APPLICATION OF WAVELET ON QUASI-PERIODIC PHYSIOLOGIC SIGNALS

A THESIS

Presented to the Department of Electrical Engineering

California State University, Long Beach

In Partial Fulfillment

of the Requirements for the Degree

Master of Science in Electrical Engineering

Committee Members:

Hen-Geul Yeh, Ph.D. (Chair)
Tulin Mangir, Ph.D.
Fei Wang, Ph.D.

College Designee:

Antonella Sciortino, Ph.D.

By Krupa S. Bhavsar

B.E., 2014, Gujarat Technological University, India

January 2017

ABSTRACT

APPLICATION OF WAVELET ON QUASI-PERIODIC PHYSIOLOGIC SIGNALS

By

Krupa S. Bhavsar

January 2017

Electrocardiogram (ECG) signals signify the electrical activity of the heart. The scrutiny of these signals is extremely crucial as it ascertains the robustness of the heart and accordingly the health of the person. An ideal ECG signal is generated synthetically in MATLAB to interpret its morphology.

This research describes an innovative method to classify the normality or abnormality of the ECG signals by considering interval estimation, specifically the P-R interval. Along with the P-R interval, an R-R interval, and a P-P interval is also considered. The intervals play a more significant role compared to the amplitudes of the waves in the ECG signals because the intervals remain invariant with respect to the ECG Recording Machine (ERM) while amplitudes can be manually altered. The characteristics of the ECG signals are analyzed with the help of a wavelet analysis.

A novel algorithm is developed using a db_4 wavelet to check the 50 Hz interference as well as eliminate the Wandering Baseline (WB) artifact and White Gaussian Noise (WGN) from the signal for an accurate estimation of the intervals. A tolerance of ±2 units is observed in the calculation of the intervals. The ECG signals 103, 105, 107, and 119 are chosen from the MIT-BIH Arrhythmia database, and the ECG signals 16420, 16272, 17052, and 17453 are chosen from the MIT-BIH Normal Sinus Rhythm Database. The developed algorithm demonstrates precise results with the simulations performed in MATLAB to conclude the normality or

abnormality of the ECG signals.

ACKNOWLEDGEMENTS

Most important, I would like to thank God for bestowing me the strength to finish this research. Without Him, I would be without strength.

I would like to express my sincere thanks to my advisor, Dr. Hen-Geul Yeh, Department Chair of Electrical Engineering, California State University Long Beach, for imparting his expertise in this research. Without his generous advice and support, this research would not have been a success. It is a great honor to work under his supervision.

I am highly indebted to the School of Nursing, California State University Long Beach, for their guidance as well as for providing the necessary information regarding this research and for their support in completing this endeavor. I would like to express my deepest gratitude to Dr. Joy Goebel, Associate Professor, School of Nursing, California State University Long Beach, for her endless encouragement as well as comprehensive advice.

My profound gratitude also goes to my panel of examiners, Dr. Fei Wang and Dr. Tulin Mangir, California State University Long Beach, for their constructive comments, suggestions, and critique.

I would also like to thank Dr. Boi Tran, Lecturer of Electrical Engineering, California State University Long Beach, for sharing his knowledge and providing innovative ideas for my research. I am grateful to Sarah Davis, Graduate Assistant, Writing and Communication Resource Center, College of Engineering, California State University Long Beach, for helping me shape my translation skills for my research.

I would like to thank my parents for having faith in me and supporting me in every way to complete my research. Last but not the least, Anubhav Jagtap deserves heartiest thanks for his encouragement and moral support without which I would not be where I am today.

TABLE OF CONTENTS

LIST OF TABLES

LIST OF FIGURES

LIST OF ABBREVIATIONS

3D	Three Dimensional
AC	Alternating Current
bpm	Beats Per Minute
CQF	Conjugated Quadrature Filter
dB	Decibels
db_4	$Daubechies_4$
DWT	Discrete Wavelet Transform
ECG	Electrocardiogram
EMG	Electromyography
ERM	ECG Recording Machine
FFT	Fast Fourier Transform
FIR	Finite Impulse Response
IDWT	Inverse Discrete Wavelet Transform
IIR	Infinite Impulse Response
LMS	Least Mean Square
MBAD	MIT-BIH Arrhythmia Database
MBNSRD	MIT-BIH Normal Sinus Rhythm Database
QMF	Quadrature Mirror Filters
SG	String Galvanometer
SWT	Stationary Wavelet Transform
WB	Wandering Baseline
WGN	White Gaussian Noise

CHAPTER 1

INTRODUCTION

An Electrocardiogram (ECG) signal is a physiological signal that precisely defines the health of the heart. This ECG signal carries vital information about the heart in its waveforms and intervals, so it is crucial to extract the minute information from the ECG signal to obtain an accurate analysis of the heart. This research focuses on extracting information from the ECG signals to conclude its normality or abnormality.

An ECG signal consists of numerous cardiac cycles, and a cardiac cycle consists of various waves. This cardiac cycle repeats continuously along the length of the signal. The consistency of the waves in the cardiac cycle repeating along the duration of the signal may or may not remain the same. There might be a possibility of the absence of a wave or group of waves in the ECG signal. Regardless of the absence or presence of all the waves in the cardiac cycle, the pattern repeats over time. This repetitive phenomenon of the cardiac cycle is similar to the periodicity property of a signal. Thus, the ECG signal is quasi-periodic in nature because a certain pattern repeats over time.

In this research, an ideal case ECG signal is generated synthetically in MATLAB to realize its morphology. The artifacts are superimposed on the ECG signal when recorded by an ECG Recording Machine (ERM). The White Gaussian Noise (WGN) is one of the most common noises observed in a signal; thus, the ECG signal consists of WGN and artifacts. The artifacts and WGN overlap the essential information necessary for the analysis of the heart. Signal processing techniques are required to eliminate these artifacts and noise from the ECG signal. The wavelets are one of the techniques to eliminate the artifacts and noise from the ECG signal. There are several wavelets and wavelet transforms available in the literature, which can be used

to process a signal. This research uses the Discrete Wavelet Transform (DWT) on Daubechies$_4$ (db_4) wavelet to eliminate the artifacts and noise from various ECG signals.

The ECG signal contains only the necessary information about its waves and intervals once the signal processing is completed using the db_4 wavelet, which is important for the heart. This information can now be extracted depending on which information from the ECG signal needs to be collected. In this research, the result of the normality or abnormality of various ECG signals depends on the detection of its peaks and intervals.

In this research, MATLAB software is used to develop the algorithm. The accuracy of the developed algorithm is verified by testing it on eight different ECG signals. The MIT-BIH Arrhythmia Database and MIT-BIH Normal Sinus Rhythm Database provide information about the numerous types of normal and abnormal ECG signals for this research. The ECG signals are selected according to the type of feature necessary for the detection. The upcoming chapters describe the specifics of the signal processing by using the db_4 wavelet and the detection of the features from numerous ECG signals.

Background of ECG Signal

According to D. Schechter [1], the Electrocardiograph records the minute electrical currents from the heart. It is a biophysical machine, which is highly reliable and accurate**.** According to B. Aehlert [2], an ECG signal represents the electrical events occurring in a cardiac cycle of the heart. The electrodes attached to the cables are connected to an ERM to observe the electrical activity in the heart [1]. The record of the potential difference between the two terminals of the ERM placed on the surface of the skin forms the ECG signal [1].

According to M. Conover [3], the analysis of the ECG signal involves an appropriate identification of the features of the ECG signal. This analysis includes the detection of the

peaks of the R-waves and the location of Q-T intervals present in the ECG signal. It also calculates the heart and breath rates from the ECG signal. The R-R interval is the time between the successive peaks of the R-waves, and the reciprocal of this time interval produces the heart rate [2] [3]. The variability of these R-R intervals reveals the vital information about the physiological condition of the heart [2].

The ECG signal provides information about the orientation of the heart, a patient's heart rate, the effects of the diseases or injuries on the function of the heart, and electrical consequences of the drugs and electrolytes. It also provides details about the function of the pacemakers, evaluation of the responses to the medications, and a baseline record before, during, and after a medical procedure [2].

History of ECG Signal

In 1878, the earliest records of the electrical activity in the heart were made by connecting the recording wires directly to the heart [1]. In 1887, A. Waller developed a method to record the electrical currents in the human heart on the surface of the body [1]. In his method, the lead wires of a capillary electrometer were connected to record and measure the shadow of its oscillation [1].

W. Einthoven, the great Dutch physiologist in 1901, invented the String Galvanometer (SG) [1]. It measured the current in millivolts, which passed through the string to set up the magnetic field to produce the deflection. A photographic plate or film moving at a desired speed focused the images of these deflections [1]. It was comparatively difficult to manage the SG; thus, the film was developed with a consequent delay in the available information. The presently used equipment has a direct writing stylus and is read from moment to moment [1]. As the SG electrocardiograph turned out to be accessible, clinically, developments were made to make it

more practical. The ECG signals described by A. Waller consisted of five electrodes. E. Schafer of the University of Edinburgh was the first person who purchased the SG electrocardiograph for clinical use in 1908.

According to M. AlGhatrif and J. Lindsay [4], W. Einthoven could diminish the quantity of the electrodes to three by excluding those that gave the minimum yield. These three leads were used to develop the Einthoven's triangle; an essential idea still used today. W. Einthoven won a Nobel Prize in Physiology and the prescription for the disclosure of the Electrocardiograph in 1924. In the United States, the first ERM was acquired by Dr. A. Cohn at Mt. Sinai Hospital, New York in 1909 [4].

During the first three decades of the twentieth century, the use of three-lead ECG signals expanded, especially after improvements were made to make it more portable. ECG signals were originally used to study arrhythmias [4]. At present, the conventional ECG signals use 12-leads.

Leads

A lead is a record of the electrical activity between two electrodes. The electrodes are placed at particular locations on the patient's chest to view the electrical activity occurring in the heart at different angles and planes [2]. The electrodes can be applied to the patient in the combinations of two, three, four, or five. One end of a monitoring cable is attached to the electrode and the other end to the ERM [1] [2]. The electrode placement is different for each lead, and different leads provide different views of the heart.

Each lead records the average current flow at a definite time in a section of the heart [2]. The lead is chosen to highlight a segment of the ECG complex, or the electrical events of the cardiac cycle [4].

The frontal (coronal) and horizontal (transverse) planes are the two planes viewing the

heart's electrical activity with the help of leads. Superior, inferior, right, and left are the directions observed in the frontal plane. The horizontal plane leads scrutinize the heart as if the heart was divided into two halves horizontally. Anterior, posterior, right, and left are the directions observed in the horizontal plane [2]. A 12-lead ECG signal interprets the heart in both the frontal and horizontal planes.

There are three types of leads namely, standard limb leads, augmented leads, and precordial (chest) leads [4]. Each lead has a negative (-) and positive (+) electrode (pole). Any of the electrodes can be made positive or negative by moving the lead selector on the ERM [2].

Morphology of ECG Signal

A typical cycle of the ECG signal consists of P, Q, R, S, and T waves. A U-wave is present in the signal in rare conditions. Figure 1 displays the waves present in a cardiac cycle of the ECG signal. An isoelectric line connects these waves. According to J. Kubicek, M. Penhaker, and R. Kahankova [5], an isoelectric line is a portion of time during which the heart is inactive for a short duration. A zero-voltage level denotes this line. This isoelectric line is called a baseline. Each wave of the ECG signal carries information that the pathologists can use to arrive at a diagnosis depending upon the abnormal wave present in the ECG signal.

P-wave. The P-wave is one of the most important features of the ECG signal. The rate or the absence of the P-wave in the ECG signal helps to establish the rhythm, and it is important in recognition of most arrhythmias [2]. Its beginning is denoted as the first abrupt or gradual deviation from the baseline, and its end is a point at which the waveform returns to the baseline. The duration between two consecutive P-waves is called a P-P interval. The normal P-wave is smooth and round in nature. The length of a normal P-wave should be no more than 0.11 seconds. Its height should not exceed 2.5 mm [1] [2]. If the P-wave is tall, pointed, broad or

notched, then it is an abnormal wave.

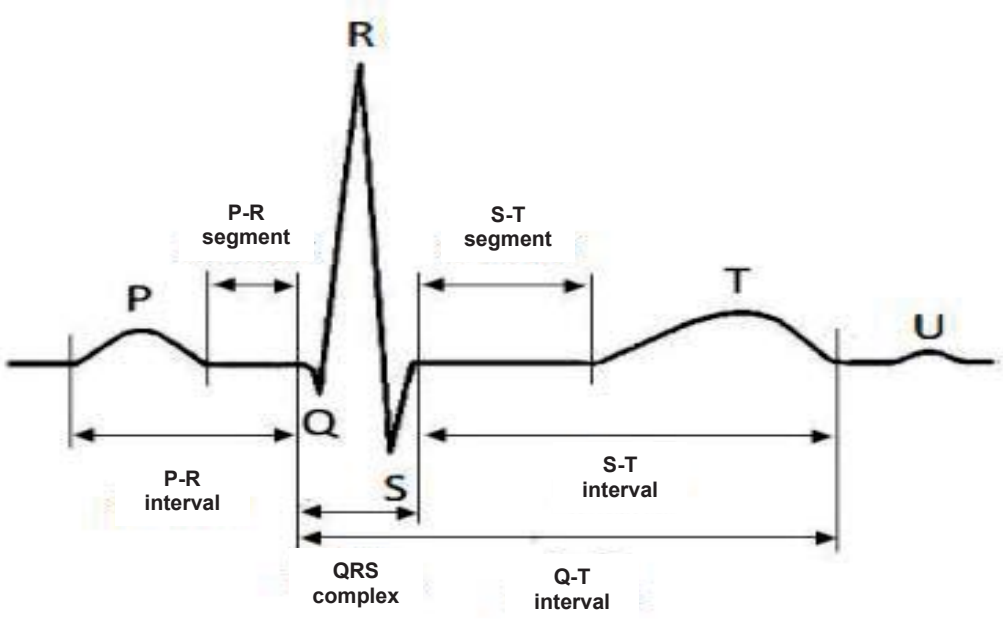

FIGURE 1. Morphology of ECG signal [2] [5].

P-R segment. A segment is a line between the waveforms and is named by the waveform that precedes or follows it. A P-R segment is a part of the P-R interval. It is a horizontal line between the terminating point of the P-wave and the starting point of the QRS complex [2]. This segment is usually isoelectric. Its duration depends on the length of the P-wave.

P-R interval. An interval is a waveform and a segment. A P-R interval includes the P-wave, the P-R segment, and a QRS complex [1] [3]. The onset of the P-wave to the beginning of the QRS complex determines this interval. The standard length of this interval is between 0.12 to 0.20 seconds, or 0.21 seconds in adults. The length of this interval may be shorter in children and longer in the elderly. This interval varies with the heart rate. According to J. Hurst and R. Myerburg [6], this interval shortened with an increase in the heart rate. If the duration of the interval is time variant, or if the interval is shorter or longer in length, then it is abnormal.

QRS complex. A complex consists of several waveforms. A QRS complex consists of

a Q-wave, an R-wave, and an S-wave. It typically arises after each P-wave. One or even two of the three waveforms that form the QRS complex may not always be present in the signal [1] [3].

The QRS complex begins with a downward deflection of the Q-wave. The Q-wave is typically a negative waveform, and its duration is usually less than 0.04 seconds. Its amplitude is approximately 25% of the amplitude of the R-wave [2].

The QRS complex continues with a large, upright, triangular waveform known as an R-wave. The R-wave is the first positive deflection above the baseline in the QRS complex and is about 5-16 mm in height [1] [2] [6]. The S-wave is the negative waveform following the R-wave.

The term QRS complex is used irrespective of the presence of a Q-wave, an R-wave, and an S-wave in the complex [2]. If the QRS complex consists entirely of a positive waveform, it is called an R-wave [2]. If the complex consists entirely of a negative waveform, it is called a Q-S wave [2]. The second wave is called an R-prime, and it is written as R' when there are two positive waves present in an unchanged complex [2]. Similarly, the second wave is called the S-prime, and it is written as S' when there are two negative deflections succeeding an R-wave.

The evaluation of the QRS complex starts from the point when the first wave of the complex begins to deviate from the baseline [2] [3]. The point at which the last wave of the complex begins to level out, above or below the baseline, indicates the termination of the QRS complex. The duration of a normal complex is between 0.06 to 0.10 seconds in adults.

S-T segment. The portion of the ECG signal between the QRS complex and the T-wave is called the S-T segment. The point where the QRS complex and the S-T segment intersect is called the junction, or a J-point. The regular S-T segment begins at the isoelectric line, extends from the end of the S-wave, and curves progressively in an upward direction to the starting point of the T-wave. It varies from -0.5 to +1 mm in a few precordial leads [1] [2]. The length of the

normal S-T segment is 1 mm. It displaces from the isoelectric line either in a positive or a negative direction depending on various conditions. This displacement determines an abnormal signal.

T-wave. A normal T-wave is slightly asymmetric because the peak of the waveform is closer to its terminating point than to the starting point, and the first half has a more gradual slope compared to the second half. The beginning of the T-wave is a point from which the slope of the S-T segment appears to become abruptly or gradually steeper [1] [2]. The T-wave ends when the wave returns to the baseline. It may be complicated to evidently define the starting and termination point of the T-wave [2]. It usually orients in the same direction as the preceding QRS complex. It is about 1 to 5 mm in height. The T-wave following an abnormal QRS complex is typically reverse in direction of the QRS complex. A tall, negative, pointed, and deeply inverted T-wave suggests that the ECG signal is abnormal.

Q-T interval. The duration between the beginning of the QRS complex and the end of the T-wave is called a Q-T interval. This interval is called a Q-T interval irrespective of whether the QRS complex begins with a Q-wave or an R-wave. The Q-T interval is calculated from the beginning of the R-wave to the end of the T-wave when the Q-wave is absent [2] [3]. Its duration varies according to the age, gender, and particularly the heart rate. It usually lasts from 0.36 to 0.44 seconds. The interval decreases as the heart rate increases and vice versa. A prolonged interval determines the abnormality of the ECG signal.

Artifacts in ECG Signal

The non-distortion of the waveforms and intervals present in the ECG signal determines its accurate analysis. According to M. Silverman, R. Myerburg, and J. Hurst [7], the distortion of an ECG signal by electrical activity that is non-cardiac in origin was called an artifact. The loose

electrodes, the broken ECG cables, or broken wires, the muscle tremor, the patient movement, and the external chest compressions are a few reasons generating the artifacts [2] [3] [6].

A proper preparation of the patient's skin and an evaluation of the ERM before use can minimize the problems associated with the artifact. The noise one hears while tuning a radio is similar to an artifact. These signal distortions may be continual or intermittent in nature [2]. The most significant artifacts that should be taken account before analyzing the ECG signal are the power line interference artifact and the Wandering Baseline (WB) artifact.

50-cycle interference. A poor ground connection of the ERM causes a phenomenon known as a 50-cycle interference in the ECG signal [2] [3]. It is also called a power line interference, or an Alternating Current (AC) interference [2]. A random spike at 50 Hz frequency denotes the presence of this interference. It can also occur at the harmonics of the power supply.

Wandering baseline interference. The isoelectric line shifts its position when the WB artifact is present in the signal. The movement of the electrodes, the patient's movement, and an improper electrode contact during the recording of the ECG signal are a few reasons causing this interference [2] [6].

Background of Wavelets

According to A. Graps [8], a wavelet is a wave, which has an amplitude beginning at zero, increases, and then decreases back to zero. It is a function that satisfies a particular mathematical condition, and it defines the data or an additional function. There are several properties of the wavelets including orthogonal, non-orthogonal, biorthogonal, and multiresolution analysis [8]. The wavelets are suitable for estimating the data with sharp discontinuities and analyzing the transient, nonstationary, or time-shifting signals [8].

A wavelet analysis provides information about the time and frequency components of the

signal simultaneously. It is a technique to execute an original wavelet function called an analyzing wavelet, or a mother wavelet [8]. According to I. Daubechies [9], the scaling and the wavelet function describes the wavelet analysis, and they are represented in the form of coefficients.

A wavelet algorithm routes the data at different scales, or resolutions [8]. The analysis of a signal or a function described by the wavelet algorithm through a large window detects significant features from the signal. Similarly, the examination of a signal via a small window detects minute features from it [8].

According to C. Torrence and G. Compo [10], a time-based calculation was conducted with a limited high-frequency form of the original wavelet, while a frequency analysis was executed by a widened low-frequency form of a similar wavelet. The data operation was executed only on the matching wavelet coefficient. The data was represented in a way that one could select the wavelet best suited for one's data by reducing the coefficients below a threshold level [10]. This sparse coding yielded the wavelet as an outstanding tool in the field of data compression.

There are various transforms associated with a wavelet. A wavelet transform generates colorful images and produces qualitative results [10]. The wavelet analysis includes a transform from a one-dimensional time series or frequency spectrum to a scattered two-dimensional time–frequency image [8]. Weather detection, signal and image processing, astrophysics, sound quality, nuclear-power engineering, neurophysiology, speech differentiation, scientific applications, and sub-band coding are the areas of the application of the wavelets [10].

Outline

The organization of this research is in the following manner. Chapter 2 describes the

literature survey. Chapter 3 explains the wavelet theory. Chapter 4 defines the characterization of ECG signals as normal or abnormal, and Chapter 5 portrays the obtained results. Finally, Chapter 6 summarizes the conclusion and provides the future expansion.

CHAPTER 2

LITERATURE SURVEY

This chapter describes the techniques previously developed for generating the synthetic ECG signal in MATLAB and the removal of the artifacts present in the signal. It also describes the methods for the elimination of the WGN and the detection of the peaks of the waves in the ECG signal. The upcoming sections describe these techniques in detail.

Techniques to Generate Synthetic ECG Signal

Chapter 1 describes the morphology of the ECG signal in detail. The construction of the synthetic ECG signal in MATLAB can be used to interpret its morphology. The various waves of the generated ECG signal have normal amplitudes and duration. Thus, the synthetic ECG signal can be used as an ideal case ECG signal. The upcoming sections describe the three techniques previously used to generate the synthetic ECG signal.

Three-Dimensional Approach

P. McSharry et al. [11] generated a dynamical model consisting of three coupled conventional differential equations, and it was used to construct the synthetic ECG signal. This model produces a trajectory in a Three-Dimensional (3D) state–space in the (x, y, z) direction as shown in Figure 2. The dashed line in Figure 2 describes a limit cycle of a unit radius, and the small circles indicate the locations of all the waves present in the ECG signal. The development of the trajectory within the unit range of the limit cycle in the (x, y) plane indicated the semi-periodicity property of the ECG signal [11]. Each transformation on this circle was related to an R-R interval or pulse.

The movement of the trajectory in the z plane replicated the interbeat variation in the ECG signal [11]. According to G. Clifford and P. McSharry [12], the occurrences of the negative

and positive attractors/repellors in the z direction portrayed the different segments of the ECG signal. θ_P, θ_Q, θ_R, θ_S, and θ_T represented the location of these occurrences at set inclines along the unit circle. When the direction of the trajectory approached one of these occurrences, it pushed itself in an upward or a downward direction, which was far from the limit cycle. After it had moved away, it was again pulled back towards the limit cycle [12].

A group of three familiar differential equations generates the dynamical equations of motion. Equations (1), (2), and (3) describe this motion [11 - 14].

$$\dot{x} = \alpha x - \omega y \tag{1}$$

$$\dot{y} = \alpha y + \omega x \tag{2}$$

$$\dot{z} = -\sum_{i\in\{P,Q,R,S,T\}} a_i \Delta\theta_i exp\left(-\frac{\Delta\theta_i^2}{2b_i^2}\right) - (z - z_0) \tag{3}$$

where $\alpha = 1 - \sqrt{x^2 + y^2}$,

$\Delta\theta_i = (\theta - \theta_i)\ mod\ 2\pi$,

$\theta = atan2(y, x)$ with $-\pi \leq atan2(y, x) \leq \pi$,

and ω = shifting of the angular velocity of the trajectory with respect to the limit cycle.

The coupling of the baseline value z_0 in Equation (1) with the respiratory frequency f_2 added the WB artifact in the signal. Equation (4) explains the relation between the respiratory frequency f_2 and the baseline value z_0 [11] [12].

$$z_0(t) = A\ sin(2\pi f_2 t) \tag{4}$$

where A = 0.15 mV.

These equations of motion given by Equation (1) were integrated numerically using a fourth order Runge–Kutta technique with a fixed time step of $\boldsymbol{\Delta t = 1 \div f_s}$, where $\boldsymbol{f_s}$ was the sampling frequency [11].

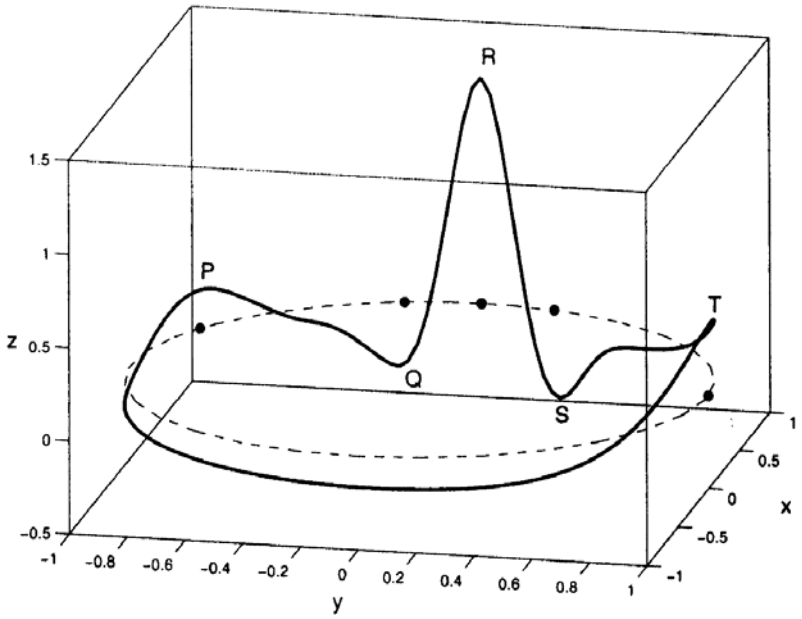

FIGURE 2. Trajectory generated by dynamical model in 3D [10] [11].

This dynamical model demonstrated how the positions of the occurrences of all the waves followed up the trajectory in the z direction as it moved around the unit circle in the (x, y) plane [11] [12]. The z variable from the 3D system in Equation (1) yielded the synthetic ECG signal. When the synthetic ECG signal was generated, there was no artifacts or noise present in it. The times and angles of the waves are specified corresponding to the position of the R-peak, which is shown in Table 1.

When one lap of the limit cycle completed, it was equivalent to the R-R interval of the synthetic ECG signal [12]. The variations in the length of the R-R interval were obeserved by changing the angular velocity ω [12].

Figure 3 displays the synthetic ECG signal generated by this dynamical model. This model was used to survey the biomedical sign preparing strategies, which were used to process the clinical insights of the ECG signal [12]. This approach determined the mean, standard deviation of the heart rate, and morphology of the ECG signal.

TABLE 1. Parameters for Dynamical ECG Model [11] [12]

Index (i)	P	Q	R	S	T
Time (seconds)	-0.2	-0.05	0	0.05	0.3
θ_i (radians)	$-\frac{1}{3}\pi$	$-\frac{1}{12}\pi$	0	$\frac{1}{12}\pi$	$\frac{1}{2}\pi$
a_i	1.2	-5.0	30.0	-7.5	0.75
b_i	0.25	0.1	0.1	0.1	0.4

Inbuilt MATLAB Functions Technique

A computer based model was used to develop the sequential waves of the ECG signal. The *synecg* function was developed and tested in MATLAB to generate the artificial ECG signal. According to J. Ackora-Prah, A. Y. Aidoo, and K. B. Gyamfi [13], the *synecg* function was designed by using the inbuilt MATLAB functions namely, *sgolayfilt*, *kron*, *ones*, *round*, and *linspace*.

The function *sgolayfilt* denotes a Savitzky-Golay filter. It is also called a digital smoothing polynomial filter, or a least-squares smoothing filter. The function is described by Equation (5) [13].

$$y = sgolayfilt\ (x,\ k,\ f) \tag{5}$$

where x = vector or a matrix,

k = order of the polynomial,

and f = frame size.

This filter is applied to the information in the vector x. If x is a matrix, then the function *sgolayfilt* works on each column. The polynomial order k should typically be smaller than the frame size f and must be odd. If the value of k is the difference between the frame size and one,

then the filter produces no smoothing [13]. The noise from the ECG signal is reduced by using the Savitzky-Golay smoothing filter [13]. The peaks and the valleys of the ECG signal are retained more efficiently with the use of the Savitzky-Golay smoothing filter when compared to the standard FIR filter [13].

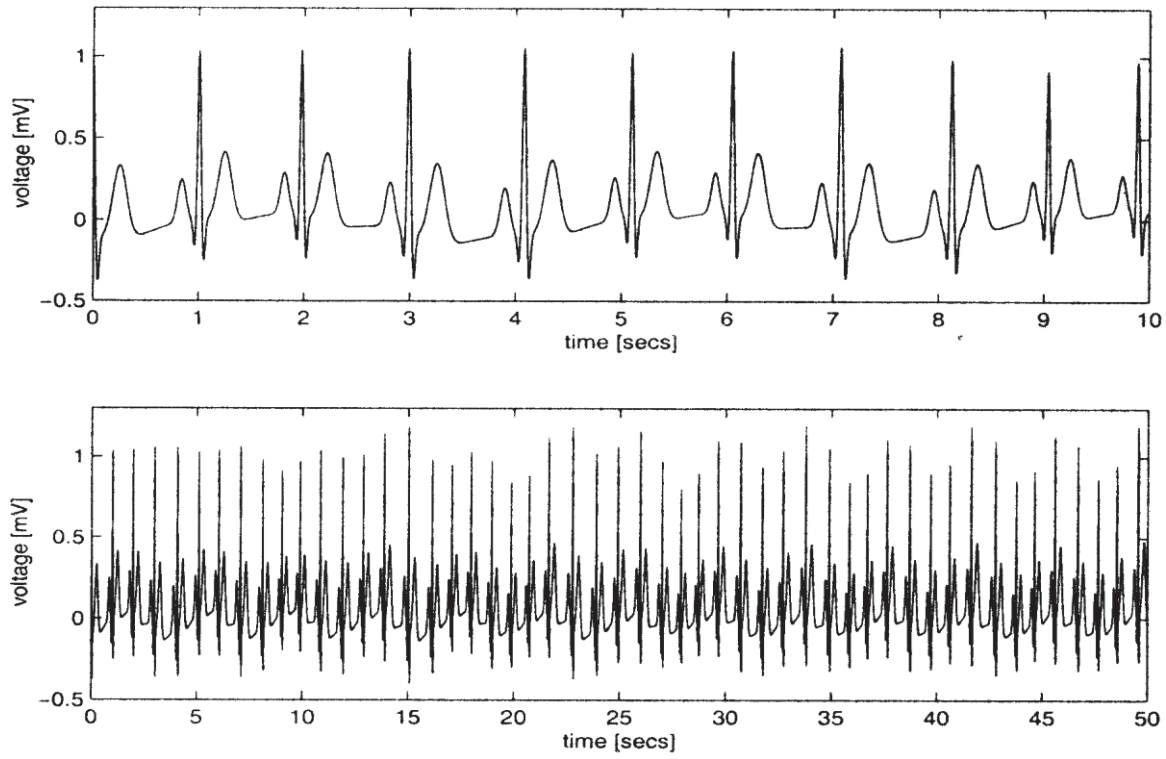

FIGURE 3. Synthetic ECG signal generated by dynamical model at 10s and 50s [10].

The function *kron* represents the Kronecker Tensor Product. The function is described by Equation (6) [13].

$$K = kron\ (X,\ Y) \tag{6}$$

where X, Y = matrices.

Equation (6) returns the Kronecker tensor product of X and Y. The outcome is a large array produced by considering all the probable products between the elements of X and Y [13]. If the size of X is m *by* n and that of Y is p *by* q, then the size of the matrix K is $m*p$ *by* $n*q$.

The function *ones* is used to create a matrix of any dimension containing ones [13]. The

command *ones (m, n)* generates a matrix of a *m by n* dimension with all ones [13].

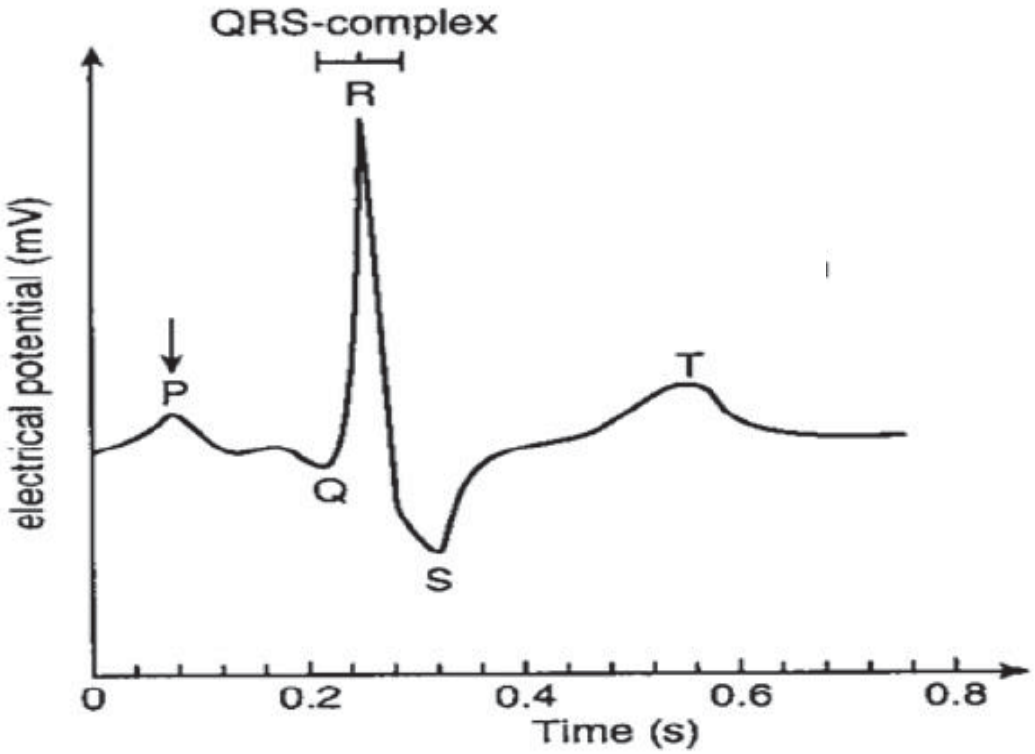

FIGURE 4. Synthetic one cardiac cycle of ECG signal [13].

The function *round* operates on a single number or the numbers in a matrix to round them to the nearest integer [13]. The solution for *round* (*2.43345534*) is 2. Similarly, if *M* is a *two by two* matrix with *M* = [2.323 5.2344; −1.234 8.4353], then *round* (*M*) will be [2 5; -1 8] [13].

The function *linspace (a, b, n)* creates a one-dimensional array of *n* uniformly spaced numbers in the interval [*a b*] [13].

The *synecg* function generated the synthetic ECG signal for 10 seconds and for various heart rates of a resting individual with a peak voltage of 1.2 mV. The cardiac cycle of the ECG signal was 0.8 seconds long. Figure 4 displays the cardiac cycle of the synthetic ECG signal. This function used the heart rate per minute and the voltages of the waves measured in millivolts to generate the synthetic ECG signal [13]. This *synecg* function generated the synthetic ECG

signals for 60 Beats Per Minute (bpm), 80 bpm, and 95 bpm in MATLAB [13]. G. A. Kumar and S. Vegi [14] also produced the ECG signals in the range of 40–100 bpm.

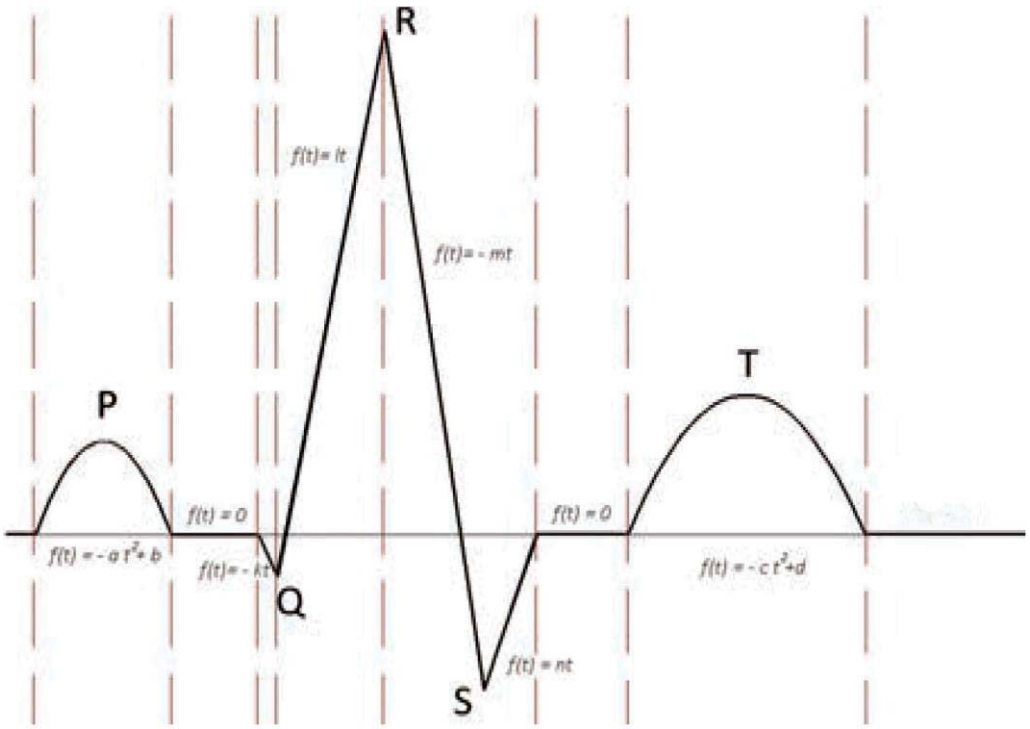

FIGURE 5. Performance of rough analysis on ECG signal [7].

Fourier Series Technique

The decomposition of the periodic functions uses a Fourier series. The ECG signal is assumed to be periodic in nature; therefore, it is decomposed using a Fourier series. Figure 5 displays a rough analysis on the ECG signal. The ECG signal consists of repeating sine waves namely, the P, T, and U waves. The triangular QRS complexes are also present in the ECG signal. The divisions of the ECG signal displayed in Figure 5 simplify the mathematical equations for each part of the signal [7]. The shifts and slopes of the elementary functions described the coefficients representing the different parts of the ECG signal. *a*, *b*, *c*, *d*, *k*, *l*, *m*, and *n* denoted the coefficients [7].

A parabolic function $f(t) = -t^2$ estimated the P and T waves [7]. The final form of the

function was denoted by the adjustable parameters including the shift or width. The mathematical formulation has the following forms as illustrated in Equations (7 – 10) [7].

$$a_0 = \int_c^{c+2\pi} -t^2 dt = \left[-\frac{t^3}{3}\right]_c^{c+2\pi} = -\frac{2}{3}\pi^2 \quad (7)$$

$$a_k = \frac{1}{\pi}\int_c^{c+2\pi} -t^2\, cos(kt)\, dt \quad (8)$$

$$b_k = \frac{1}{\pi}\int_c^{c+2\pi} t\, sin(tx)\, dt\ = 0 \quad (9)$$

$$f(t) = 4\sum_{k=1}^{\infty} \frac{(-1)^k}{k^2} \cos(kt) \quad (10)$$

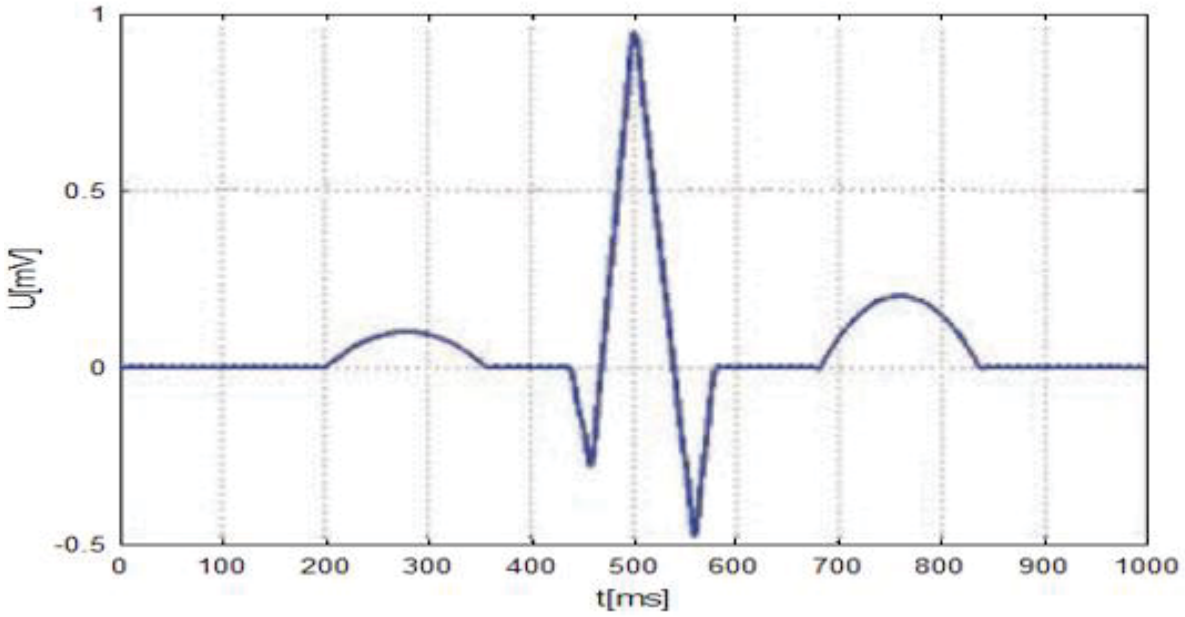

FIGURE 6. Synthetic ECG signal [7].

The Q, R, and S waves are triangular, so their division is into two parts namely, the falling and rising segments. The basic functions $(\boldsymbol{t}) = -\boldsymbol{t}$ and $\boldsymbol{f}(\boldsymbol{t}) = \boldsymbol{t}$ denoted each wave with a diverse shift and slope [7]. For the formation of a rising segment of the QRS complex, a basic function of the form $\boldsymbol{f}(\boldsymbol{t}) = \boldsymbol{t}$ was selected. The decomposition of the waves using the Fourier series is described by Equations (11 – 14) [7].

$$a_0 = \frac{1}{\pi}\int_c^{c+2\pi} t\ dt = \frac{1}{\pi}\left[\frac{t^2}{2}\right]_c^{c+2\pi} = 0 \quad (11)$$

$$a_k = \frac{1}{\pi}\int_c^{c+2\pi} t\ cos(kt)\ dt = 0 \quad (12)$$

$$b_k = \frac{1}{\pi}\int_c^{c+2\pi} t\ sin(tx)\ dt\ = (-1)^{k+1}\frac{2}{k} \quad (13)$$

$$f(t) = 2\sum_{k=1}^{\infty}\frac{(-1)^{k+1}}{k}\sin(kt) \quad (14)$$

The falling segment of these waves, by contrast, is described by the decomposition of the Fourier series in Equations (15 – 18) [7]. For the formation of the signal, the most basic function $\boldsymbol{f(t) = -t}$ was chosen [7].

$$a_0 = \frac{1}{\pi}\int_c^{c+2\pi} -t\ dt = \frac{1}{\pi}\left[\frac{-t^2}{2}\right]_c^{c+2\pi} = 0 \quad (15)$$

$$a_k = \frac{1}{\pi}\int_c^{c+2\pi} -t\ cos(kt)\ dt = 0 \quad (16)$$

$$b_k = \frac{1}{\pi}\int_c^{c+2\pi} -t\ sin(tx)\ dt\ = -\left((-1)^{k+1}\frac{2}{k}\right) \quad (17)$$

$$f(t) = -2\sum_{k=1}^{\infty}\frac{(-1)^{k+1}}{k}\sin(kt) \quad (18)$$

This technique adapts to the shape of the ECG signal with the help of the corresponding variables *a* – *g* described in Table 2 [7]. The slopes of the lengths of the segments corresponded to the physiological parameters of the ECG signal. Thus, the synthetic ECG signal was constructed using MATLAB software. Figure 6 displays the constructed synthetic ECG signal. This technique had a higher accuracy of approximations and computational time [7].

50 Hz Component Removal Techniques

Chapter 1 describes the artifacts present in the ECG signal and its effects on the signal. The interference of the power supply is one of the artifacts in the signal, and it changes the information of the ECG signal. There are various techniques to remove the effect of the power

supply from the ECG signal, and two of those techniques are described as follows.

TABLE 2. Parameters for Fourier Series Technique [7]

Variable	Function in Synthetic ECG Signal	Physiological Interval
a	Amplitude of P-wave	0 – 0.3 mV
b	Length of P-wave	0 – 160 ms
c	Amplitude of the QRS complex	0 – 0.5 mV
d	Length of QRS complex	50 – 120 ms
e	Amplitude of T-wave	0 – 0.8 mV
f	Length of T-wave	0 – 300 ms

Sliding Window Approach

Chapter 3 describes the soft threshold technique of the wavelet denoising in detail. If a detail level consisting of a 50 Hz component in the decomposition tree was selected, then this approach removed the 50 Hz interference without changing the ECG waveform. The approximation of the detail signal, the ECG time margins, and the duration of the noise indirectly helped to remove the 50 Hz component from the signal.

According to P. Agante and J. Marques de Sa [15], a sliding window was used to approximate the time margins because the samples of the ECG signal had higher coefficient values than noise. The improved detail signal performed a preprocessing operation by using the squared coefficient values, which in return indicated a greater difference among the noise and the ECG sample values [15].

When the mean of the coefficient values in the sliding window was greater than the standard deviation of the samples of the signal, then the ECG signal coefficients were formed.

Figure 7 illustrates how this 50 Hz interference is removed using a sliding window (w) [15]. This approach was operated on both the starting and the ending point of the detail signal. Numbers 1 and 2 in Figure 7 describe the edges of the window for the detail signal. The average of the four largest coefficients of the signal provided the noise level. This approach diminished all the probable approximation errors by specious and arbitrary glitches. The use of the approximation value of the signal as a threshold level in the soft threshold technique created a clean and a filtered ECG signal [15]. This approach used the Daubechies and Coiflet wavelets with three levels of the decomposition and reconstruction process [15].

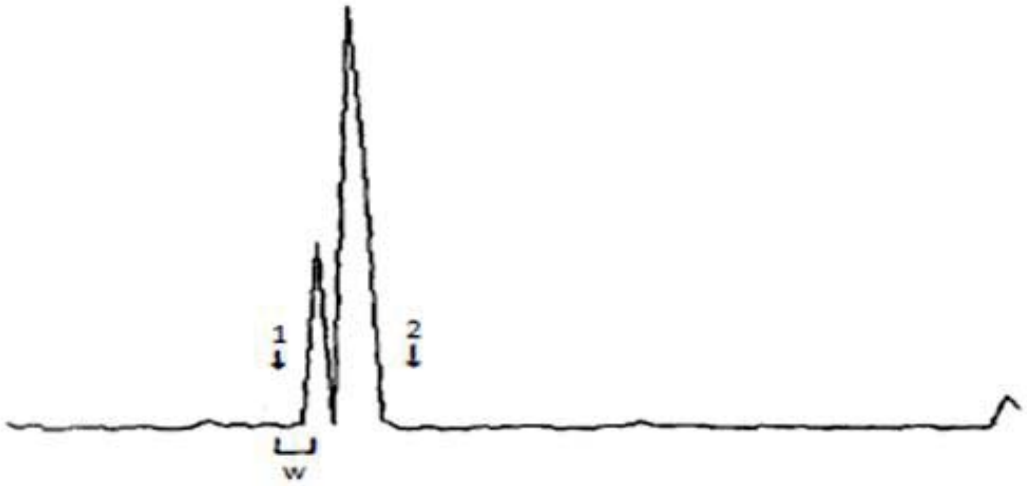

FIGURE 7. Establishment of soft threshold with the help of sliding window (w) [15].

Signed Regressor Technique

According to M. Rahman, R. Shaik, and D. Reddy [16], the ECG signal consisted of 4000 samples corrupted with the synthetic interference of the power supply. The primary input to the adaptive filter was this corrupted ECG signal. Figure 8 displays the structure of the adaptive filter. The ECG signal represented by s_1 with additive noise n_1 is displayed in Figure 8 [16]. The reference input is n_2, which is noise; y is the output of the filter, and e is the error occurred in the filter [16]. This logic of the adaptive filter was also explained by Y. Sharma and A. Shrivastava

[17]. The application of this signed regressor technique removed the WB artifact from the ECG signal. This technique was obtained from the conventional Least Mean Square (LMS) algorithm by replacing the tap-input vector $x(n)$ with the vector $sgn\{x(n)\}$. The signed regressor LMS adaptive filter processes the input signal $x(n)$ and generates the output $y(n)$, which is described by Equation (19) [16].

$$y(n) = w^t(n)x(n) \tag{19}$$

where $w(n) = [w_0(n),\ w_1(n), \ldots, w_{L-1}(n)\ ]^t$ is an L^{th} order adaptive filter.

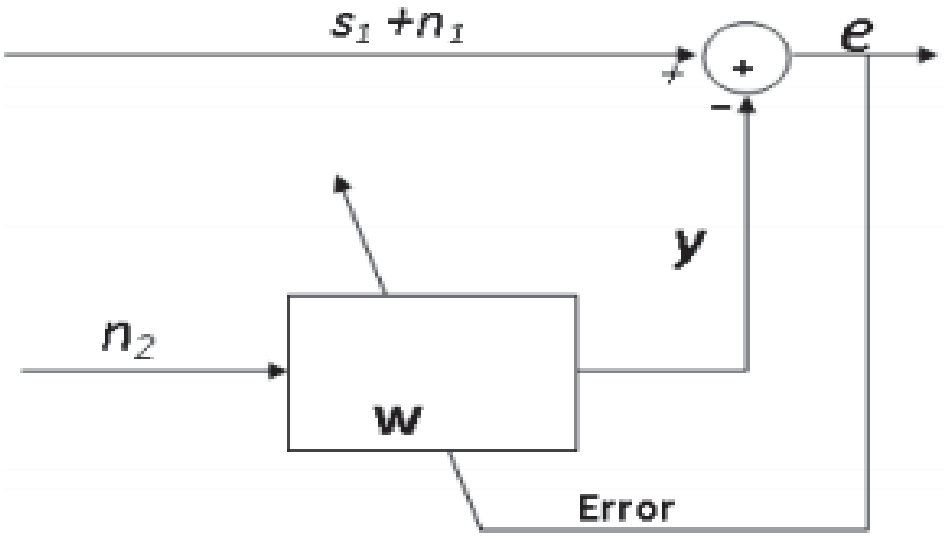

FIGURE 8. Adaptive filter structure [15] [16].

The signed-regressor LMS algorithm updates the adaptive filter coefficients as described by Equation (20) [16].

$$w(n+1) = w(n) + \mu\, sgn\{\Phi(n)\}e(n) \tag{20}$$

Figure 9 displays the ECG signal with noise, and Figure 10 displays the signal in which the interference of the power supply is removed using the signed regressor technique.

Wandering Baseline Elimination Techniques

The WB is another important artifact present in ECG signal. There are various techniques to eliminate the WB artifact, and a few of those techniques are described in detail as follows.

Butterworth Filter Approach

According to Z. H. Slimane and A. Naït-Ali [18], the implementation of a fifth order high-pass Butterworth filter eliminated the WB artifact from the ECG signal in the frequency range of 0–1 Hz.

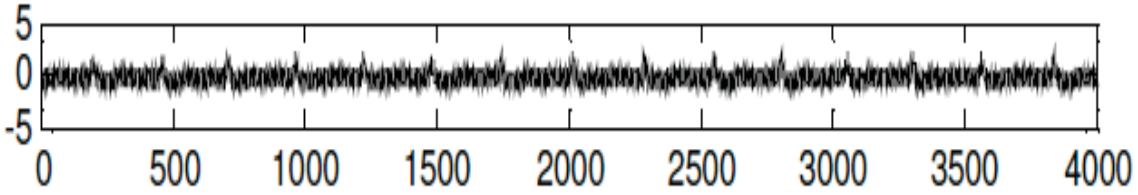

FIGURE 9. ECG signal with noise [16].

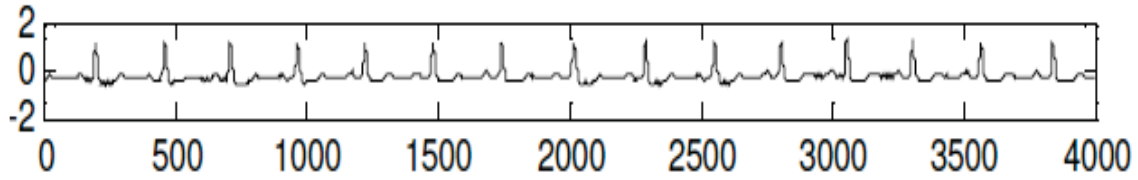

FIGURE 10. 50 Hz interference removed from ECG signal [16].

Filtration of Zero-Phase Technique

A bidirectional filter filters the signal in a forward direction over a selected window, and then the same window is filtered in a reverse direction again. According to M. Kaur and B. Singh [19], the filter was used to select a brief window for the computation purposes of actual time resolutions. In this manner, the delay of every frequency module was operated in a forward direction, then in a reverse direction in time and hence was void. The result then had a zero-phase filtration [19]. The transfer function of the filter corresponded to the squared magnitude of the fundamental transfer function of the filter. The order of the filter was double the order of the filter defined by its values in the numerator and the denominator [19].

This technique reduced the beginning and terminating transients of the filter by using the complementary preliminary states. It precisely conserved the characteristics of the filtered time waveform [19]. The Finite Impulse Response (FIR) and the Infinite Impulse Response (IIR) filters were used in this zero-phase filtering technique [19].

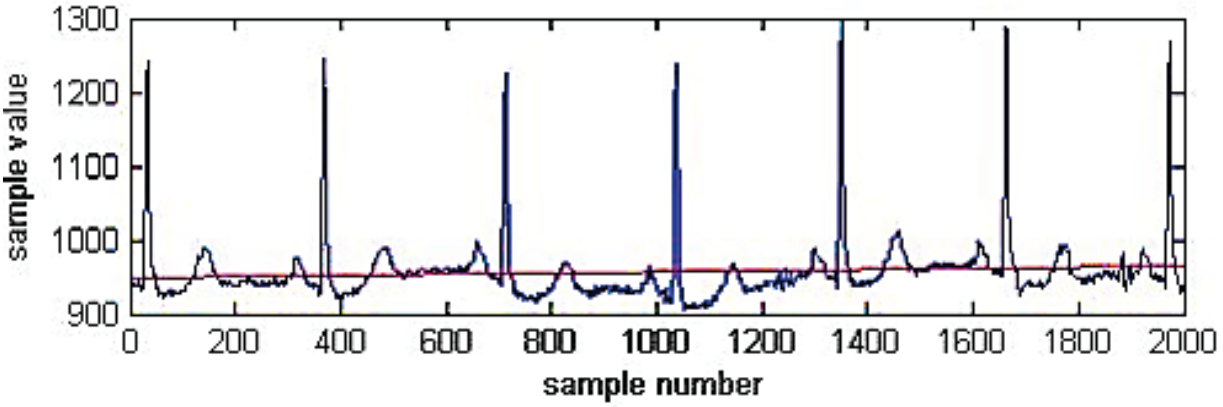

FIGURE 11. Fundamental ECG signal [19].

The denominator vector *a* and the numerator vector *b* defines the zero-phase filter. When this filter is operated on the data in the vector *x*, it produces the filtered data *y* at its output terminal. This filter is represented by Equations (21) and (22) [19].

$$y[n] = a_0x[n] + a_1x[n+1] + a_2x[n+2] + a_3x[n+3] + \cdots + b_1y[n+1] + b_2y[n+2] + b_3y[n+3] \quad (21)$$

Equation (21) describes an implementation of the recursive filter in the forward direction, and Equation (22) uses the recursive filter but in the backward direction [19].

$$y[n] = a_0x[n] + a_1x[n-1] + a_2x[n-2] + a_3x[n-3] + \cdots + b_1y[n-1] + b_2y[n-2] + b_3y[n-3] \quad (22)$$

The filtered sequence was reversed and routed across the filter once again after the completion of the filtration of the signal in the forward direction [19]. Figure 11 depicts the original ECG signal. By using the zero-phase filtering technique in the IIR and FIR filters,

Figures 12 and 13, respectively, display the removal of the WB artifact from the ECG signal described in Figure 11 [19].

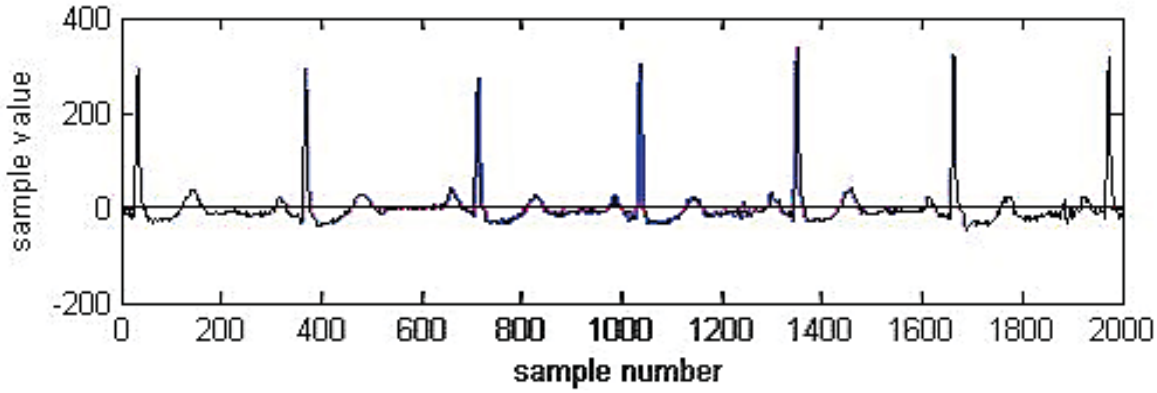

FIGURE 12. WB artifact removed in ECG signal by zero-phase filtering in IIR filter [19].

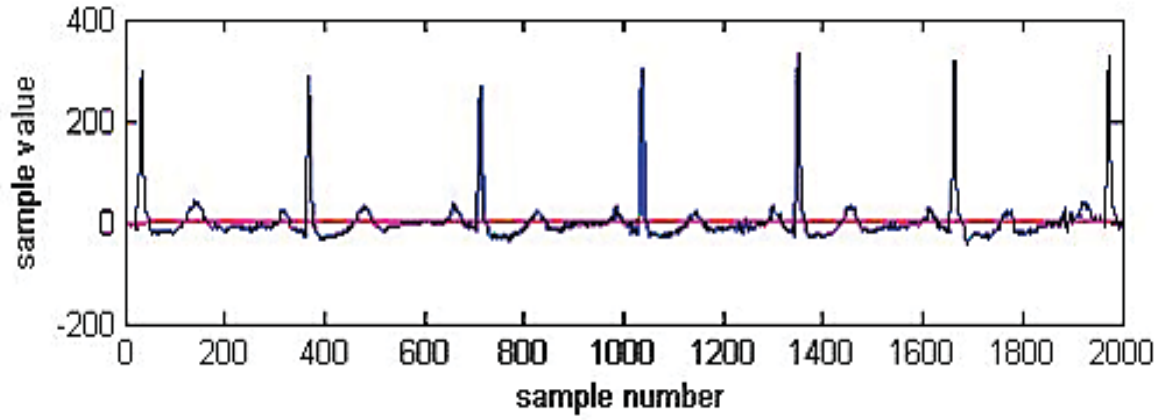

FIGURE 13. WB artifact removed in ECG signal by zero-phase filtering in FIR filter [19].

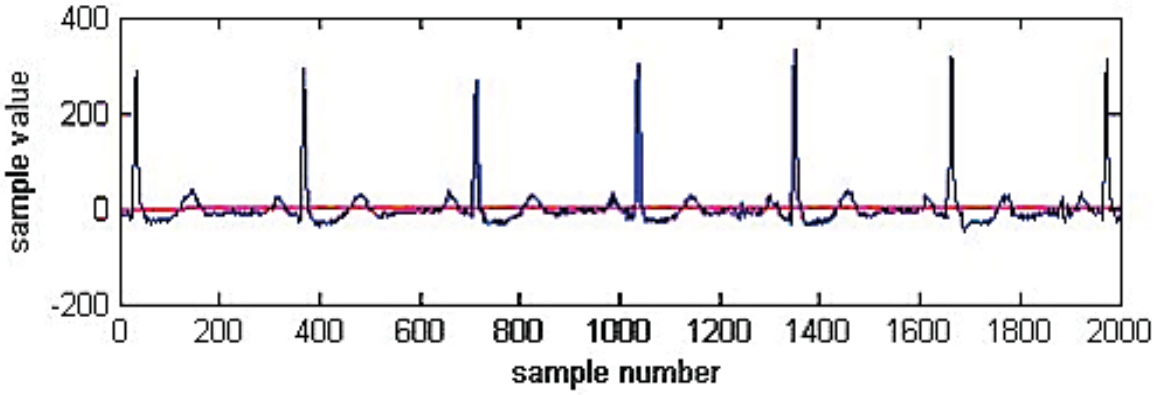

FIGURE 14. WB artifact removed in ECG signal using wavelets [19].

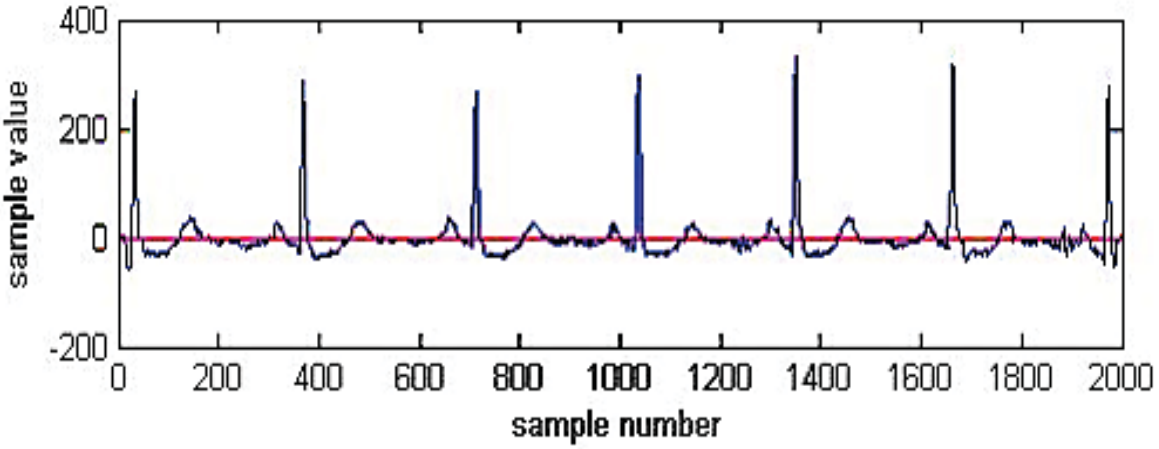

FIGURE 15. WB artifact removed in ECG signal using moving average [19].

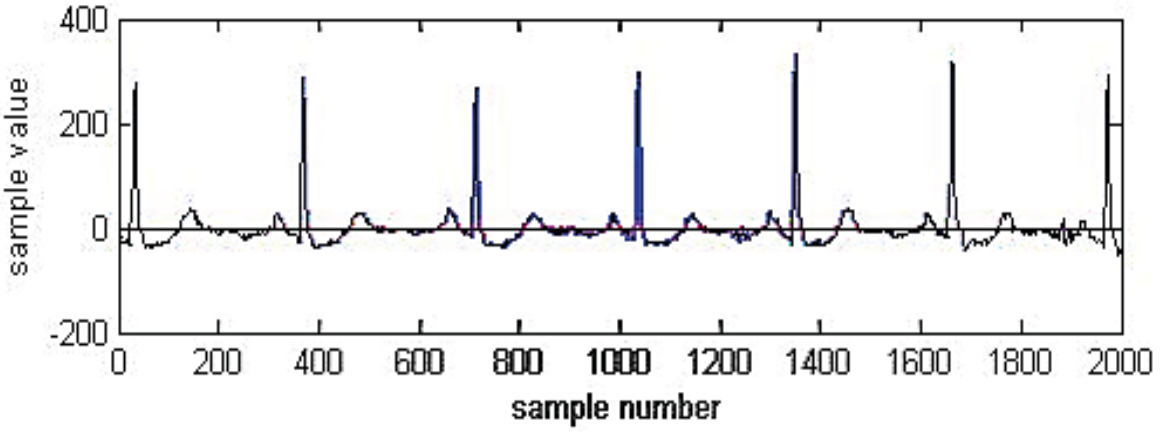

FIGURE 16. WB artifact removed in ECG signal using Savitzky-Golay filter [19].

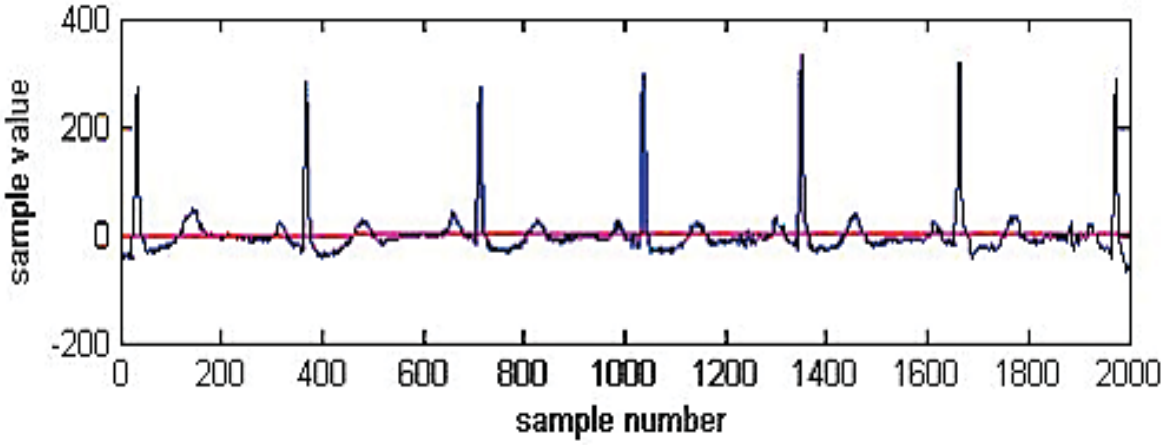

FIGURE 17. WB artifact removed in ECG signal by means of polynomial fix [19].

This technique produced the best results when compared to methods 3-6 in the wandering baseline elimination techniques for removing the WB artifact from the ECG signal [19].

Wavelet Approach

The ECG signal was decomposed up to level 8 by applying the Daubechies$_6$ wavelet. The detail coefficients of all the levels were superimposed to remove the WB artifact from the ECG signal [19]. Chapter 3 describes the wavelet in detail. Figure 14 displays the removal of the WB artifact from the ECG signal in Figure 11 using the wavelet approach.

Moving Average Method

A moving average filter leveled the information by substituting every data point with the average of the neighboring data points outlined in that duration [19]. This method corresponded to the low-pass filtering with the response of the flattening given by Equation (23) [19].

$$Y_s(i) = \frac{1}{2N+1}\big(Y(i+N) + Y(i+N-1) + \cdots + Y(i-N)\big) \tag{23}$$

where $Y_s(i)$ = the smoothed value for the i^{th} data point,

N = number of neighboring data points on either side of $Y_s(i)$,

and $2N + 1$ = span.

The moving average smoothing method used the Curve Fitting Toolbox. There are two rules for this toolbox. The first rule is that the duration of the signal must be odd. The second rule is that the focal point of the length of the signal represents the samples that can be smoothed [19]. The duration of the signal was modified in such a way that the sample values failed to hold the stated quantity of the neighbors on either side [19]. The terminating location of the sample values was not defined because the duration of the signal was undefined. Figure 15 displays the WB artifact removed from the ECG signal in Figure 11 using the moving average method [19].

Savitzky-Golay Filter Technique

A Savitzky-Golay filter has a simplified moving average. The filter coefficients were derived by an unweighted linear least square fit, which consisted of a polynomial of a suitable degree [19]. This filter conserved the peaks and valleys of the ECG signal more efficiently compared to the standard FIR filter. Figure 16 depicts the WB artifact removed from the ECG signal in Figure 11 by using the Savitzky-Golay filter technique [19].

Polynomial Fix Technique

The polynomial fitting was a technique to remove the WB artifact by fixing the polynomials to the characteristic details of the ECG signal [19]. The low-frequency information was preserved, and the high-frequency baseline noise was eliminated from the signal. The order of the polynomial was increased by selecting a knot per beat through which the baseline approximation passed [19]. The sample of every beat was called a knot [19]. This technique was beneficial for the operation of other procedures after removing the WB artifact from the signal. The computational complexity of the polynomial was increased by using the higher order polynomials to generate a precise baseline approximation. The polynomial was constructed in such a way that when one sample was deducted from the original signal, the value of the knot was zero [19]. The polynomial of degree 6 was used to generate the ECG signal using the polynomial fix technique. Figure 17 indicates the removal of the WB artifact from the ECG signal displayed in Figure 11 by using the polynomial fix technique.

Signed Regressor Method

Figure 8 displays the adaptive filter in which the primary input is the ECG signal 105 of the MIT–BIH database. The signed regressor algorithm [16] [17] as described in Equations (19) and (20) is applied to the ECG signal to remove the WB artifact [16]. Figures 18 and 19 display

the results of the algorithm. Figure 18 exhibits the ECG signal composed of the WB artifact, and Figure 19 demonstrates the ECG signal free from the WB artifact.

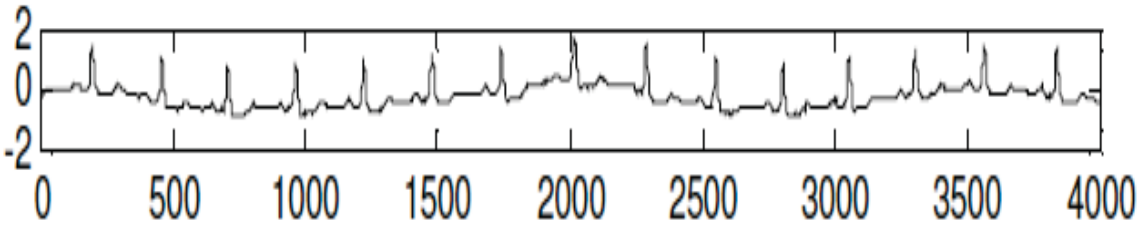

FIGURE 18. ECG signal consisting of the WB artifact [16].

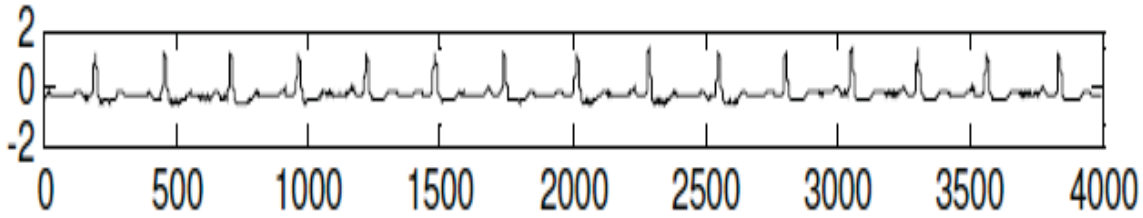

FIGURE 19. WB artifact removed in ECG signal [16].

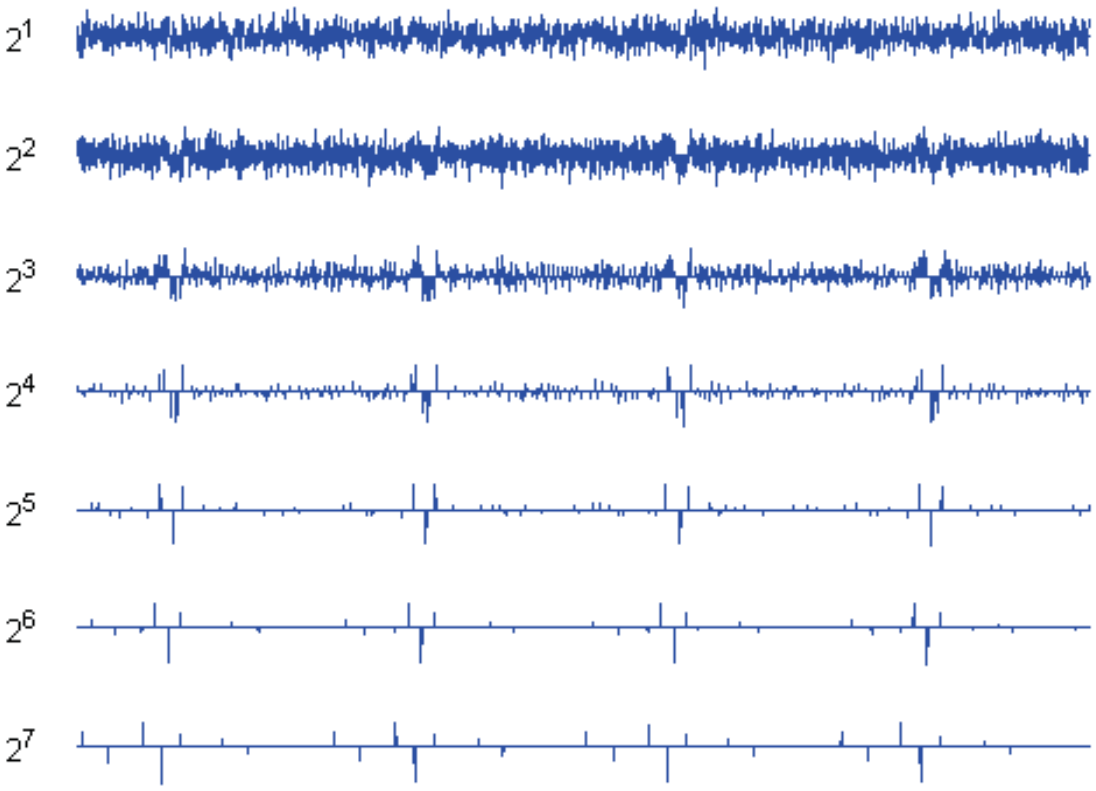

FIGURE 20. Modulus maxima of noisy ECG signal [20].

White Gaussian Noise Elimination Methods

The presence of the WGN modifies the information in the ECG signal; thus, it is necessary to eliminate the WGN from the ECG signal for the detection of its features. A few methods previously developed for removing the WGN are discussed in detail as follows.

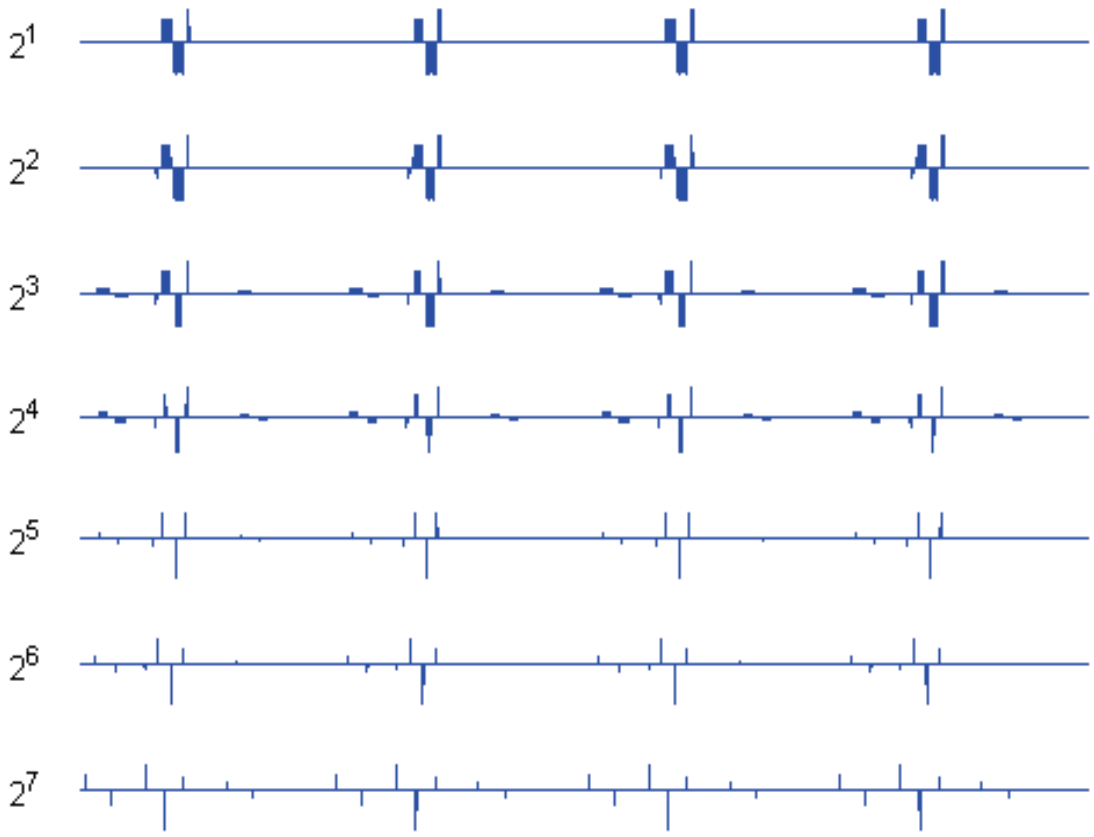

FIGURE 21. Modulus maxima of noisy ECG signal after thresholding [20].

Modulus Maxima Approach

According to M. Ayat et al. [20], the ECG signal was decomposed into various levels from 1 to 7 using the Daubechies$_6$ wavelet. Chapter 3 describes the hard and the soft threshold techniques in detail. The discrete modulus maxima of the wavelet transform reduced the white noise from the ECG signal by applying this approach [20]. The noise modulus maxima were only visible on the lower levels of the decomposition process [20]. The amplitudes of the noise

modulus maxima were smaller than the ECG modulus maxima. The soft threshold technique of the wavelet removed the white noise from the ECG signal when it was reconstructed [20]. Figure 20 illustrates the modulus maxima of the noisy ECG signal, and Figure 21 depicts the modulus maxima of the noisy ECG signal after the thresholding operation.

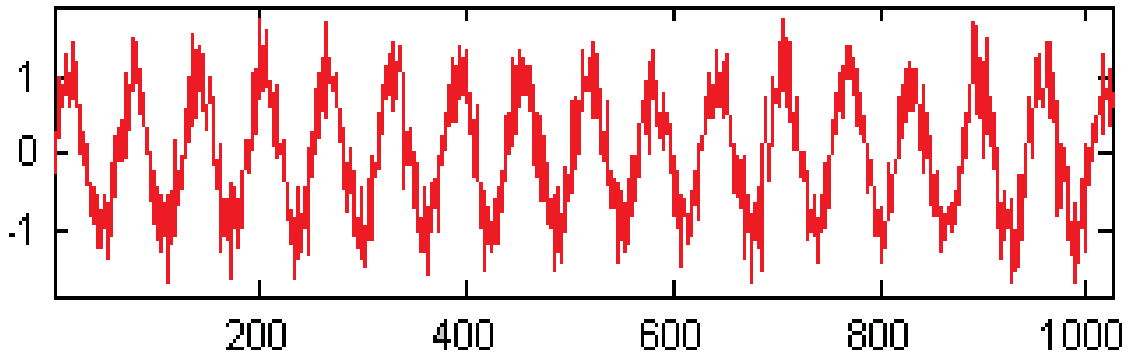

FIGURE 22. ECG signal with noise [21].

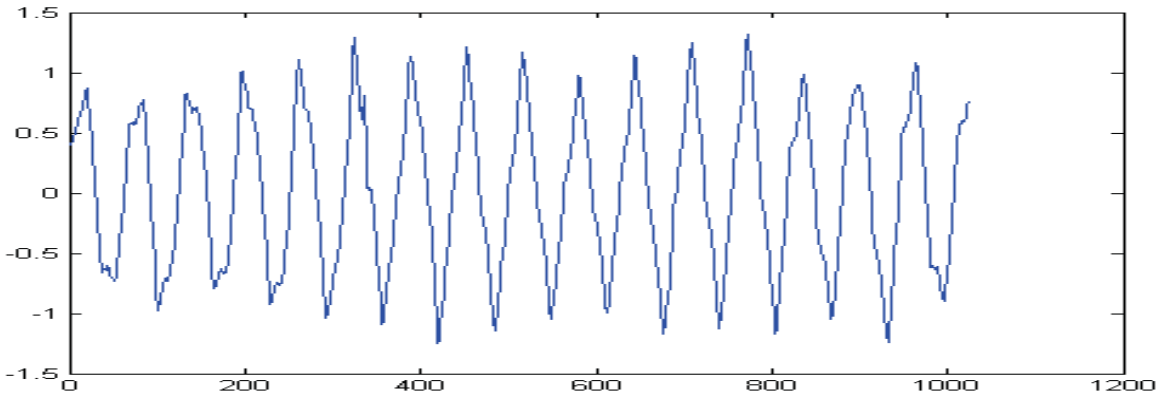

FIGURE 23. ECG signal denoised by universal threshold rule in DWT [21].

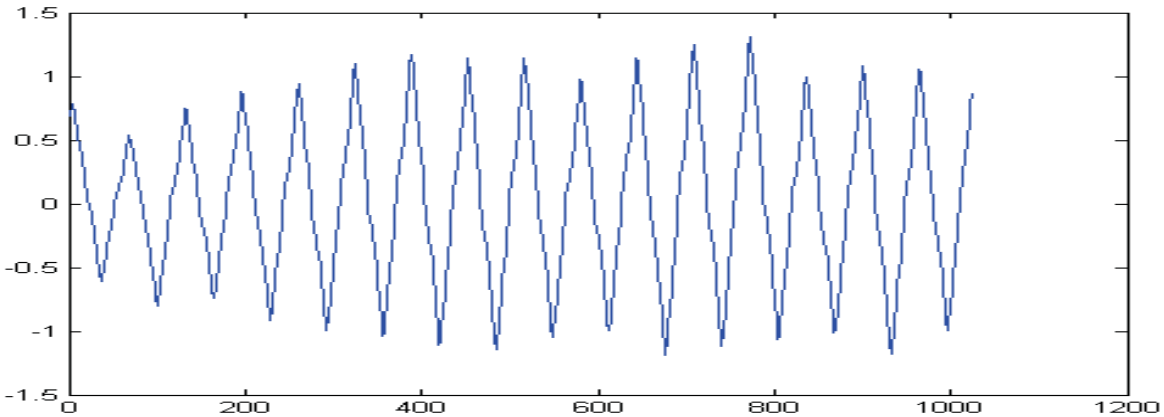

FIGURE 24. ECG signal denoised by interval dependent threshold selection in DWT [21].

Adaptive Filters Technique

The Fast Fourier Transform (FFT) technique, an LMS algorithm, a normalized LMS algorithm, a comb filter, the Gaussian Reproducing Kernel Hilbert Space technique, a kernel least mean square algorithm, and a dynamic kernel least mean square algorithm are the techniques to eliminate the noise from the ECG signal using the adaptive filters.

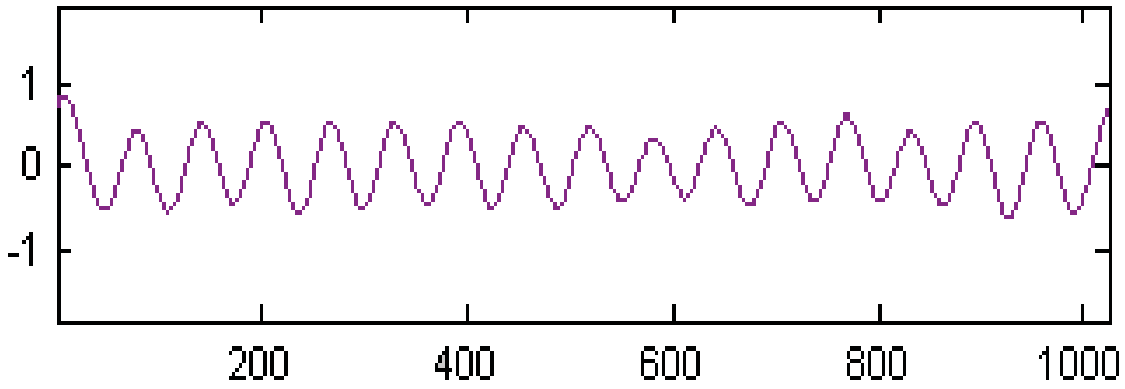

FIGURE 25. ECG signal denoised by universal threshold rule in SWT [21].

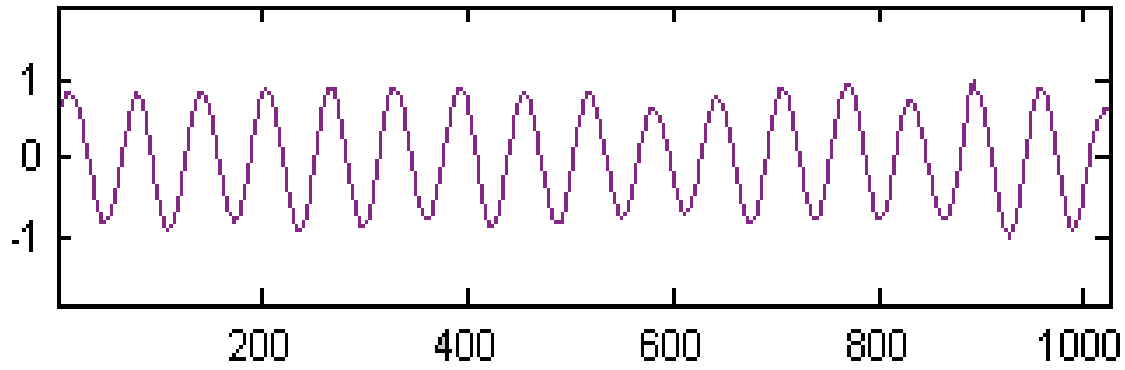

FIGURE 26. ECG signal denoised by interval dependent threshold selection in SWT [21].

Stationary and Discrete Wavelet Transforms Approach

According to R. Kumar and P. Patel [21], the Daubechies$_6$ wavelet was used to remove the noise from the ECG signal by using the DWT and Stationary Wavelet Transform (SWT) approaches. A universal threshold rule and an interval dependent threshold selection were the two methods used to implement this algorithm.

Figures 22 – 26 demonstrate the plots of the SWT and DWT with both these threshold methods [21]. Figure 22 displays the noisy ECG signal. Figures 23 and 24, respectively, depict the obtained noise-free ECG signal by performing the DWT on the signal. Figures 25 and 26, respectively, display the obtained noise-free ECG signal by performing the SWT on the signal.

Threshold Technique

According to M. Alfaouri and K. Daqrouq [22], the ECG signal was decomposed into five levels by applying the DWT on the Daubechies_8 wavelet. The soft threshold technique was applied to each level of the decomposition process. The reconstruction of the ECG signal removed the noise.

On the other hand, S. Chen, H. Chen, and H. Chan [23] removed the noise from the ECG signal by applying three levels of the DWT. Each level of the decomposition process applied the hard threshold technique of the wavelet. The reconstruction of the ECG signal eliminated the noise from it [22] [23]. Figure 27 displays the noisy ECG signal, and Figure 28 displays a clean ECG signal after the application of the hard threshold technique.

Peak Detection Methods

It is crucial to detect the exact peaks of the various waves present in the ECG signal to extract the information from it. An accurate peak detection results in a precise estimation of the intervals namely, the R-R intervals, the P-P intervals, and the P-R intervals. The precise calculations of these mentioned intervals will result in either a normal or an abnormal ECG signal depending upon the invariability or variability of the intervals throughout the duration of the ECG signal. There are various methods to detect the peaks of the R-waves and the P-waves in the ECG signal. Four of these methods are summarized as follows.

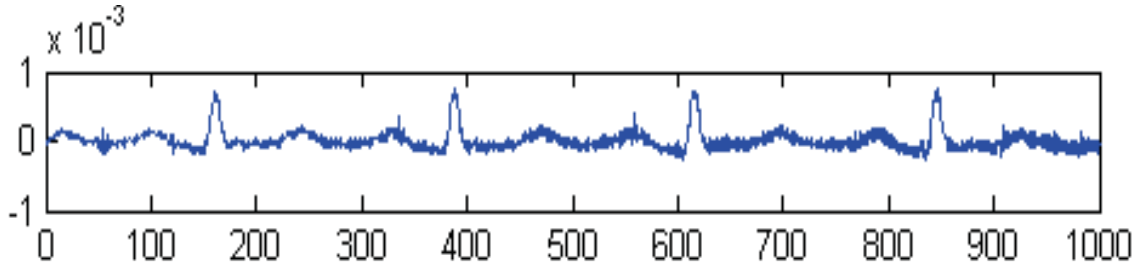

FIGURE 27. Noisy ECG signal [23].

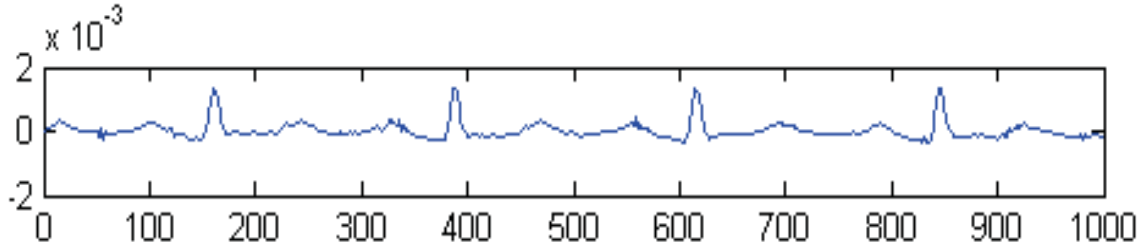

FIGURE 28. Noise-free ECG signal [23].

So and Chan Method

According to K. Tan, K. Chan, and K. Choi [24], the So and Chan QRS detection method was executed on the ambulatory ECG screen. The computational prerequisite was kept at a suitable level without trading off its accuracy. Let $X(n)$ denote the amplitude of the ECG signal at the discrete time n. Equation (24) defines the slope of the ECG signal [24].

$$slope(n) = -2X(n-2) - X(n-1) + X(n+1) + 2X(n+2) \quad (24)$$

Equation (25) describes the threshold level of the slope for the ECG signal [24].

$$slope\_thresh = \frac{thresh\_param}{16} \times maxi \quad (25)$$

$$maxi = \frac{first\_max - maxi}{filter\_param} + maxi \quad (26)$$

where *slope_thresh* = slope threshold,

thresh_param = threshold parameter,

first_max = height of R point – height of QRS onset,

and *filter_param* = filter parameter.

Equations (25) and (26) were also studied by D. Nithya and S. Ravindrakumar [25]. When two successive ECG signals fulfilled the condition: $slope(n) > slope\_thresh$, the onset of the QRS complex was identified [24]. The parameter *thresh_param* was set to specific values namely, 2, 4, 8, or 16. After the identification of the onset of the QRS complex, the most extreme point (*maxi*) was observed. This observed point was the R point [24].

This method was a one-pole filter, which smoothed the consequence of any sudden change in the signal [24]. The parameter filter_param was set to the values 2, 4, 8, or 16 [24]. The introductory *maxi* was the maximum slope of the first 250 data points in the ECG signal. This algorithm was written in *C* language underneath the platform of the Pentium PC, and the sensitivity achieved with this algorithm was 95.60% [24].

Pan and Tompkins Method

The Pan and Tompkins QRS detection method recognized the QRS complexes based on the computerized examinations of the slope, amplitude, and width of the ECG signal [24]. This method executed an exceptional digital band-pass filter [24]. The filter reduced the false detection brought by the different types of interferences present in the ECG signal [24] [25]. This filtering allowed the utilization of the low threshold values, and in this manner, it increased the recognition sensitivity [24]. This method modified the threshold values and parameters of the signal to adjust to the changes in the QRS morphology and heart rate. It consisted of the following stages namely, a band-pass filtering block, a differentiation block, a square block, a moving window integration, a fiducial mark determination, the adjustments of the threshold values block, an average R-R interval and the rate limits adjustment block, as well as the T-wave identification block [24] [25]. Equation (27) describes the slope threshold, *pt_thresh*, for the P-wave identification [24].

$$pt\_thresh = pt\_param \times slope\_thresh \quad (27)$$

where *pt_param* = a set between 0.1 to 0.3.

This method successfully detected the onset, peak, and offset of the P-waves. The location of the P-wave offset was at the beginning of the QRS onset [24]. The search distance was set in such a way that the data of the P-R interval was less than 0.2 second [24]. When the distance between the two sequential data points in the signal was $\boldsymbol{slope(n) > pt\_thresh}$, the first data point was recognized as the P-wave offset [24].

The P-wave onset was located by the forward search from a sufficient distant data point before the QRS onset and the discovered P-wave offset [24]. When the distance between the two sequential data points was $\boldsymbol{slope(n) > pt\_thresh}$, the first data point was characterized as the P-wave onset [24]. The peak was effectively recognized between the onset and offset of the P-wave by inspecting the amplitude of the data in the ECG signal [24]. This algorithm was written in *C* language underneath the platform of the Pentium PC, and the sensitivity achieved with this algorithm was 88.96% [24].

Extracting Coefficients at Various Levels of Wavelet Transform Technique

According to S. Mahmoodabadi, A. Ahmadian, and M. Abolhasani [26], the process of extracting and retaining the detail and approximation coefficients at various levels of the DWT and the continuous wavelet transform detected the peaks of the waves present in the signal. Y. Zhong et al. [27]; M. Bahoura, M. Hassani, and M. Hubin [28]; C. Li, C. Zheng, and C. Tai [29]; and I. Nouira et al. [30] also proposed this technique to detect the peaks of the waves present in the signal.

Filter Approach

According to M. Akay [31], the application of a direct FFT on the sampled ECG signal

data followed by the windowed filters removed the low-frequency components and retained the high-frequency components at various levels to detect the peaks of the R-waves in the signal.

Bionic Wavelet Transform Method

According to U. Zaka et al. [32], the ECG signal was decomposed up to level 4 by applying the bionic wavelet transform. The next step was to apply the hard threshold technique to the level 4 coefficients for the detection of the peaks of the R-waves present in the ECG signal [32].

CHAPTER 3

WAVELET THEORY

History

Wavelets came into existence during the last fifteen years. They are associated with numerous different fields including physics, engineering, pure and applied mathematics, as well as computer science. Wavelets are named after the scientists who invented them and are grouped into families, or basis, depending upon its properties, and there are several wavelet transforms.

A. Harr invented the first wavelets in 1910 and called them *Harr wavelets*. As these wavelets operated only on the square functions, they were not continuous and differentiable, so they cannot be used to analyze the continuous signals.

In 1981, J. Morlet discovered *wavelets of a constant shap*e by finding a replacement for the short time Fourier transform [33]. The signals that he examined consisted of diverse characteristics in both the time and frequency domains. His signals characteristically had high-frequency segments for a brief duration compared to its low-frequency segments. He created the transform functions by using windowed cosine waves to include both these segments in a single transform. These waves were compressed in the time domain to achieve higher frequency functions or lower frequency functions. He also shifted the functions in the time domain to examine these segments at various times [33]. The transform functions rested on two parameters namely, their position in the time domain and their amount of compression, or their scale. There was one vital modification with the transform functions as compared to the standard Fourier transform that is, in his method, the low-frequency functions were broad compared to the high-frequency functions.

After Morlet's wavelets existed, another scientist named A. Grossman created a precise

reverse formulation of his wavelets. In 1984, J. Morlet and A. Grossman developed wavelets by combining their individual research.

In 1985, Y. Meyer developed *orthogonal wavelet basis* with good time-frequency localization properties. He generalized the basis to *N* dimensions by working with P. G. Lemarie´ [33]. A couple of months later, P. Lemarie´ worked with G. Battle to develop the wavelet basis containing spline functions with improved decay compared to Meyer's wavelets at the expense of a shortfall in consistency. Thus, the wavelet decompositions consisted of the narrow functions for the fine scale features and broader functions for the unrefined features [33].

In the meantime, S. Mallat formulated an analogous layered arrangement for the wavelet basis in which all the terms equivalent to a unique scale in the wavelet decomposition of a function yielded the differentiation amongst the two consecutive approximations [33]. In 1988, S. Mallat and Y. Meyer presented the idea of the multiresolution analysis. This analysis described all the marvels in the wavelet basis, and it became simple to compose supplementary orthonormal wavelet basis. The significance of the multiresolution analysis was that it led to a straightforward and recursive filtering algorithm to calculate the wavelet decomposition of a function from its best scale approximation. A suitable FIR filter was developed to inspect its resemblance with an orthonormal wavelet basis. This idea of developing a FIR filter was the root to create the orthonormal wavelet bases for a compactly supported wavelet [33].

In 1988, I. Daubechies discovered orthogonal wavelets with compact support. This research uses the orthogonal wavelets developed by her. She described the wavelets as a tree whose roots stretch deeply in many directions [33]. The trunk of the tree resembled the development of the wavelet tools in the second half of the 1980's [33]. These wavelet tools came into existence because of the contributions from the scientists in a wide range of fields. The top

of the tree with its numerous branches resembled the various directions and applications in which wavelets turned into a standard part of the scientific toolbox. [33].

She grouped the frequencies of the wavelets in bands with a width corresponding to the mean frequency in that band [33]. This concept was called a steady relative bandwidth, or a constant-Q filtering [33]. One approach to get a portion of the frequency band was to work iteratively. The first step was to divide the full range of frequencies of a bandlimited function into two channels namely, one high-pass and one low-pass [33]. The second step was to partition the lower frequency half again into two halves until the researcher needed to stop according to his/her application. Since the distinctive parts that outcome from this iterative process had diverse bandwidths, they resembled various Nyquist sampling rates. This research uses this iterative process developed by her. This iterative process was a simple approach to acquire the accurately sampled versions of a considerable number of segments and hold just the part of the output samples at each filtering step [33]. This crucial sampling generated aliasing, which prompted unsatisfactory artifacts at the reconstruction stage because the filters were constructed carelessly [33].

Later in 1989, S. Mallat modified the work of I. Daubechies by inventing the fast wavelet transforms.

Wavelet Analysis

The wavelet analysis is described by the scaling function and the wavelet function. According to I. Daubechies [33], the scaling function $\varphi(t)$ is called a father wavelet, and a wavelet function $\psi(t)$ is called a mother wavelet. The coefficients of the scaling function obtained after analysis are called the approximation coefficients, and those of the wavelet function are called the detail coefficients. Equation (28) represents a basic scaling function [9].

$$\varphi_k(t) = \varphi(t-k) \qquad ,k \in Z, \varphi \in L^2 \tag{28}$$

where t = time,

and k = no of translations.

A. Boggess, F. J. Narcowich [34] and D. F. Walnut [35] also described Equation (28). An accurate interpretation of the fundamental scaling function characterizes the arrangement of the derived scaling function in a signal. The wavelet and the scaling functions are the square integrable functions. Equation (29) defines the subspace L^2 (R) for the square integrable functions [9] [35].

$$v_0 = \overline{\underset{k}{Span\{\varphi_k(t)\}}} \tag{29}$$

where v_0 = the subspace,

k = integer from minus infinity to plus infinity,

and t = time.

The dashed solid line in Equation (29) is called an over-bar, and it denotes a closure for a subspace. It is an interval that not only contains all the signals linked by a direct combination of the basic function but also additionally contains the signals, which are at the ending instants of the infinite expansions of the subspace [9] [35]. A one-dimensional scaling function in this subspace is characterized by Equation (30) [9] [34].

$$f(t) = \sum_k a_k \varphi_k(t), \qquad for\ any\ f(t) \in v_0 \tag{30}$$

where k = number of translations,

φ = scaling function,

t = time,

and a = function in the subspace.

The scaling and translation of the basic scaling function described in Equation (28) generates a two-dimensional scaling function, which is described by Equation (31) [9] [34].

$$\varphi_{j,k}(t) = 2^{j/2}\varphi\left(2^j t - k\right) \tag{31}$$

where t = time,

k = number of translations,

and j = scale factor.

A wavelet function usually refers to either an orthogonal or a non-orthogonal wavelet [4]. It navigates through the dissimilarities between the spaces of the different sizes of the scaling function. A weighted and a time-shifted scaling function $\varphi(2t)$ represents a wavelet function. The wavelet function is depicted by Equation (32) [19] [33] [34].

$$\boldsymbol{\psi(t) = \sum_n h_1(n)\sqrt{2}\,\varphi(2t - n),} \quad \boldsymbol{n \in Z} \tag{32}$$

The wavelet transform involves both the scaling and the wavelet functions. The wavelet transform is used to examine the time series data that consist of the nonstationary power at various frequencies [4]. For a sequence $x(n)$, the wavelet transform is given by Equation (33) [20] [26].

$$W(j,b) = \sum_n \frac{1}{2^j} x(n)\psi^*\left(\frac{n-b}{2^j}\right) \tag{33}$$

$$b = K \times 2^j \tag{34}$$

where ψ = wavelet function,

j = scale,

b = time delay,

and K = integer.

The wavelet function is expanded or contracted by the integer scale factor j and delayed

in time by a parameter b. For an N-point arrangement, the scale component j assumes the quantities $j = 0, 1, \ldots, log2(N)$ to produce a multiresolution decomposition of the input signal [26].

Factors for Opting Wavelet Functions

There are various factors, which need to be considered before choosing the wavelet functions, and they are described in detail as follows.

Orthogonal or Non-Orthogonal Wavelet

The property of an orthogonal wavelet is that the number of convolutions at every scale are proportional to the width of the wavelet basis at that scale. This property delivers a range of wavelets that consist of separate sections of the wavelet power and is important for the signal processing as it gives the most reduced representation of the signal [10].

On the other hand, a non-orthogonal wavelet evaluation is unnecessary at large scales. In this evaluation, the range of the wavelets at adjacent times is substantially correlated [10]. The non-orthogonal transform predicts a smooth and uninterrupted alteration in the amplitude of the wavelet for a time series examination.

Complex or Real Function

A complex wavelet function will return the data for both the amplitude and phase of the signal. A better modification of the function encapsulates its oscillatory behavior [10].

A real wavelet function returns only a component of the signal and can be used to segregate the peaks or the discontinuities present in the signal [10].

Wavelet Width

The e-folding time of the amplitude of the wavelet characterizes the width of the wavelet function [10]. The resolution of the wavelet function is defined by its width in an actual space

and the Fourier space [10]. A contracted (in time) function has a clear time resolution, but an inadequate frequency resolution, while an expanded function has an inadequate time resolution but clear frequency resolution [10].

Wavelet Shape

The wavelet function mirrors the type of the characteristics present in the time series of a signal [10]. A Harr function can be selected for a time series with pointed jumps or steps, while an even function, for example a damped cosine, can be selected for a fluctuating time series [10]. The wavelet function produces the same subjective results as other functions when the wavelet power spectra are considered [10].

Discrete Wavelet Transform

The DWT is characterized by the decomposition and reconstruction of the input signal, which is described in Figure 29. Figure 29 demonstrates an *n* level tree diagram for the decomposition of the samples in the signal [9] [15]. F. N. Ucar, M. Korurek, and E. Yazgan [36] also proposed this *n* level tree diagram.

In Figure 29, let X[n] be the original signal, which needs to be decomposed. $LD_1[n]$, $LD_2[n]$, and $LD_3[n]$ represent the decomposition low-pass filter coefficients at levels 1, 2, and 3, respectively. $HD_1[n]$, $HD_2[n]$, and $HD_3[n]$ represent the decomposition high-pass filter coefficients at level 1, 2, and 3, respectively. The signal X[n] convolves with $LD_1[n]$ and $HD_1[n]$, and then both these signals are downsampled by a factor of two. At this stage, the total number of coefficients of the original signal X[n] are retained. The output of the high-pass filter after downsampling by a factor of two is called the level 1 DWT coefficients (detail coefficients at level 1), and the output of the low-pass filter is called the approximation coefficients at level 1 [9].

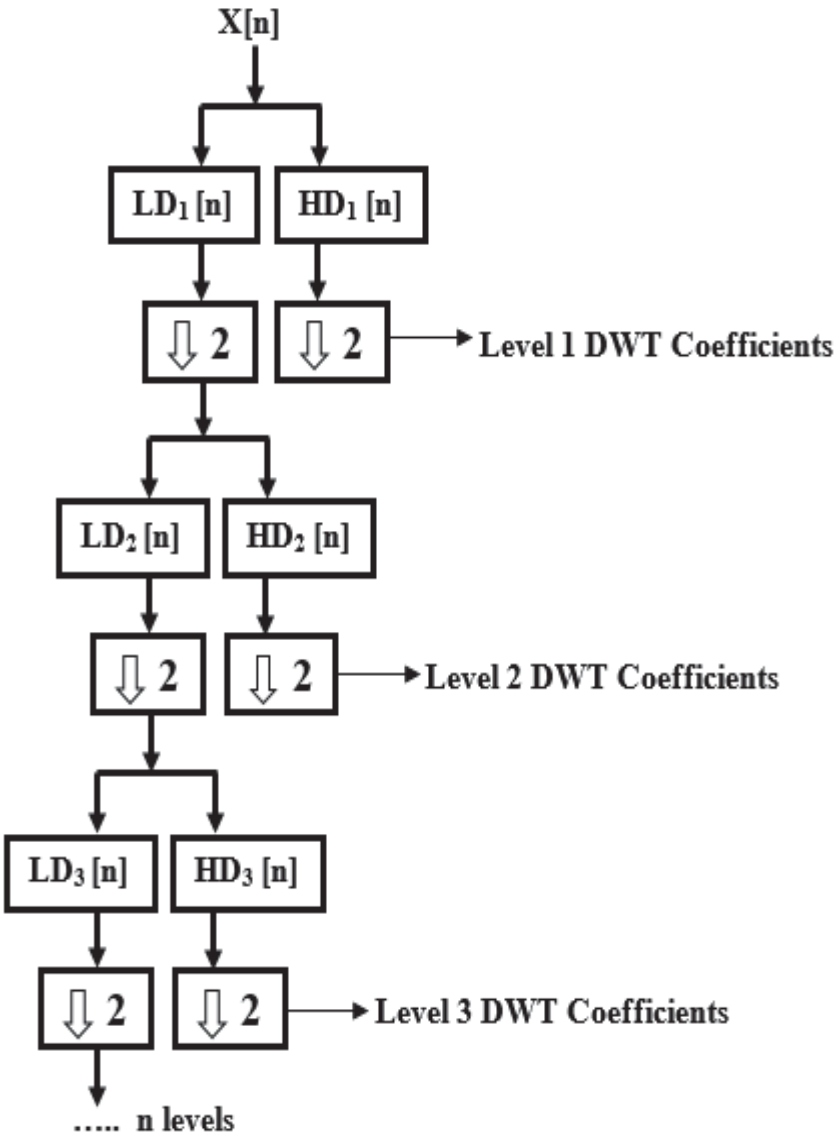

FIGURE 29. Decomposition tree [9].

The level 1 approximation coefficients convolve with $LD_2[n]$ and $HD_2[n]$. The outputs of $LD_2[n]$ and $HD_2[n]$ then downsample by a factor of two to obtain the level 2 approximation and detail coefficients. The length of the signal at level 2 is n/2 [9]. This decomposition procedure repeats until the desired level is achieved. The level 1 decomposition and reconstruction process are described in detail as follows.

Figure 30 illustrates the level 1 decomposition of the input samples. $F[n]$ and $G[n]$ are the

outputs of the low-pass filter and the high-pass filter, respectively. cA_1 and cD_1 are the approximation and detail coefficients at level 1, respectively. The mathematical equations of $F[n]$ and $G[n]$ are given by Equations (35) and (36) [9].

$$F[n] = (x * LD_1)[n] \sum_{k=-\infty}^{k=\infty} x[k]\, LD_1\,[n-k] \tag{35}$$

$$G[n] = (x * HD_1)[n] \sum_{k=-\infty}^{k=\infty} x[k]\, HD_1\,[n-k] \tag{36}$$

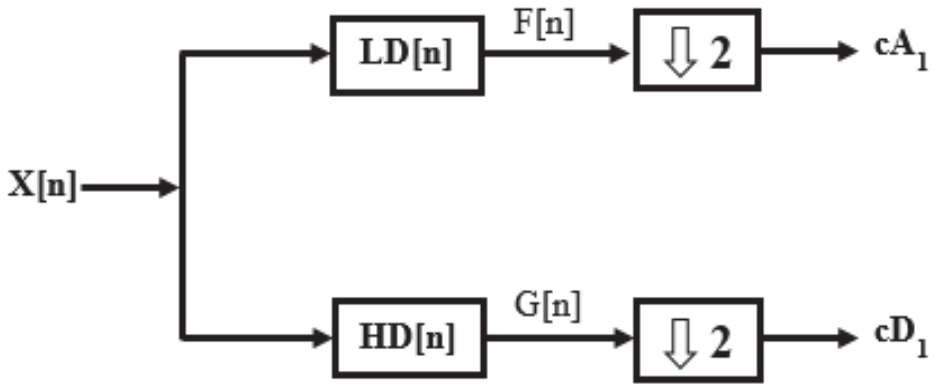

FIGURE 30. One level decomposition structure.

Equations (37) and (38), respectively, define the mathematical equations to obtain cA_1 and cD_1 [9].

$$cA_1[n] = (x * LD_1)[n] \sum_{k=-\infty}^{k=\infty} x[k]\, F\,[2n-k] \tag{37}$$

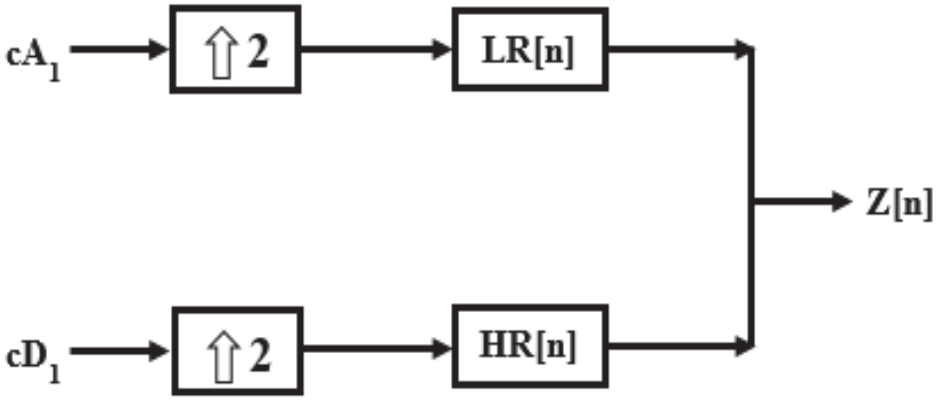

FIGURE 31. One level reconstruction structure.

$$cD_1[n] = (x * HD_1)[n] \sum_{k=-\infty}^{k=\infty} x[k]\, G\,[2n - k] \quad (38)$$

The reconstruction process is the reverse of the decomposition process. The coefficients cA_1 and cD_1 are first upsampled by a factor of two and then are convolved with the reconstruction level 1 low-pass filter coefficients (LR[n]) and high-pass filter coefficients (HR[n]) to obtain the reconstructed signal Z[n] [9]. Figure 31 illustrates this process.

Daubechies Wavelet

The Daubechies wavelets invented by I. Daubechies are a group of orthogonal wavelets. These wavelets use the DWT, and they are described by the maximal number of vanishing moments for a given support [9]. The Daubechies wavelets contain numerous levels (*N*) ranging from *N = 1,2,3, …, 45*. This *N* specifies the number of moments present in the wavelet.

Denoising

The objective of the denoising procedure is to evaluate the coefficients of a noisy signal of all the sub-groups present in the decomposition tree. The estimation techniques are used to provide a threshold level for reducing the coefficients. These techniques use a threshold strategy, which typically is applied to the coefficients of the detail segments in the decomposition tree. The signal is reproduced by ascending the decomposition tree after the application of the threshold operation.

Eliminating White Gaussian Noise

The WGN is one of the most common noises observed in the high-frequency segment of any signal, in this case, the ECG signal. D. Donoho and I. Johnstone developed a universal threshold rule, which effectively removes the random Gaussian noise from the signal. Equation (39) describes the universal threshold rule [15] [20] [27].

$$\lambda = \sigma\sqrt{2logN} \quad (39)$$

$$\sigma = \frac{MAD}{0.6745} \tag{40}$$

where λ = threshold value,

N = length of the coefficients in the signal,

σ = standard deviation of the noise,

and MAD = median absolute deviation of the thresholds.

The expression described in Equation (40) considers the value of the standard deviation of the noise, and it remains constant for different time intervals [20].

Soft and Hard Threshold Techniques

Once the value of the threshold parameter λ is calculated, the soft and hard threshold techniques are then applied to the signal depending on the application. Assume $c_{j,k}$ represents the coefficients of the wavelet transform at level j. $c'_{j,k}$ and $c''_{j,k}$, respectively, represent the thresholded coefficients of the hard threshold [20] [27] [28] and soft threshold [20] [27] techniques.

$$c'_{j,k} = \begin{cases} c_{j,k} & |c_{j,k}| \geq \lambda \\ 0 & otherwise \end{cases} \tag{41}$$

$$c''_{j,k} = \begin{cases} sign(c_{j,k})\,(|c_{j,k}| - \lambda) & |c_{j,k}| \geq \lambda \\ 0 & otherwise \end{cases} \tag{42}$$

where *sign* (*) is a signum function represented by Equation (43).

$$sign(n) = \begin{cases} 1 & if\ n > 0 \\ -1 & if\ n < 0 \end{cases} \tag{43}$$

Equations (41) and (42), respectively, represent the hard and soft threshold techniques to remove the WGN from the signal. M. S. Chaudhary, R. K. Kapoor, and A. K. Sharma [37] also illustrated this technique.

In the hard threshold technique, if the absolute values of all the coefficients at level j are

greater than the threshold value, then only they are retained, while the other coefficients are set to zero. In the soft threshold technique, the values of coefficients are shrinked except those lower than the threshold, which are set to zero [20].

CHAPTER 4

CHARACTERIZATION OF ECG SIGNALS AS NORMAL OR ABNORMAL

Synthetic ECG Generation

The ECG signal is generated synthetically in MATLAB by considering the morphology of the ECG signal and the physiological parameters of its waves described in Chapter 1. The P and T waves of the ECG signal are round in nature, so they are constructed using the sine waves. The QRS complex has peaked waves, so the triangular waves construct the complex. The duration of each wave, as well as the time interval between the waves, are precisely taken into account. Table 3 displays the amplitudes and duration of the waves for constructing the synthetic ECG signal. The conversion used is 1 mm = 0.1 mV.

A cardiac cycle of an ideal ECG signal is 0.5 seconds long. The ECG signal is constructed synthetically in MATLAB and has less computational time. It also resembles the statistics described in Chapter 1. Chapter 5 describes the results for generating the synthetic ECG signal. The length of the QRS complex in the generated synthetic ECG signal is much shorter than its ideal case, so the generated signal is more rapid compared to the ideal ECG signal.

The ECG signals are processed using the db_4 wavelet. The db_4 wavelet is chosen because it strongly resembles the morphology of the ECG signal, so it is the best wavelet to detect the peaks of the various waves present in the ECG signal. The filter coefficients of the decomposition and reconstruction process are derived before analyzing the ECG signals as normal or abnormal signals.

Derivation of Filter Coefficients

This section describes the analysis for generating the low-pass and high-pass filter coefficients for the decomposition and the reconstruction process of the db_4 wavelet. Let

$P_N(z) = \frac{1}{2}\sum_{k=0}^{2N-1} p_k z^k$ be a polynomial that satisfies Equations (45-47) [9] [34].

$$P(0) = 1 \tag{45}$$

$$|P(\xi)|^2 + |P(\xi + \pi)|^2 = 1 \tag{46}$$

$$|P(\xi)| > 0 \; for \; \frac{-\pi}{2} \leq \xi \leq \frac{\pi}{2} \tag{47}$$

For a given polynomial $P(z)$ [34]:

$$\text{let } p(\xi) = P\left(e^{-i\xi}\right) \tag{48}$$

Equation (49) describes the trigonometric identity.

$$cos^2\left(\frac{\xi}{2}\right) + sin^2\left(\frac{\xi}{2}\right) = 1, where \; \frac{-\pi}{2} \leq \xi \leq \frac{\pi}{2} \tag{49}$$

Both sides of Equation (49) are raised to the power *n*. The value of *n* is given by Equation (50) [34].

$$n = 2N - 1 \tag{50}$$

where *N* = the number of vanishing moments.

This research uses the db_4 wavelet; hence, the value of *N* is 4. The parameter *n* can take only the odd values. Thus, the value of *n* is 7. I. Daubechies illustrated that for each value of *N,* there were *2N* nonzero, real scaling coefficients $p_0, p_1, \ldots, p_{2N-1}$, resulting in a scaling function and a wavelet function that satisfied the interval $0 \leq t \leq 2N - 1$ [34]. They are selected according to the degree *2N – 1*. The polynomial $P_N(z) = \frac{1}{2}\sum_{k=0}^{2N-1} p_k z^k$ thus has the factorization as explained in Equation (51) [34].

$$P_N(z) = (z + 1)^N P'_N(z) \tag{51}$$

where the degree of P'_N is *N - 1*, and $P'_N(-1) \neq 0$.

Equation (51) ensures that the associated wavelet precisely has *N* vanishing moments. Thus, using Equation (49) and elevating it to the 7^{th} power produces Equation (52).

$$\left(cos^2\left(\frac{\xi}{2}\right)+sin^2\left(\frac{\xi}{2}\right)\right)^7=(1)^7=1 \quad (52)$$

Rearranging the power of Equation (52) results in Equation (53).

$$\left(cos^2\left(\frac{\xi}{2}\right)+sin^2\left(\frac{\xi}{2}\right)\right)^2\left(cos^2\left(\frac{\xi}{2}\right)+sin^2\left(\frac{\xi}{2}\right)\right)^2\left(cos^2\left(\frac{\xi}{2}\right)+sin^2\left(\frac{\xi}{2}\right)\right)^3=1 \quad (53)$$

Expansion of Equation (53) yields Equation (54).

$$1=\ cos^{14}\left(\frac{\xi}{2}\right)+7cos^{12}\left(\frac{\xi}{2}\right)sin^2\left(\frac{\xi}{2}\right)+21cos^{10}\left(\frac{\xi}{2}\right)sin^4\left(\frac{\xi}{2}\right)+35cos^8\left(\frac{\xi}{2}\right)sin^6\left(\frac{\xi}{2}\right)+$$

$$35cos^6\left(\frac{\xi}{2}\right)sin^8\left(\frac{\xi}{2}\right)+21cos^4\left(\frac{\xi}{2}\right)sin^{10}\left(\frac{\xi}{2}\right)+7cos^2\left(\frac{\xi}{2}\right)sin^{12}\left(\frac{\xi}{2}\right)+sin^{14}\left(\frac{\xi}{2}\right) \quad (54)$$

Now, applying the trigonometric identities $cos(x)=sin\left(x+\frac{\pi}{2}\right)$ and $sin(x)=-cos\left(x+\frac{\pi}{2}\right)$ to the last four terms on the right-hand side of Equation (54) determines Equation (55).

$$1=\ cos^{14}\left(\frac{\xi}{2}\right)+7cos^{12}\left(\frac{\xi}{2}\right)sin^2\left(\frac{\xi}{2}\right)+21cos^{10}\left(\frac{\xi}{2}\right)sin^4\left(\frac{\xi}{2}\right)+35cos^8\left(\frac{\xi}{2}\right)sin^6\left(\frac{\xi}{2}\right)+$$

$$35sin^6\left(\frac{\xi+\pi}{2}\right)cos^8\left(\frac{\xi+\pi}{2}\right)+21sin^4\left(\frac{\xi+\pi}{2}\right)cos^{10}\left(\frac{\xi+\pi}{2}\right)+7sin^2\left(\frac{\xi+\pi}{2}\right)cos^{12}\left(\frac{\xi+\pi}{2}\right)+$$

$$cos^{14}\left(\frac{\xi+\pi}{2}\right) \quad (55)$$

Taking the first four terms of Equation (55), Equation (56) is produced.

$$|p(\xi)|^2=cos^{14}\left(\frac{\xi}{2}\right)+7cos^{12}\left(\frac{\xi}{2}\right)sin^2\left(\frac{\xi}{2}\right)+21cos^{10}\left(\frac{\xi}{2}\right)sin^4\left(\frac{\xi}{2}\right)+35cos^8\left(\frac{\xi}{2}\right)sin^6\left(\frac{\xi}{2}\right) \quad (56)$$

Thus, Equation (55) can be written in the form of $1=|P(\xi)|^2+|P(\xi+\pi)|^2$, and it satisfies Equation (46). Equation (47) is also satisfied since $cos\left(\frac{\xi}{2}\right)\geq\frac{1}{\sqrt{2}}$ for $|\xi|\leq\frac{\pi}{2}$. Also note that, $|p(0)|=1$ as per Equation (45) [34]. The next step is to obtain the square root of Equation (56) and use the trigonometric identities $cos\left(\frac{\xi}{2}\right)=\frac{e^{i\frac{\xi}{2}}+e^{-i\frac{\xi}{2}}}{2}$ and $sin\left(\frac{\xi}{2}\right)=\frac{e^{i\frac{\xi}{2}}-e^{-i\frac{\xi}{2}}}{2}$ to obtain the

coefficients of the $P_N(z)$ polynomial. The coefficients of the $P_N(z)$ polynomial are listed in Equation (57).

$$p[n] = [-0.0150, 0.0465, 0.0435, -0.2644, -0.0396, 0.8922, 1.0109, 0.3258] \quad (57)$$

According to M. Vetterli and C. Herley [38], the decomposition low-pass filter coefficients $LD[n]$ are obtained by using Equation (58).

$$LD[n] = \frac{p[n]}{\sqrt{2}} \quad (58)$$

Therefore, using Equation (57) in Equation (58) yields Equation (59).

$$LD[n] = [-0.0106, 0.0329, 0.0308, -0.1870, -0.0280, 0.6309, 0.7148, 0.2304] \quad (59)$$

The reconstruction low-pass filter coefficients are obtained by reversing the coefficients of $LD[n]$. An example of the reversal is described in Equation (60) [38].

$$LR[n] = [LD(L-1), LD(L-2), \dots, LD(1), LD(0)] \quad (60)$$

where $L - 1 = n$.

Therefore, Equations (59) and (60) result in Equation (61).

$$LR[n] = [0.2304, 0.7148, 0.6309, -0.0280, -0.1870, 0.0308, 0.0329, -0.0106] \quad (61)$$

The decomposition high-pass filter coefficients $HD[n]$ are obtained by Equation (62) [38].

$$HD[n] = (-1)^n LD(L-1-n) \quad (62)$$

Therefore, Equation (63) is obtained using Equations (60), (61), and (62).

$$HD[n] = [-0.2304, 0.7148, -0.6309, -0.0280, 0.1870, 0.0308, -0.0329, -0.0106] \quad (63)$$

The reconstruction high-pass filter coefficients $HR[n]$ are obtained by Equation (64) [38].

$$HR[n] = [HD(L-1), HD(L-2), \dots, HD(1), HD(0)] \quad (64)$$

where $L - 1 = n$.

Thus, Equations (63) and (64) create Equation (65).

$$HR[n] = [-0.0106, -0.0329, 0.0308, 0.1870, -0.0280, -0.6309, 0.7148, -0.2304] \quad (65)$$

The four coefficients namely, $LD[n]$, $LR[n]$, $HD[n]$, and $HR[n]$ are thus obtained.

Algorithm to Detect Normal and Abnormal ECG Signals

After the construction of the synthetic ECG signal in MATLAB, the normality or abnormality in the ECG signal is determined. For this, consider the block diagram shown in Figure 32. The input is the sample based ECG signal obtained from the MIT – BIH database. PI represents the power line interference check, WBR represents the WB removal, and WGN represents the removal of WGN. The first step is to remove the artifacts from the ECG signal so that its minute features are clearly distinguished. The next step is to remove the random WGN and then detect the necessary features from the noise-free ECG signal.

TABLE 3. Parameters for Synthetic ECG Signal Generation

Characteristics of ECG Signal	Amplitude (mV)	Width (sec)
P-wave	0.25	0.10
P-R Interval	-	0.18
Q-wave	0.3	0.02
QRS Complex	-	0.06
R-wave	1.6	0.02
S-T Segment	-	0.04
T-wave	0.3	0.12

50 Hz Interference Verification

The input ECG signal first checks whether the PI artifact is present in the signal or not. This artifact is verified by converting the signal into the frequency domain using the FFT.

Equation (44) describes the FFT for a discrete time signal $x[n]$ [34].

$$X(e^{j\omega}) = \sum_{n=-\infty}^{n=\infty} x[n]e^{-j\omega n} \quad (44)$$

where $X(e^{j\omega})$ = the frequency response of the input ECG signal $x[n]$.

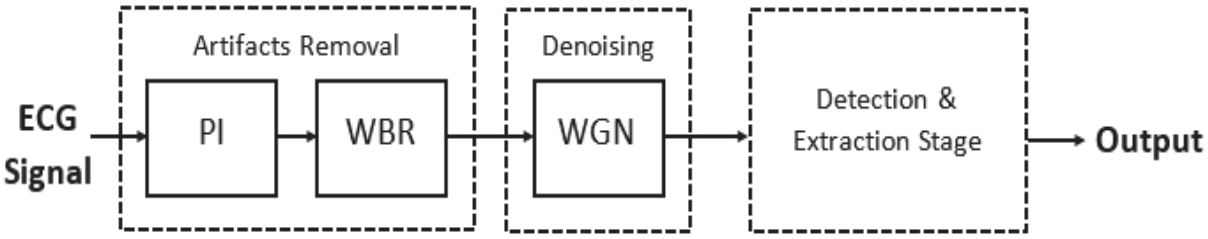

FIGURE 32. Block diagram.

If a significant spike is observed at 50 Hz in the frequency domain of the signal, then there is an effect of the power line interference artifact on the ECG signal. If there is no significant spike at 50 Hz frequency, then there is no effect of the power line interference artifact on the ECG signal.

Elimination of Wandering Baseline

After checking the effect of the PI artifact on the ECG signal, the second step is to eliminate the WB artifact present in the ECG signal.

Figure 33 shows the block diagram to remove the WB artifact from the ECG signal. $LD1$ and $LR1$ are the level 1 coefficients of the low-pass filter for the decomposition and reconstruction process, respectively. $HD1$ and $HR1$ are the level 1 decomposition and reconstruction high-pass filter coefficients, respectively. $x(n)$ is the input ECG signal. $y'(n)$ is the reconstructed signal.

The level 1 decomposition and reconstruction of the signal $x(n)$ is performed using the DWT. After generating these coefficients, the mode of the input signal $x(n)$ is so adjusted that the extreme samples are not discarded. The samples are adjusted to select the smallest length of

the DWT. The outputs of the low-pass and high-pass filters at the reconstruction stage are concatenated to obtain the reconstructed signal $y'(n)$. The WB artifact is removed when the values of the samples in the reconstructed signal are removed from those of the original signal $x(n)$. This signal with the eliminated WB artifact is represented by $y(n)$.

White Gaussian Noise Deduction

The third step is to remove the WGN from the ECG signal. There are still distortions present in the high-frequency segment of the signal after removing the WB artifact from it. These distortions are due the WGN. Equation (66) indicates the existence of the WGN in the ECG signal.

$$y(n) = z(n) + w(n) \tag{66}$$

where $y(n)$ = the signal containing the WGN,

$z(n)$ = the noise-free signal that is a clean signal,

and $w(n)$ = WGN.

After performing the wavelet transform, the resultant signal consists of the original samples of the signal as well as the noise. The chief concept is to eliminate the noise components from the signal using the threshold technique of the wavelets described in Chapter 3.

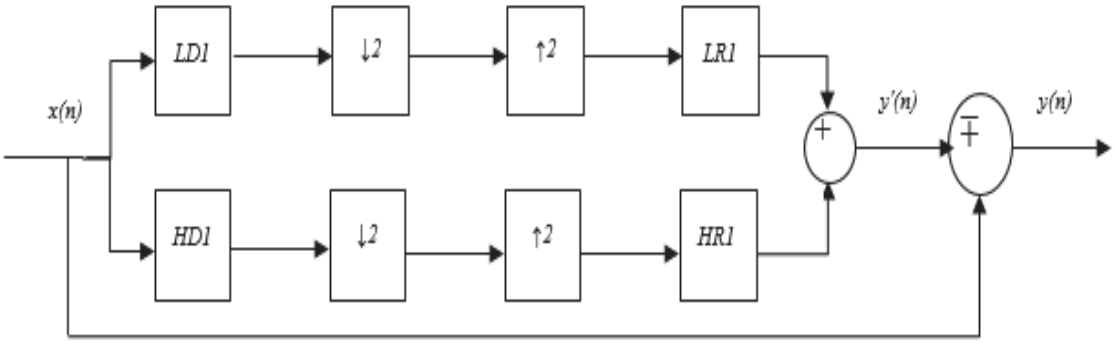

FIGURE 33. Block diagram to remove WB artifact.

Figure 34 demonstrates the block diagram to remove the WGN from the signal $y(n)$. $LD1$, $LD2$, $LD3$, and $LD4$ represent the decomposition low-pass filter coefficients for levels 1, 2, 3, and 4, respectively. $HD1$, $HD2$, $HD3$, and $HD4$ represent the decomposition high-pass filter coefficients for levels 1, 2, 3, and 4, respectively. $LR1$, $LR2$, $LR3$, and $LR4$ represent the reconstruction low-pass filter coefficients for levels 1, 2, 3, and 4, respectively. $HR1$, $HR2$, $HR3$, and $HR4$ represent the reconstruction high-pass filter coefficients for levels 1, 2, 3, and 4, respectively. The ST block represents the soft threshold technique.

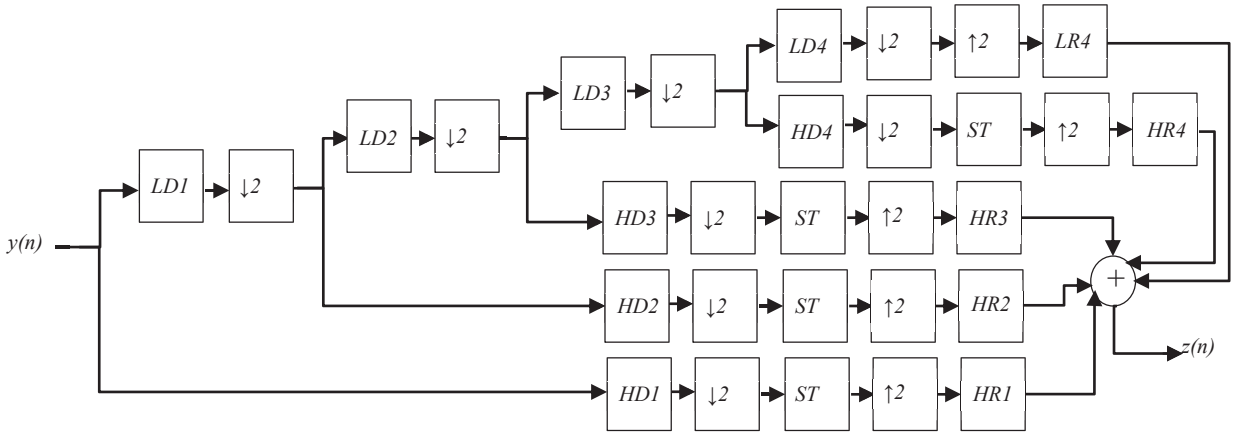

FIGURE 34. Block diagram describing the removal of white Gaussian noise.

The input signal $y(n)$ obtained after removing theWB artifact from the ECG signal $x(n)$ is applied as an input signal to remove the WGN from the ECG signal.

Decomposition into four levels. The first step for removing the WGN is to decompose the signal $y(n)$ for four levels using the db_4 wavelet.

Threshold selection. The second step is to select the threshold value to be applied to the detail coefficients of the decomposed signal at each level using the universal threshold rule described in Equation (39). This threshold value is different for each signal as the value of the standard deviation varies for all the signals.

Application of soft threshold technique. The third step is to apply the soft threshold technique described by Equation (42) to the obtained detail coefficients at all levels. A level dependent estimation of noise observed at each level of decomposition rescales the samples of the ECG signal at this stage.

Signal reconstruction. The fourth step is to reconstruct the ECG signal using the obtained approximation coefficients at level 4 and the revised detail coefficients at all the levels of the decomposition process.

By performing these steps, denoising of the ECG signal is executed using the wavelets to obtain a clean, noise-free ECG signal $z(n)$. This obtained signal $z(n)$ has no effect of the random WGN present in the ECG signal.

Now, the ECG signal is ready for the detection and extraction stage. After removing these artifacts from the signal, its minute details are more clearly visible when compared to the original ECG signal obtained from the database. Thus, the extraction process has become less complex.

Detection and Extraction Stage

The fourth step in the algorithm is to detect and extract the peaks of the P and R waves present in the ECG signals by using the hard threshold technique described in Equation (41). This peak detection is crucial because the estimation of the ECG signals as normal or abnormal depends on the accurate evaluation of its R-R intervals, P-P intervals, and P-R intervals.

As mentioned in Chapter 1, the P-R interval is measured from the onset of the P-wave to the starting of the Q-wave or the R-wave if the Q wave is not present in the QRS complex of the ECG signal. But, for the calculation of the mentioned intervals, the detection of the onset of the waves in the ECG signal is complex as the duration and amplitudes of all the waves in the signal are minute. Thus, to estimate these intervals, instead of the onset of the waves in the ECG signal,

the peaks of the waves are detected. This process of detecting peaks instead of the onset of the waves is similar to estimating the intervals after detecting the onset of the waves, which is described in Chapter 1.

The conclusion of the normality or abnormality of the ECG signal is made with the help of the intervals instead of the amplitudes of the waves because the amplitudes might vary, but the intervals remain stagnant. The normality or abnormality of the ECG signal depends on the flowchart depicted in Figure 35. It can be clearly seen from Figure 35 that if the values of all the intervals, specifically the R-R intervals, P-P intervals, and P-R intervals, remain constant throughout the duration of the ECG signal, then the ECG signal is normal. If the duration of these intervals changes even once, then the ECG signal is abnormal, and the person must visit a doctor for further guidance regarding the type of the abnormality. The intervals are calculated precisely with the tolerance of ±2 units. Out of these three estimated intervals, the most important is the P-R interval. If the P-R interval changes during the duration of the signal, then the signal is said to be abnormal, and the person has a major heart disorder.

ECG Signal's Database

The ECG signals used as a part of this research are chosen from the MIT-BIH Arrhythmia Database (MBAD) and the MIT-BIH Normal Sinus Rhythm Database (MBNSRD). A. Goldberger et al. [39] created this database. The MBAD consists of 48 half-hour, two-lead ECG signals acquired from 47 subjects [39]. The recordings were digitized at 360 samples for each second per channel with 11-bit resolution over a 10 mV range.

The MBNSRD consists of 18 long–term ECG recordings of five men aged 26 to 45 and thirteen ladies aged 20 to 50. This research uses selected recordings from both these databases [39]. To be specific, the 16420, 16272, 17052, and 17453 signals are taken from MBNSRD, and

signals 103, 105, 107, and 119 are taken from MBAD. The ECG signals used in this study are only 10 seconds long because the shorter the duration of the ECG signal the less complex it is to extract its minute information.

This algorithm is tested on these described ECG signals obtained from these two databases. Chapter 5 describes the results of the simulations performed on ECG signals 107 and 16420 using the proposed algorithm.

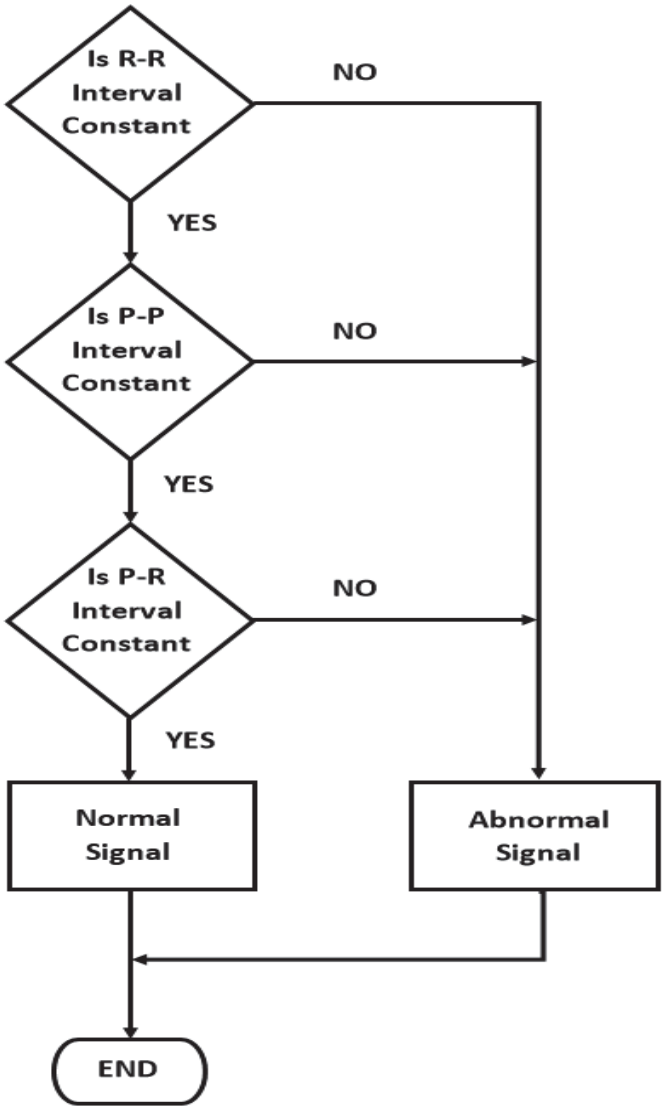

FIGURE 35. Interval estimation flow chart.

CHAPTER 5

RESULTS

Figure 36 displays a cardiac cycle of the synthetic ECG signal generated in MATLAB, and Figure 37 shows multiple cardiac cycles of the generated synthetic ECG signal. Figures 38 – 55 display the results of the developed algorithm for the database signals 107 and 16420. The results of the other ECG signals except 107 and 16420 are described in detail in Appendix A. The simulations are performed in MATLAB.

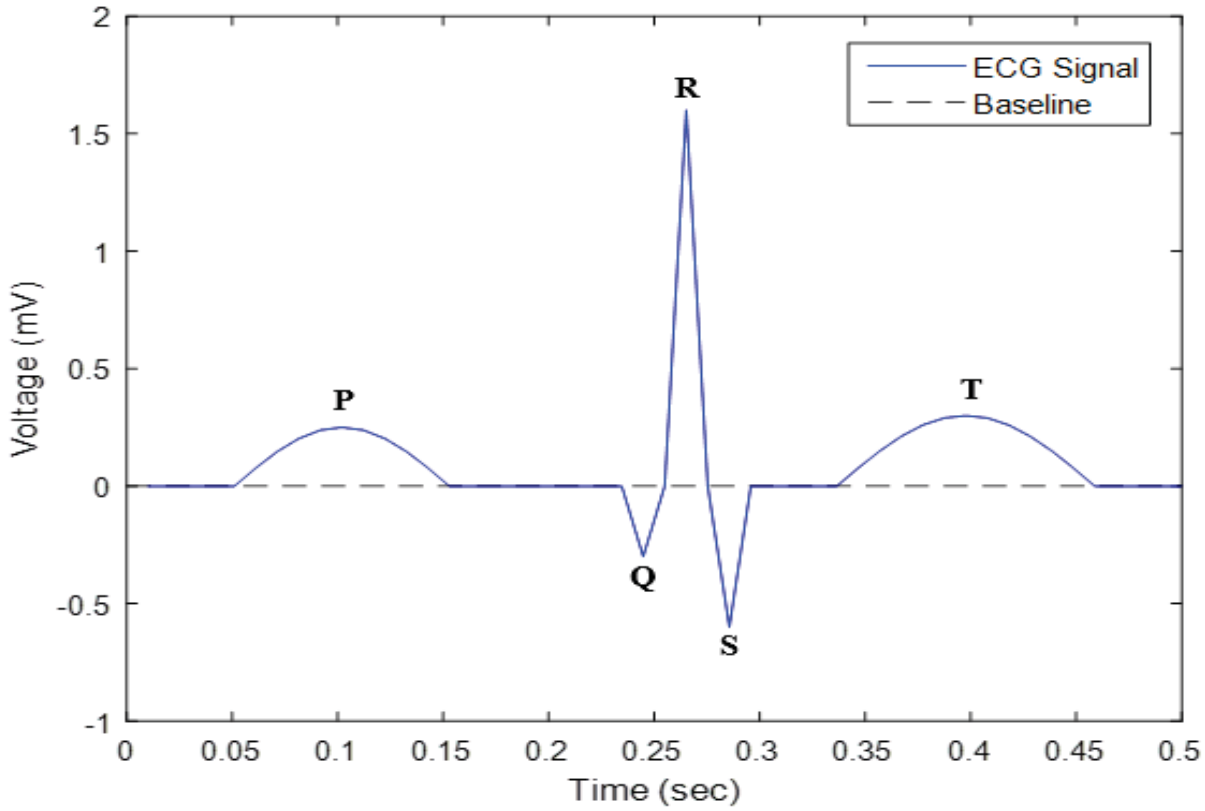

FIGURE 36. One cardiac cycle of synthetic ECG signal.

Signal 107

Figure 38 displays the original ECG signal 107 consisting of the WB artifact. Figure 39 demonstrates the frequency response of the signal in Decibels (dB) and Hz. There is no relevant

spike present at 50 Hz; so there is no effect of the PI artifact on the ECG signal 107.

Figures 40, 41, and 42, respectively, show the WB artifact removal from the ECG signal 107, the WGN removal after eliminating the WB artifact, and the WGN elimination without removing the WB artifact. Therefore, by comparing Figures 41 and 42, it can be realized that how clean the signal becomes after removing the WGN and WB artifact. Figure 41 proves that by removing the WGN before the detection stage distinguishes the peaks and valleys of the waves in the ECG signal.

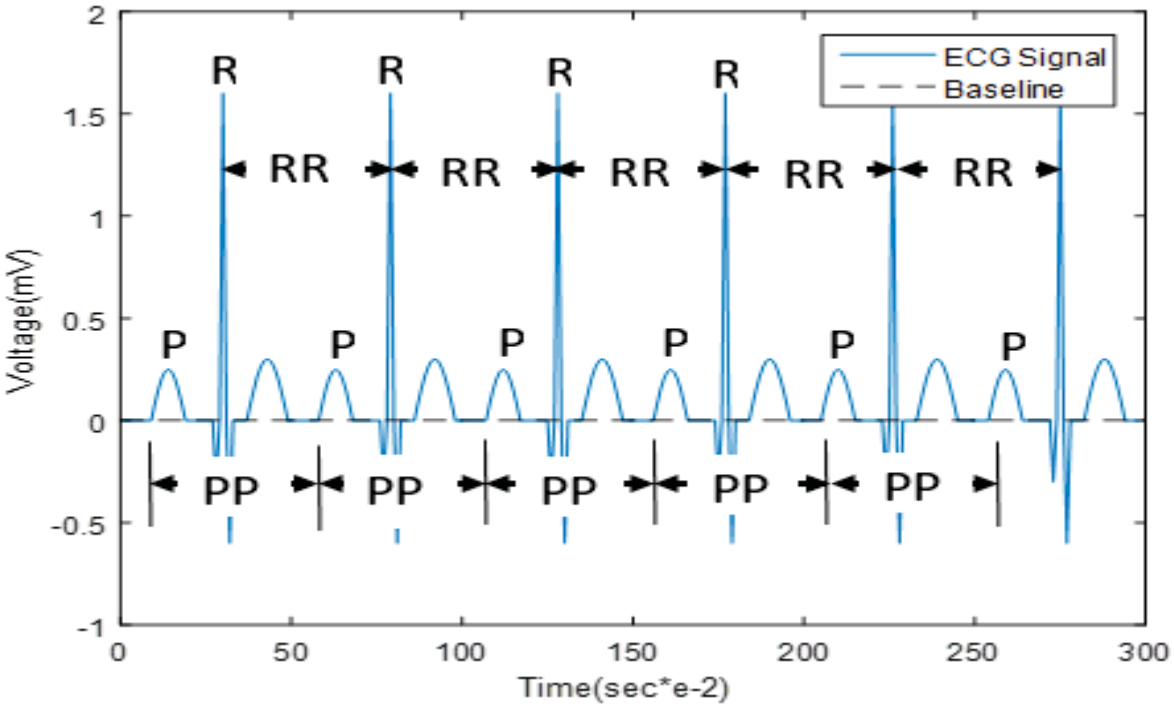

FIGURE 37. Synthetic ECG signal.

Figures 43, 44, and 45, respectively, display the detected peaks of the R-waves, P-waves, and the concatenation of the peaks to calculate the P-R interval of the ECG signal 107. The peaks of the waves are detected with respect to Figure 41. This proves that the signal processing using the wavelets does not change the morphology of the ECG signal.

Figure 46 describes the ECG signal 107 as abnormal because all the three intervals vary

in the signal. The total peaks of the R-waves and P-waves present in the ECG signal 107 are also calculated by the developed algorithm.

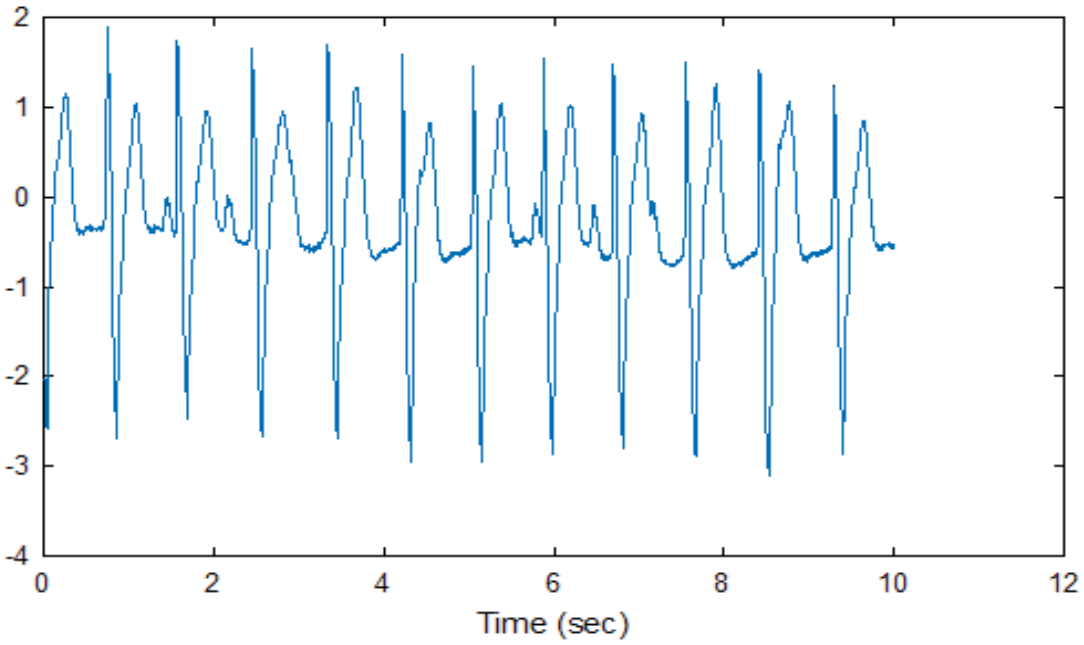

FIGURE 38. ECG signal 107.

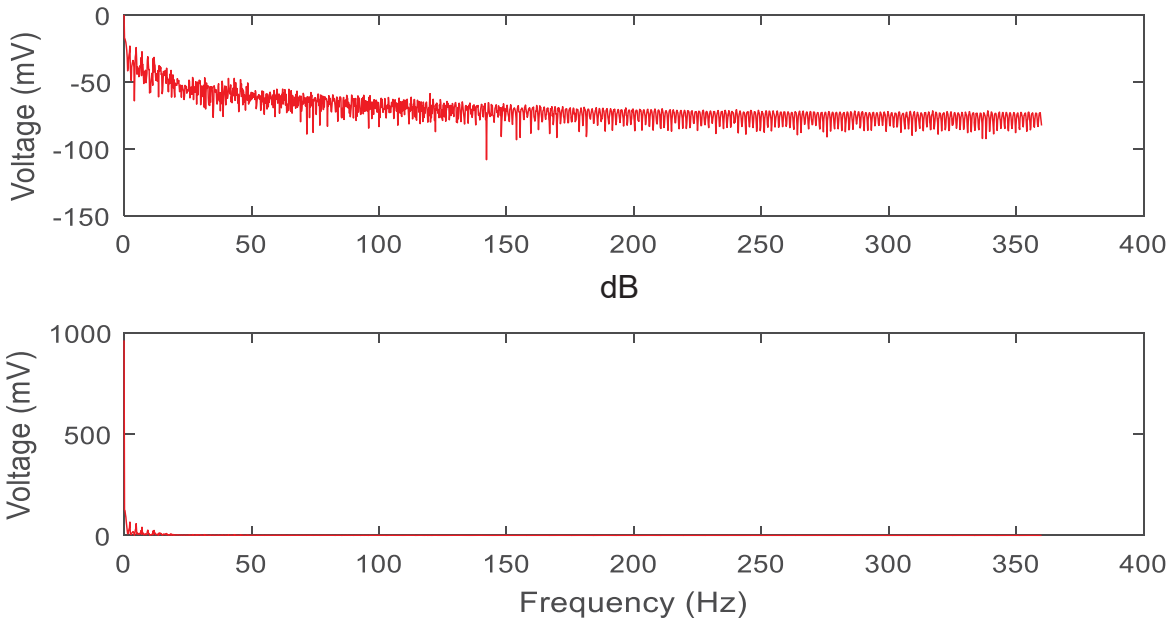

FIGURE 39. Check for spike at 50 Hz in dB and Hz in signal 107.

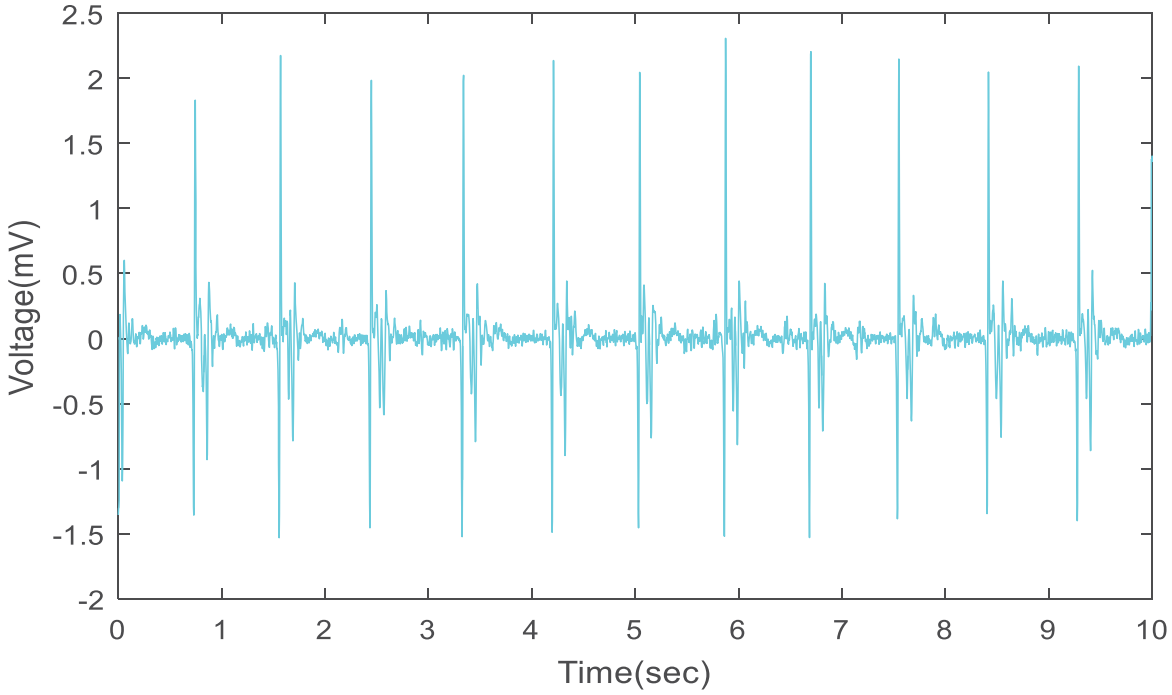

FIGURE 40. WB artifact removed in ECG signal 107.

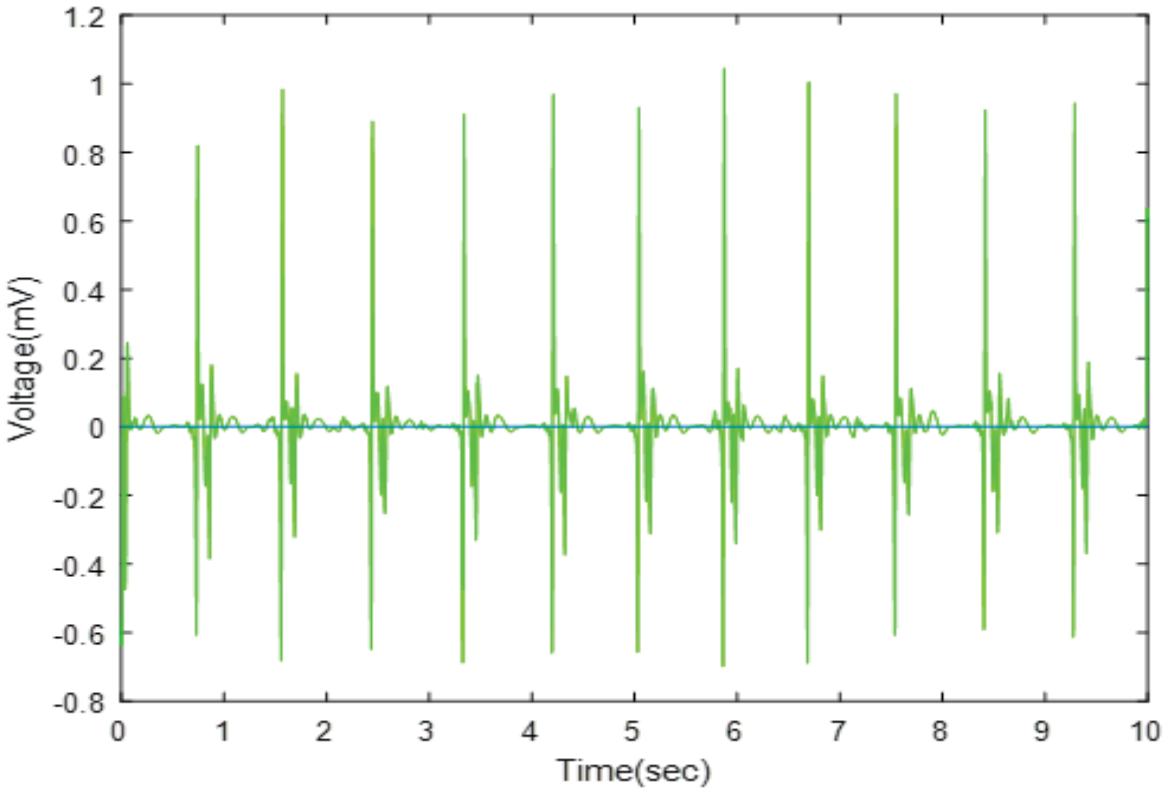

FIGURE 41. WGN removed in ECG signal 107 after eliminating the WB artifact.

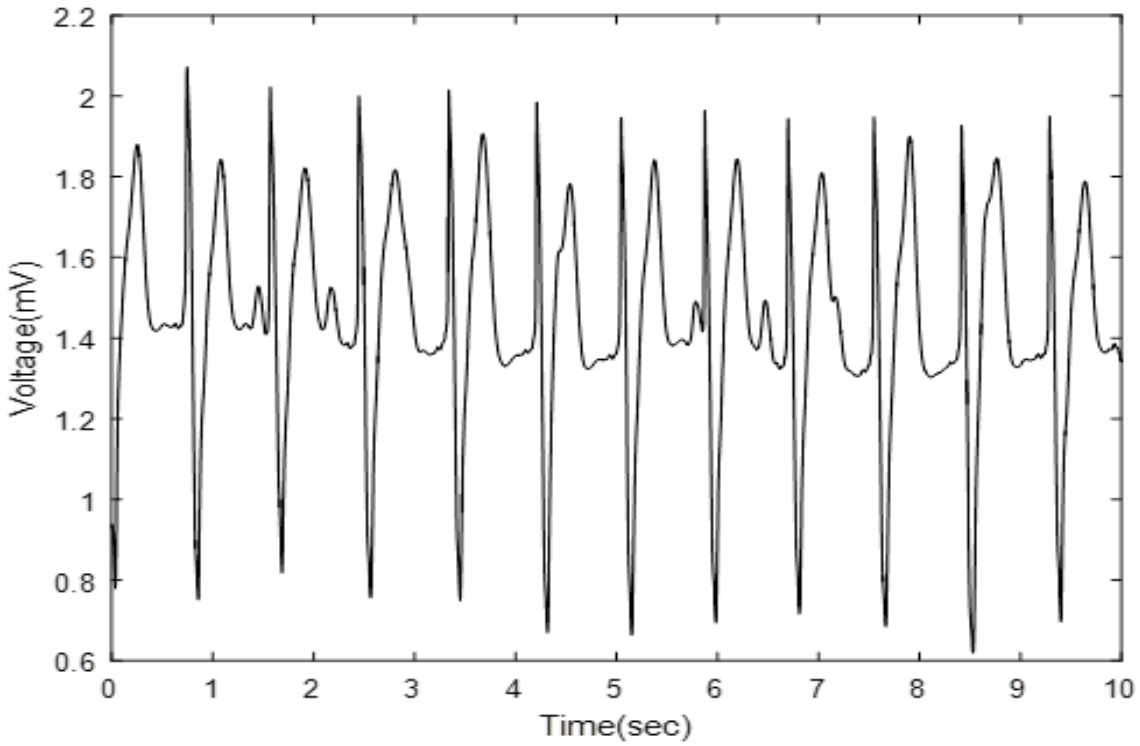

FIGURE 42. WGN eliminated in ECG signal 107 without removing the WB artifact.

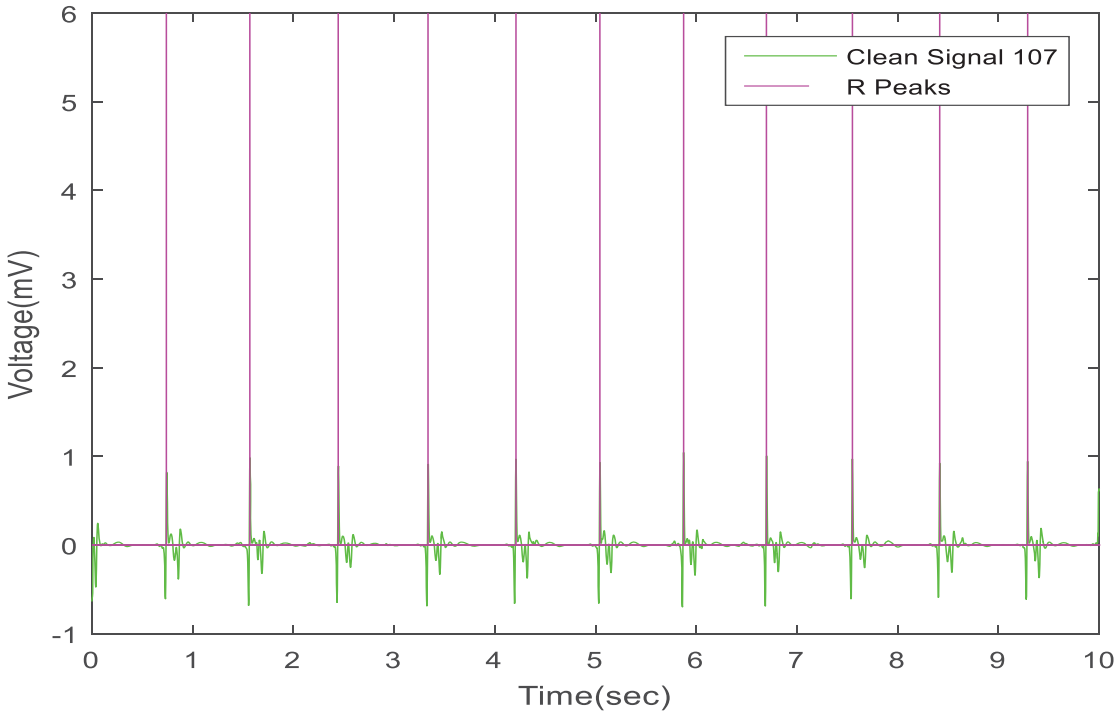

FIGURE 43. Detected peaks of R-waves in ECG signal 107.

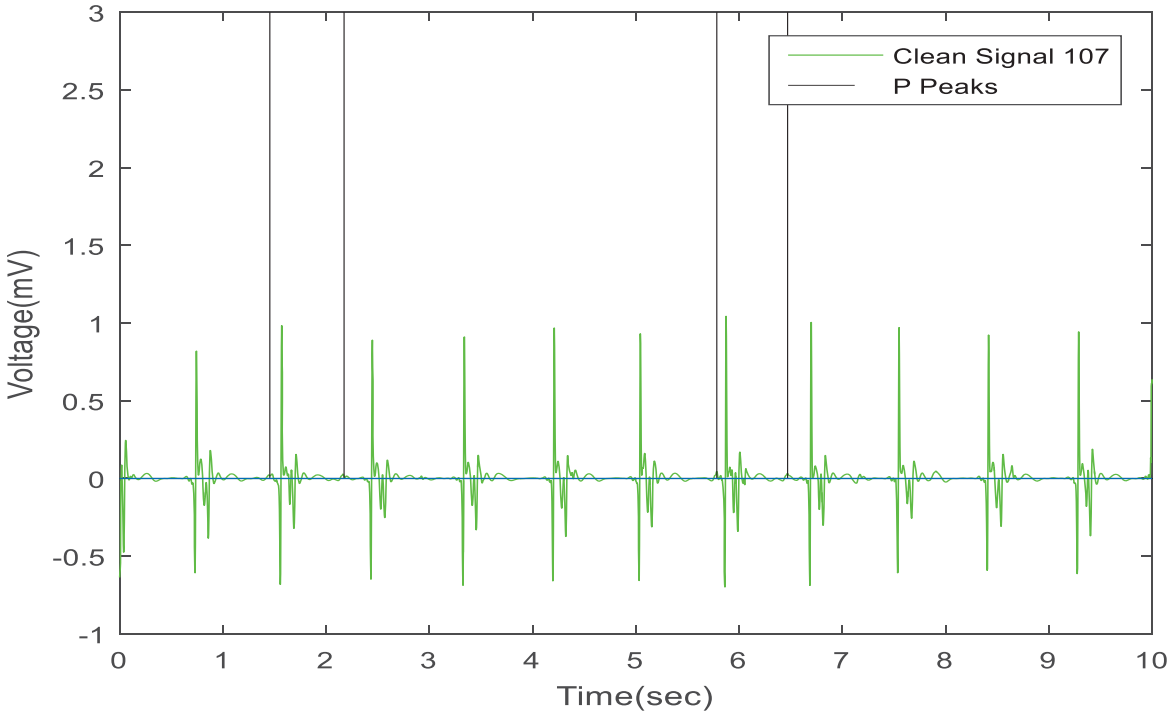

FIGURE 44. Detected peaks of P-waves in ECG signal 107.

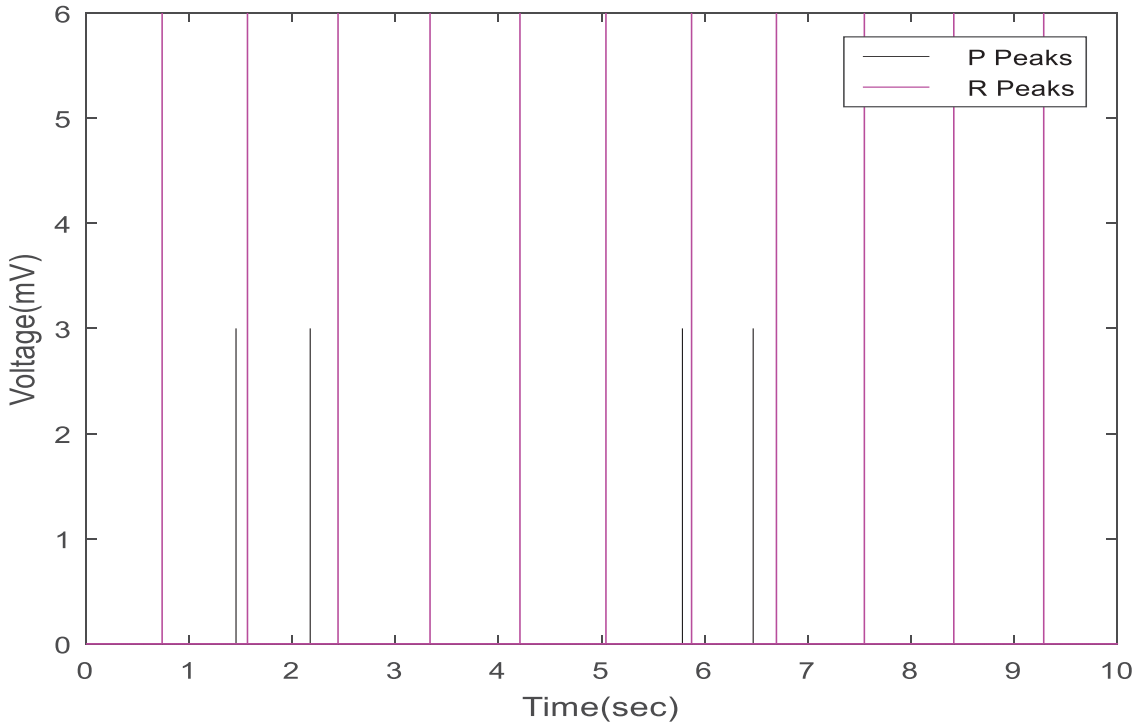

FIGURE 45. Concatenated detected peaks for P-R interval calculation in ECG signal 107.

```
The total R peaks in the signal are 11
R-R Interval is not constant!!!!
The signal is abnormal!!!!
Still check P-P Interval???
The total P peaks in the signal are 4
P-P Interval is not constant!!!!
The signal is abnormal!!!!
Still check P-R Interval???
P-R Interval is not constant!!!!
As all the three intervals are varying, the signal is abnormal!!!!
Please visit a doctor immediately.
```

FIGURE 46. ECG signal 107 characterization.

Signal 16420

Figure 47 displays the original ECG signal 16420 consisting of the WB artifact, and Figure 48 shows the frequency response of the signal in dB and Hz. There is no significant spike at 50 Hz; therefore, there is no effect of the PI artifact on the ECG signal 16420.

Figure 49 indicates the removal of the WB artifact from the ECG signal 16420. Figures 50 and 51, respectively, display the WGN removed from the ECG signal in which the WB artifact was previously eliminated and the WGN eliminated from the signal without removing the WB artifact. Therefore, by comparing both the figures it can be realized how clean the signal becomes after removing the WGN in the signal in which the WB artifact was previously removed. Figure 50 proves that by removing the WGN before the detection stage distinguishes the peaks and valleys of the waves in the ECG signal.

Figures 52 and 53, respectively, show the detected peaks of the R-waves and P-waves in the ECG signal 16420. The detected peaks of the waves coincide with the signal obtained in

Figure 50, which concludes the accurate detection of the peaks of the R-waves and P-waves of the signal. The execution of the signal processing using the wavelets not changing the morphology of the ECG signal is clearly seen from the figures. Figure 54 demonstrates the concatenation of the peaks of the R-waves and P-waves in the ECG signal 16420 for calculating the P-R interval. Figure 55 describes the ECG signal 16420 as normal because of the intervals remaining constant along the length of the signal. It also depicts the total number of the R-waves and P-waves present in the ECG signal 16420.

Table 4 summarizes the results of the ECG signals chosen in this research and concludes them as normal or abnormal signals based on the estimation of the mentioned intervals.

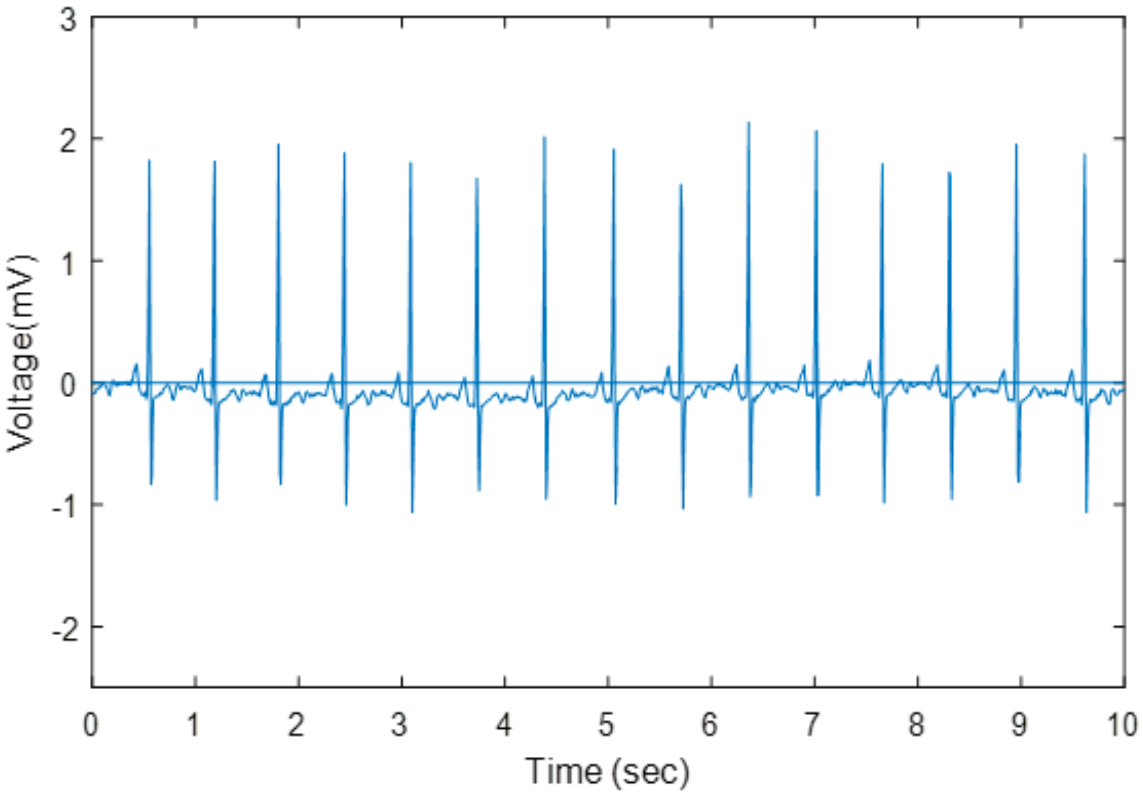

FIGURE 47. ECG signal 16420.

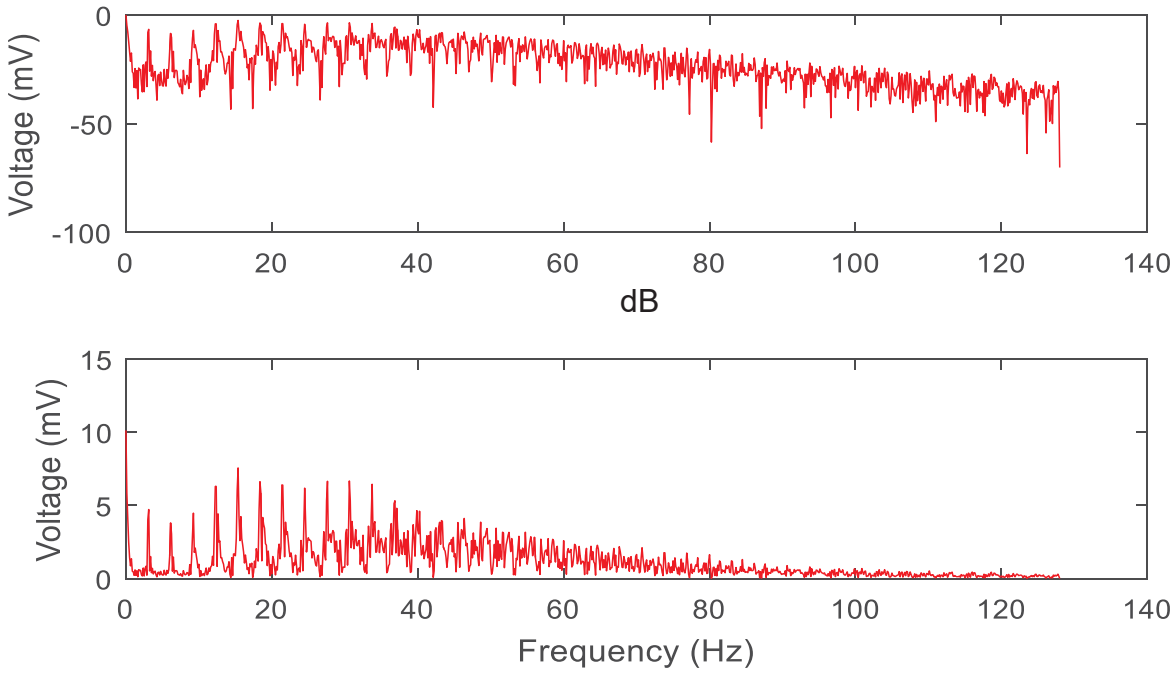

FIGURE 48. Check for spike at 50 Hz in dB and Hz in signal 16420.

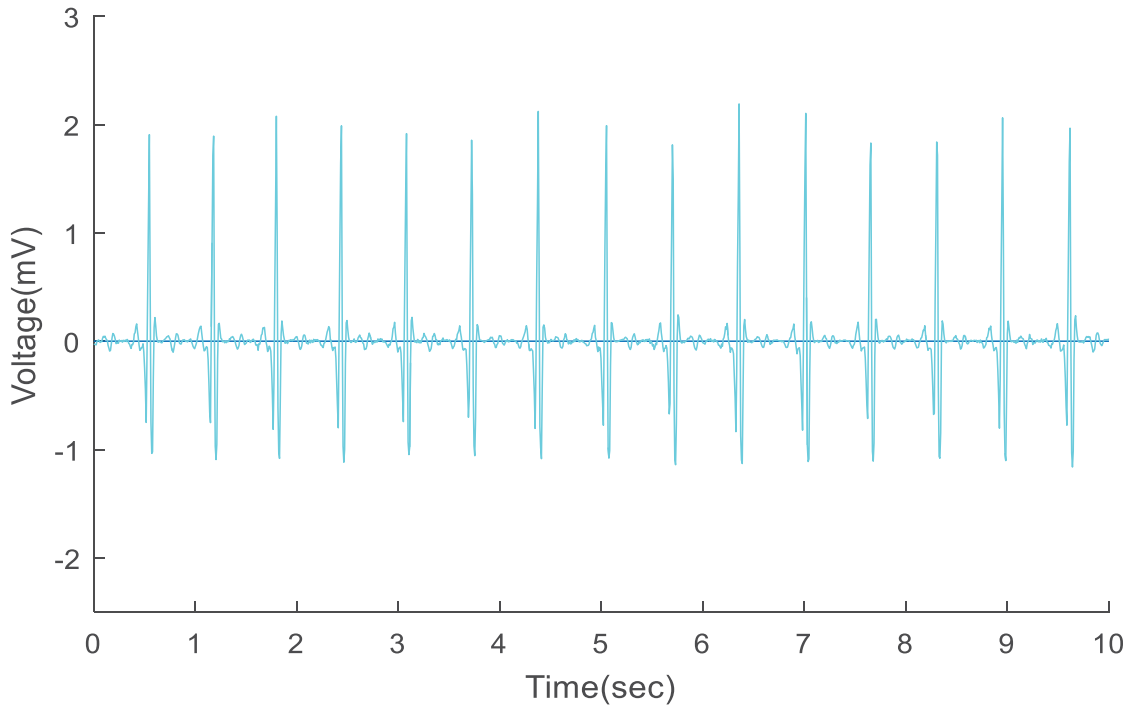

FIGURE 49. WB artifact removed in ECG signal 16420.

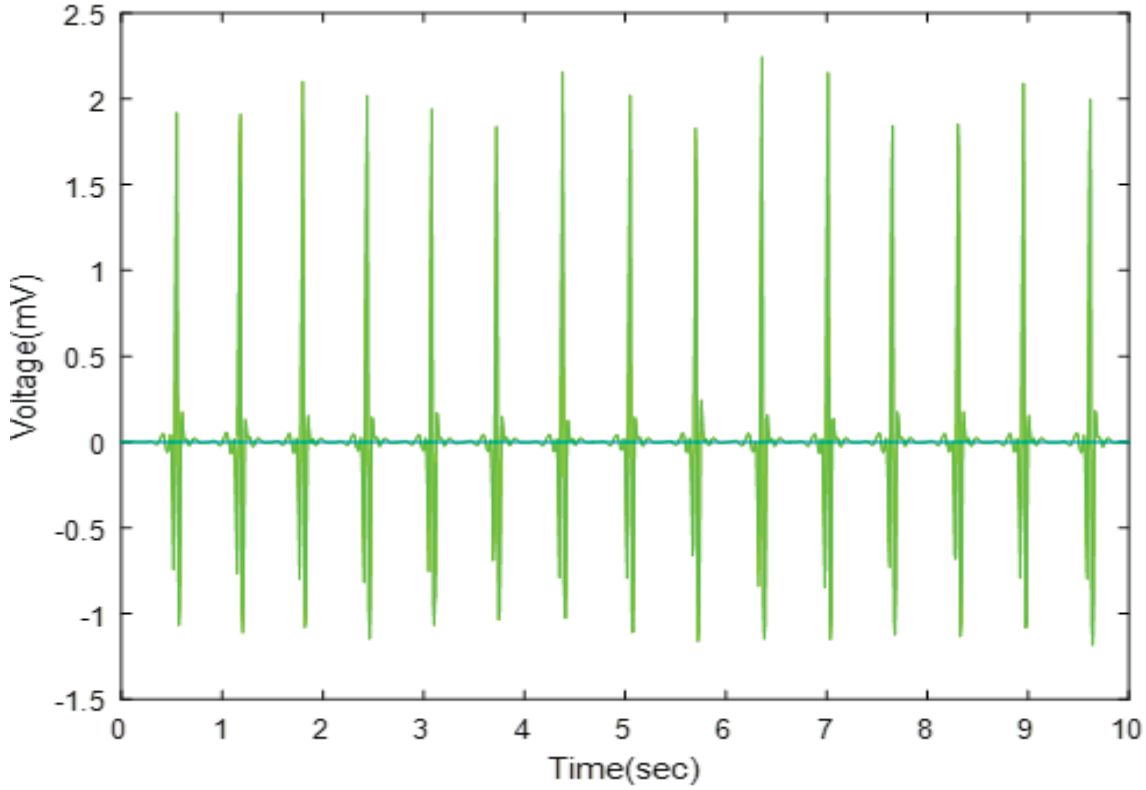

FIGURE 50. WGN removed in ECG signal 16420 after eliminating the WB artifact.

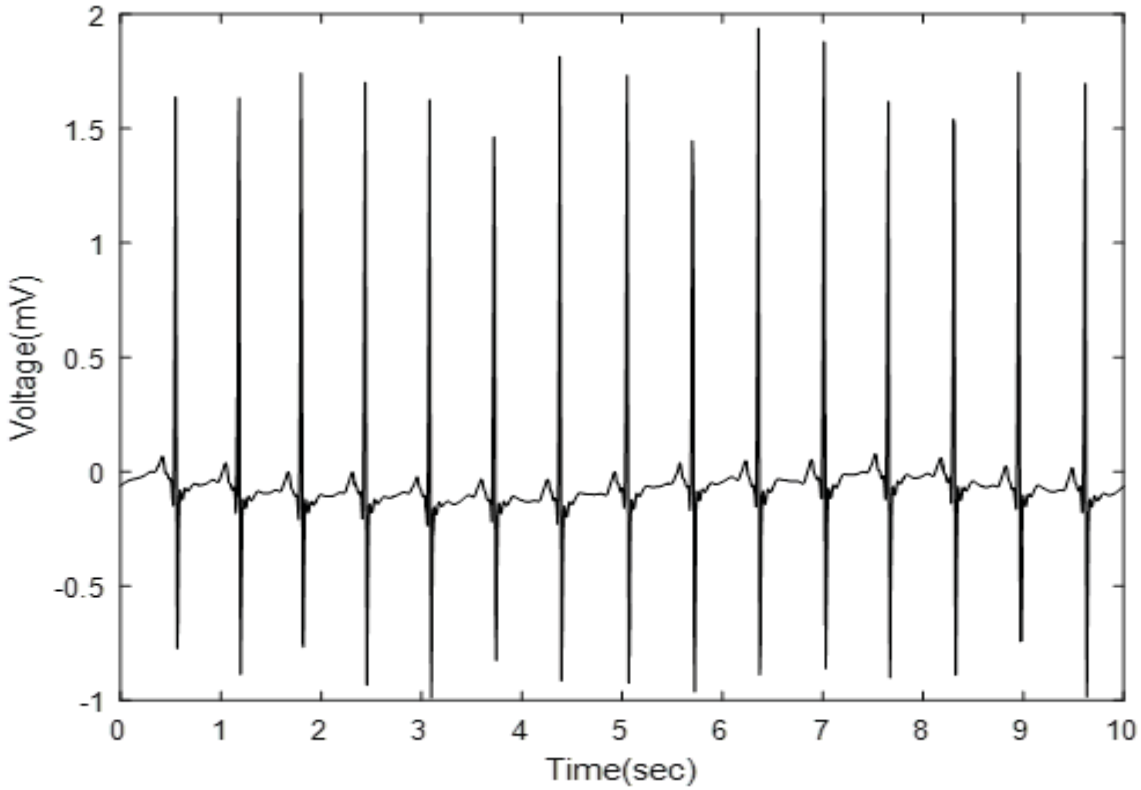

FIGURE 51. WGN eliminated in ECG signal 16420 without removing the WB artifact.

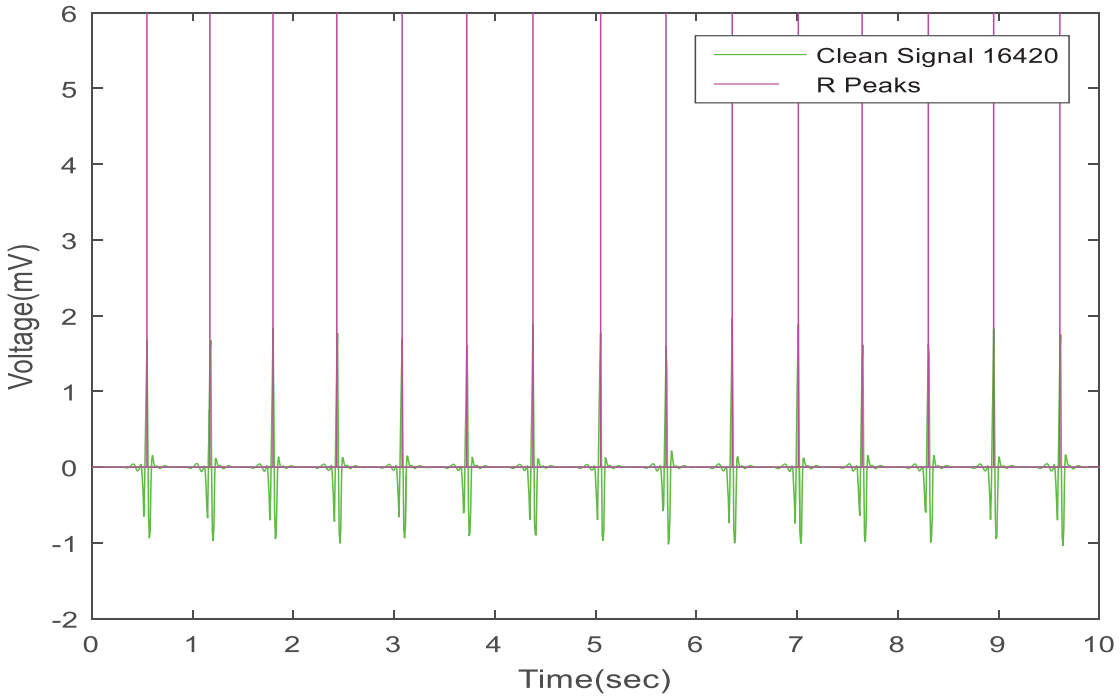

FIGURE 52. Detected peaks of R-waves in ECG signal 16420.

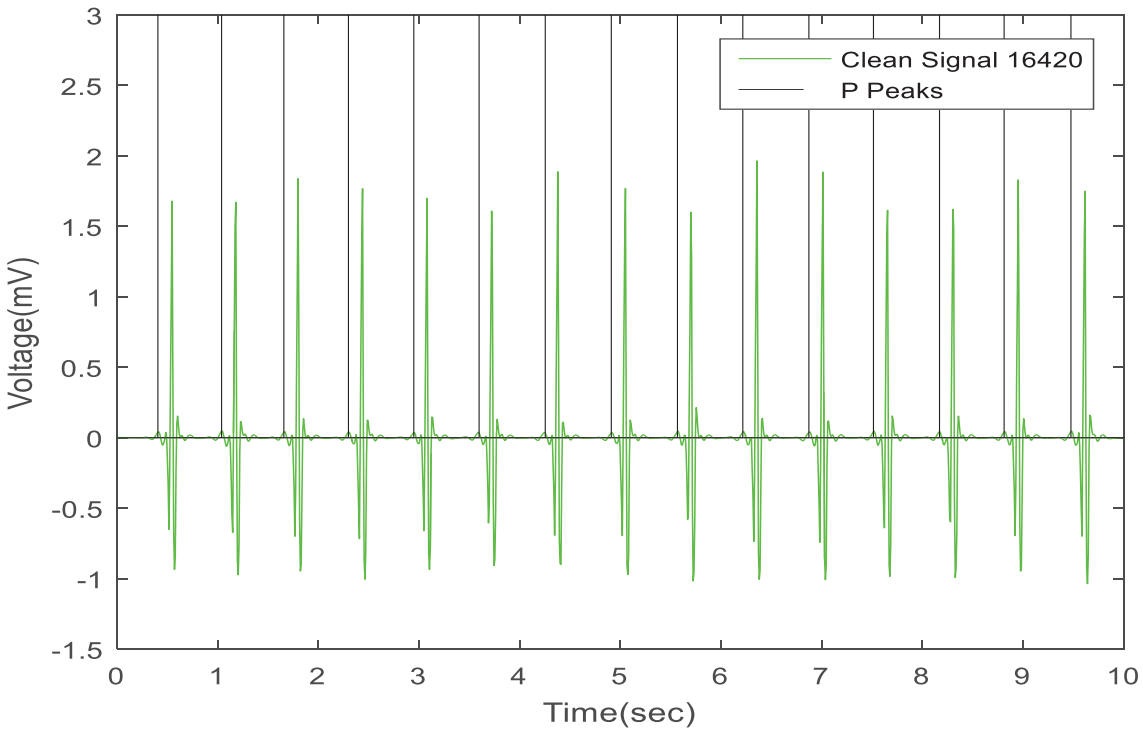

FIGURE 53. Detected peaks of P-waves in ECG signal 16420.

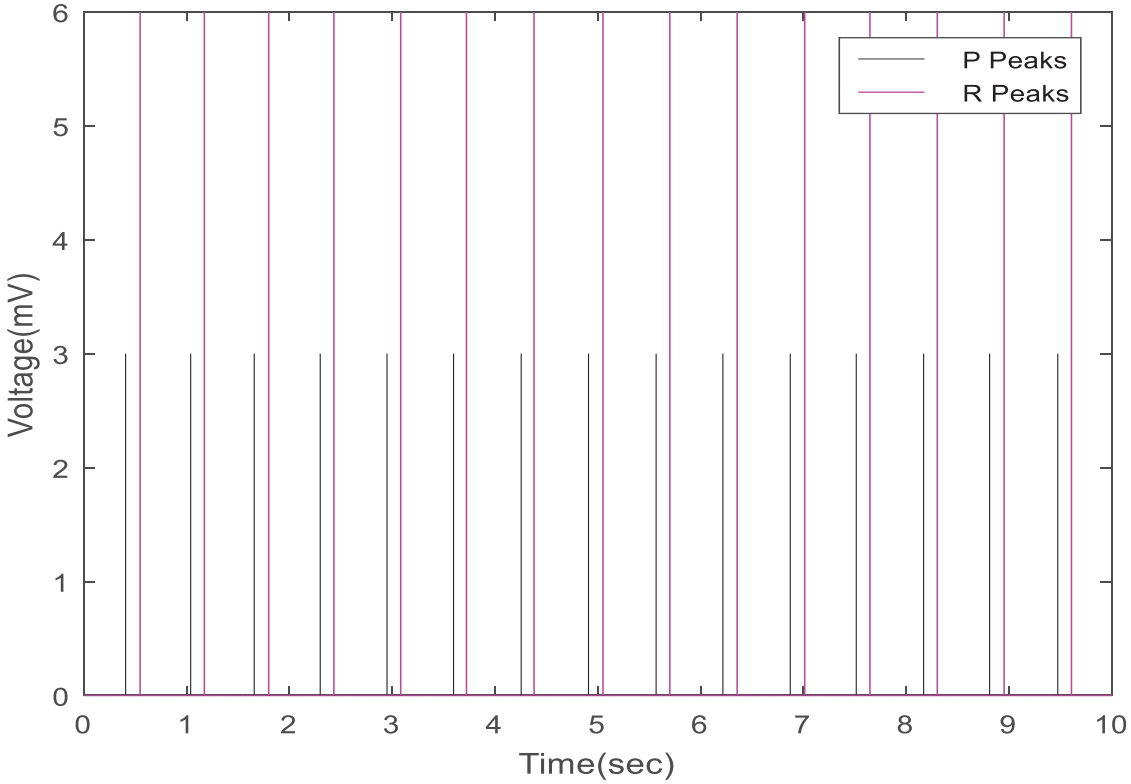

FIGURE 54. Concatenated detected peaks for P-R interval estimation in ECG signal 16420.

```
The total R peaks in the signal are 15
R-R Interval is constant.
Check for P-P Interval.....
The total P peaks in the signal are 15
P-P Interval is constant!!!!
Check for P-R Interval.....
P-R Interval is constant.
The signal is normal.
```

FIGURE 55. ECG signal 16420 characterization.

TABLE 4. Normal and Abnormal ECG Signals

ECG Signals	R-R Interval	P-P Interval	P-R Interval	Normal Signal	Abnormal Signal
16420	Constant	Constant	Constant	Yes	
16272	Constant	Constant	Constant	Yes	
17052	Constant	Constant	Constant	Yes	
17453	Not Constant	Constant	Constant		Yes
103	Not Constant	Not Constant	Not Constant		Yes
105	Not Constant	Not Constant	Not Constant		Yes
107	Not Constant	Not Constant	Not Constant		Yes
119	Not Constant	Not Constant	Not Constant		Yes

CHAPTER 6

CONCLUSION AND FUTURE EXPANSION

Conclusion

A novel scheme to classify the Electrocardiogram (ECG) signal as a normal signal or an abnormal signal is proposed using the db_4 wavelet. The db_4 wavelet is used in the described algorithm as it best resembles the morphology of the ECG signal. The developed algorithm demonstrates accurate and optimum results for the removal of the Wandering Baseline (WB) artifact using only level 1 decomposition and reconstruction of the ECG signal instead of levels 6 through 13. The White Gaussian Noise (WGN) is eliminated successfully from the ECG signal using the level 4 Discrete Wavelet Transform (DWT) along with the soft threshold technique without altering the morphology of the ECG signal.

The hard threshold technique of the wavelets precisely and accurately detects the peaks of the R-waves and P-waves in the ECG signals. The intervals of the ECG signals are estimated once the peaks of the signals are detected. A tolerance of ±2 units is considered for the estimation of the intervals. The signals are thus classified as normal signals only if all the intervals namely, the

R-R intervals, the P-P intervals, and the P-R intervals are constant. If a specific interval or all the intervals are fluctuating along the duration of the signals, then the signals are abnormal. Along with this estimation of these mentioned intervals, the ECG signal is also generated synthetically in MATLAB to realize its morphology.

The developed algorithm is tested on eight ECG signals, which are obtained from the MIT-BIH Arrhythmia Database and MIT-BIH Normal Sinus Rhythm Database. The ECG signals tested are 103, 105, 107, 119, 16420, 16272, 17052, and 17453. Thus, the db_4 wavelet

accurately classifies these ECG signals as normal or abnormal signals depending on the calculation of these mentioned intervals. Hence, 16420, 16272, and 17052 ECG signals are normal signals; 103, 105, 107, 119, and 17453 ECG signals are abnormal signals.

Therefore, the wavelet analysis is an efficient and effective tool to estimate the intervals present in the ECG signals compared to the traditional filter approach. This analysis will be a great benefit to pathologists to analyze the signal effortlessly and accurately so that the type of treatment needed for a person can be instantaneously provided if an abnormality is detected. This analysis will help to reduce major heart problems.

Future Expansion

The ECG signal consists of many features. The algorithm described in this thesis to detect the P-R interval along with the R-R interval and the P-P interval with the help of Daubechies$_4$ wavelet is not the only wavelet to detect the intervals. There are numerous other wavelets and wavelet transforms that can be used in the future to detect the intervals.

Apart from using different wavelets and wavelet transforms, other features of the ECG signal such as Q-T intervals, S-T segments, amplitudes, and duration of all the waves present in the ECG signal can also be detected in the future using the Daubechies$_4$ wavelet.

In the future, this algorithm can be used to detect the intervals from other ECG signals present in the MIT-BIH Arrhythmia Database and MIT-BIH Normal Sinus Rhythm Database to conclude its normality or abnormality. Apart from these two databases, other databases can also be used in the future.

An automatic system can be designed in the future with the described algorithm in this research, and a new algorithm can also be developed to detect the severity of the abnormality present in the ECG signal. Depending on the severity of the abnormality present in the ECG

signal, an alert can be set so that the person can contact the doctor immediately and start the medication if needed. Features such as USBs and different adapters can also be fixed on the hardware of the automatic system so that the developed system can effortlessly be connected to several computers and equipment present in the operation theater in a hospital.

A portable hardware model can also be developed using the described algorithm in the future so that the person can check his/her heart condition at his/her convenient time and place without the need of visiting a doctor immediately.

APPENDICES

APPENDIX A

SIGNAL RESULTS

The results obtained by the developed algorithm for the ECG signals 103, 105, 119, 16272, 17052, and 17453 are described as follows.

Signal 103

Figure 56 displays the original ECG signal 103 obtained from the database. This ECG signal consists of the WB artifact. Figure 57 demonstrates whether or not a spike is present at 50 Hz in the ECG signal 103 by inspecting its frequency response in dB and Hz. Fortunately, no significant spike is observed at 50 Hz. Therefore, there is no effect of the PI artifact on the ECG signal 103.

Figure 58 indicates the elimination of the WB artifact from the ECG signal 103. Figure 59 shows the removal of the WGN from the ECG signal 103 with and without removing the WB artifact. Therefore, by comparing both the graphs in Figure 59, it can be realized how clean the signal in which the WB artifact was eliminated becomes after removing the WGN from it. It proves that by removing the WGN before the detection stage distinguishes the peaks and valleys of the waves in the ECG signal.

Figures 60 and 61, respectively, display the detected peaks of the R-waves and P-waves of the ECG signal 103 by using the hard threshold technique of the wavelets. Accurate peaks of the R-waves and P-waves are detected with the algorithm described in Chapter 4. Therefore, the execution of the signal processing using the wavelets does not change the morphology of the ECG signal. Figure 62 demonstrates the concatenation of the peaks of the R-waves and P-waves of the ECG signal 103 for estimating the P-R interval.

Figure 63 describes that the ECG signal 103 is abnormal as all the three intervals vary along the length of the signal. The algorithm also calculates the total number of the R-waves and P-waves present in the ECG signal 103. It also displays the total R-waves and P-waves present in

the signal.

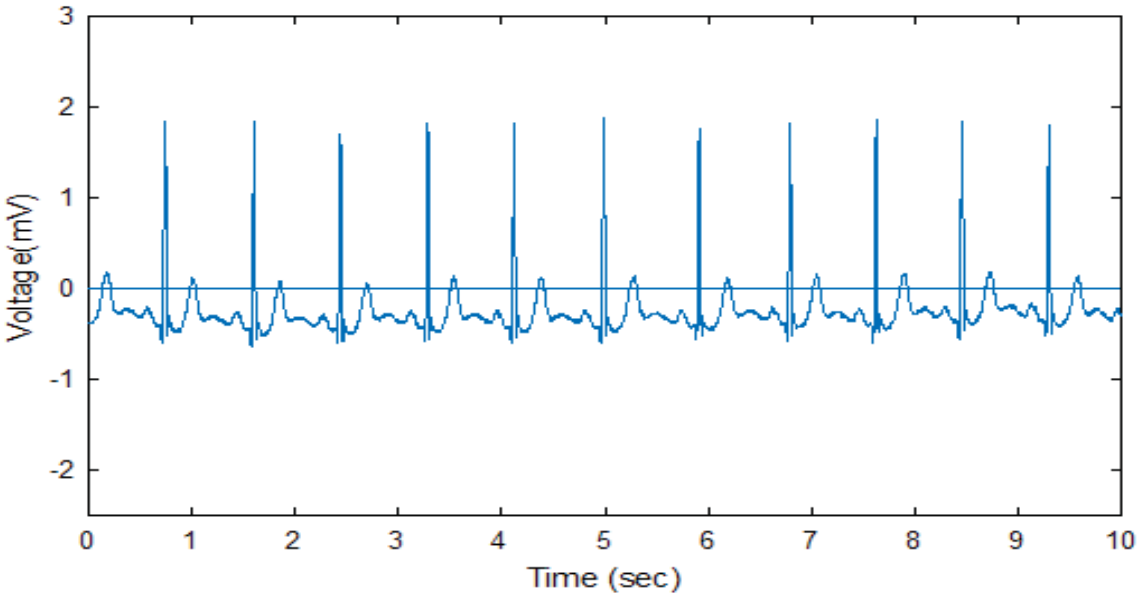

FIGURE 56. ECG signal 103.

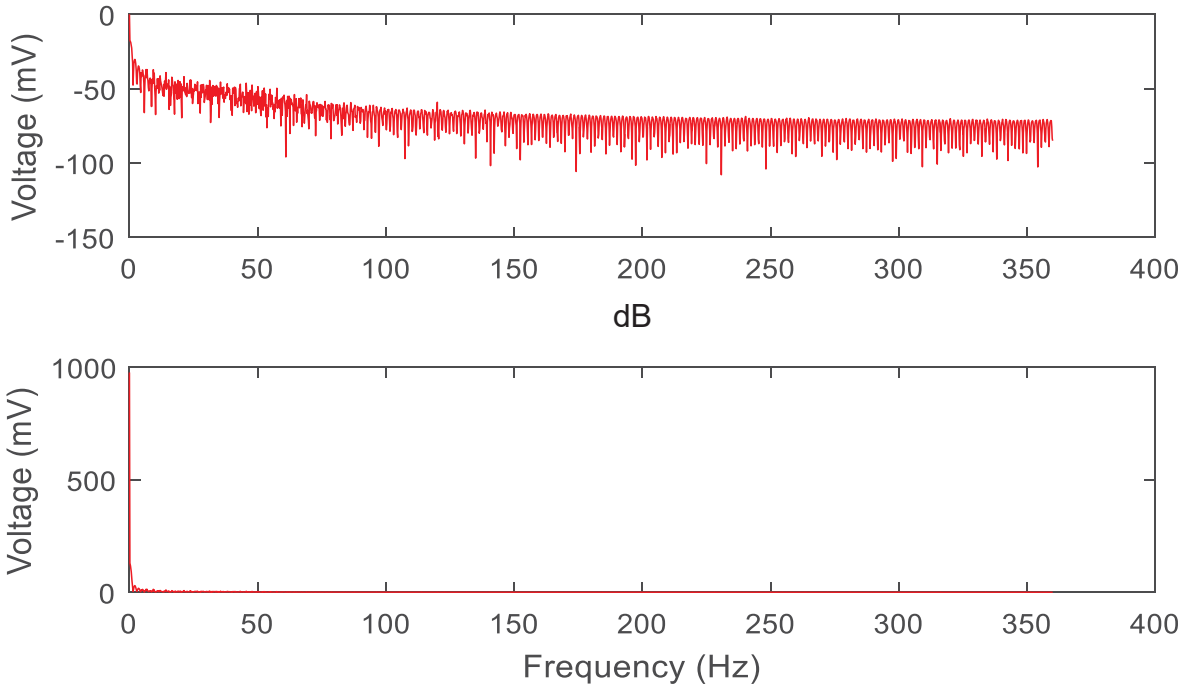

FIGURE 57. Check for spike at 50 Hz in dB and Hz in ECG signal 103.

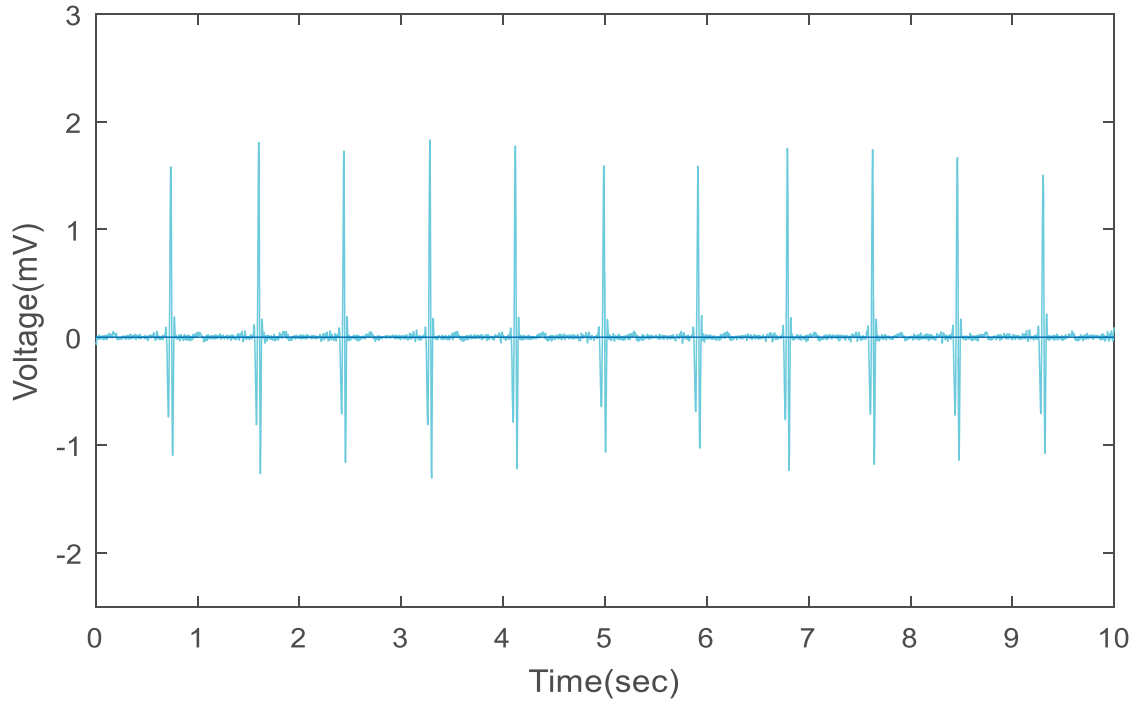

FIGURE 58. WB removed in ECG signal 103.

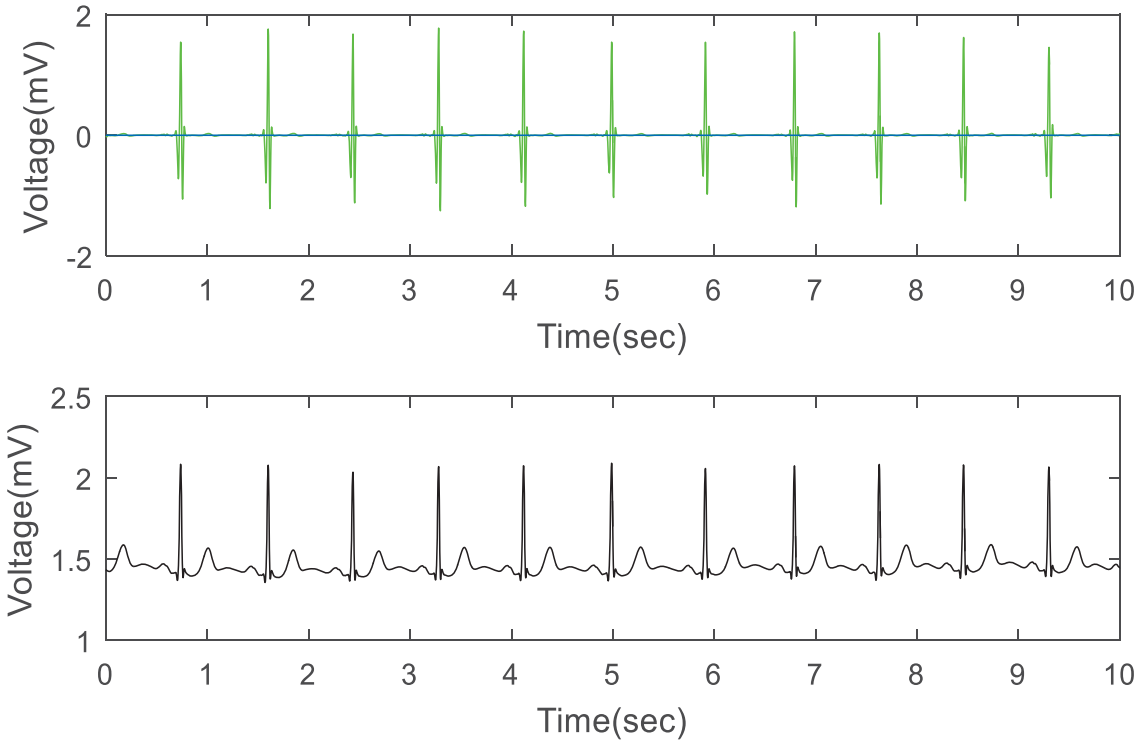

FIGURE 59. WGN removed in ECG signal 103 with and without removing the WB artifact.

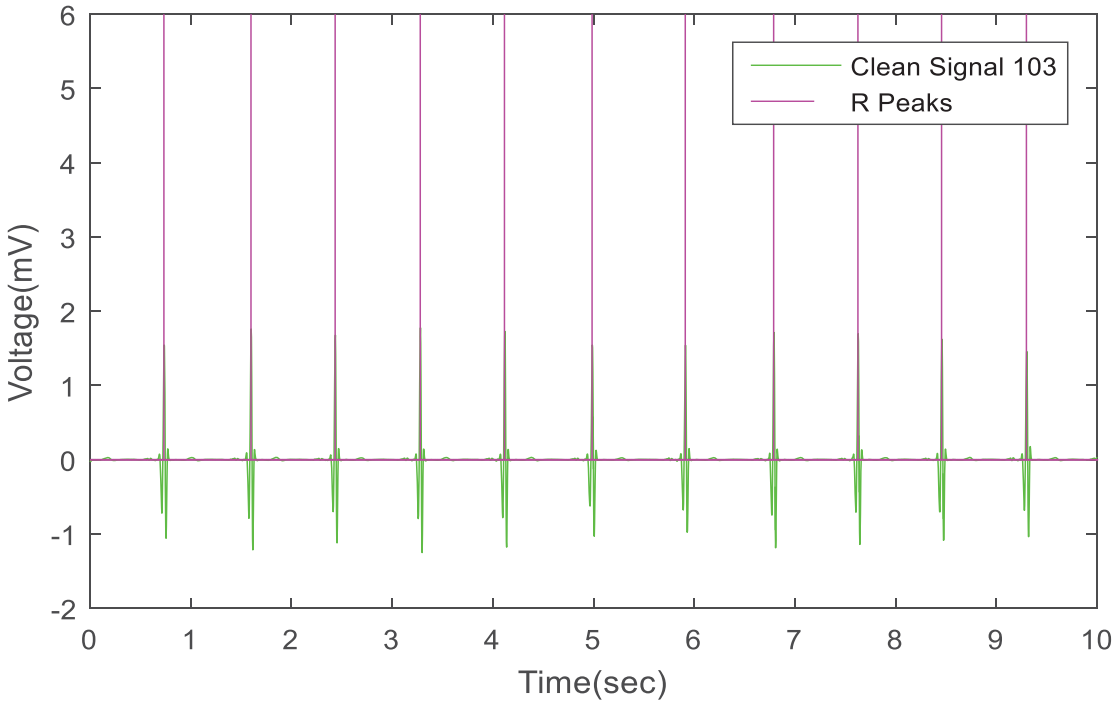

FIGURE 60. Detected peaks of R-waves in ECG signal 103.

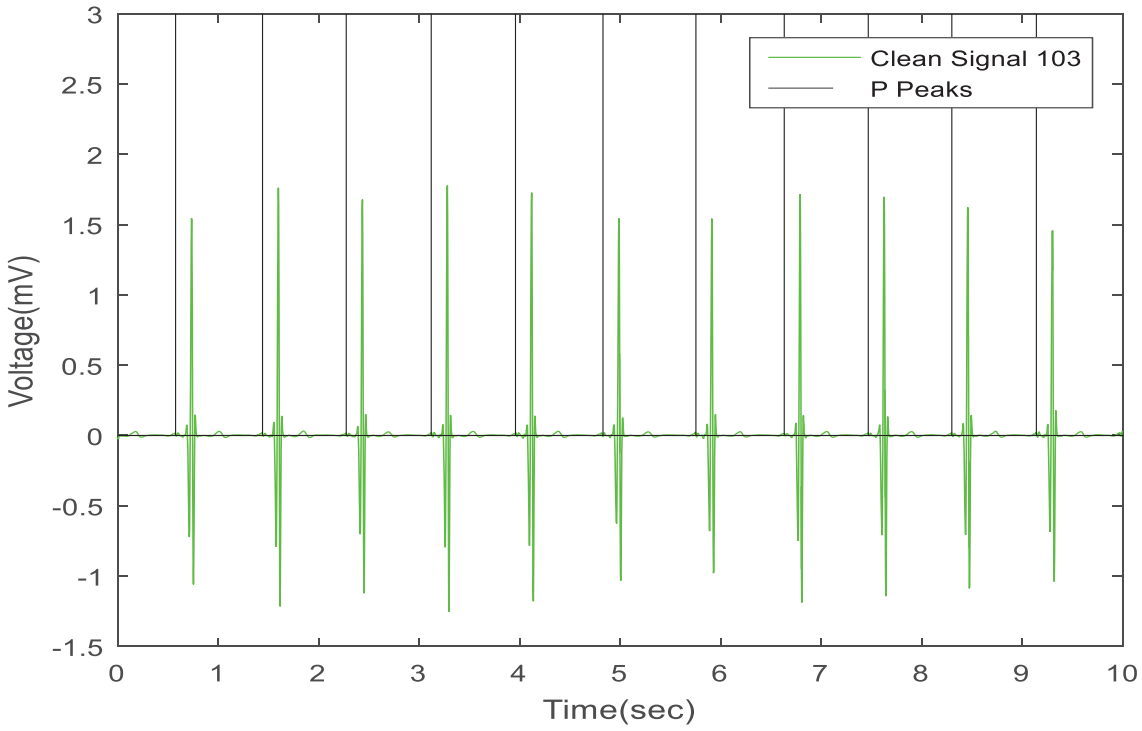

FIGURE 61. Detected peaks of P-waves in ECG signal 103.

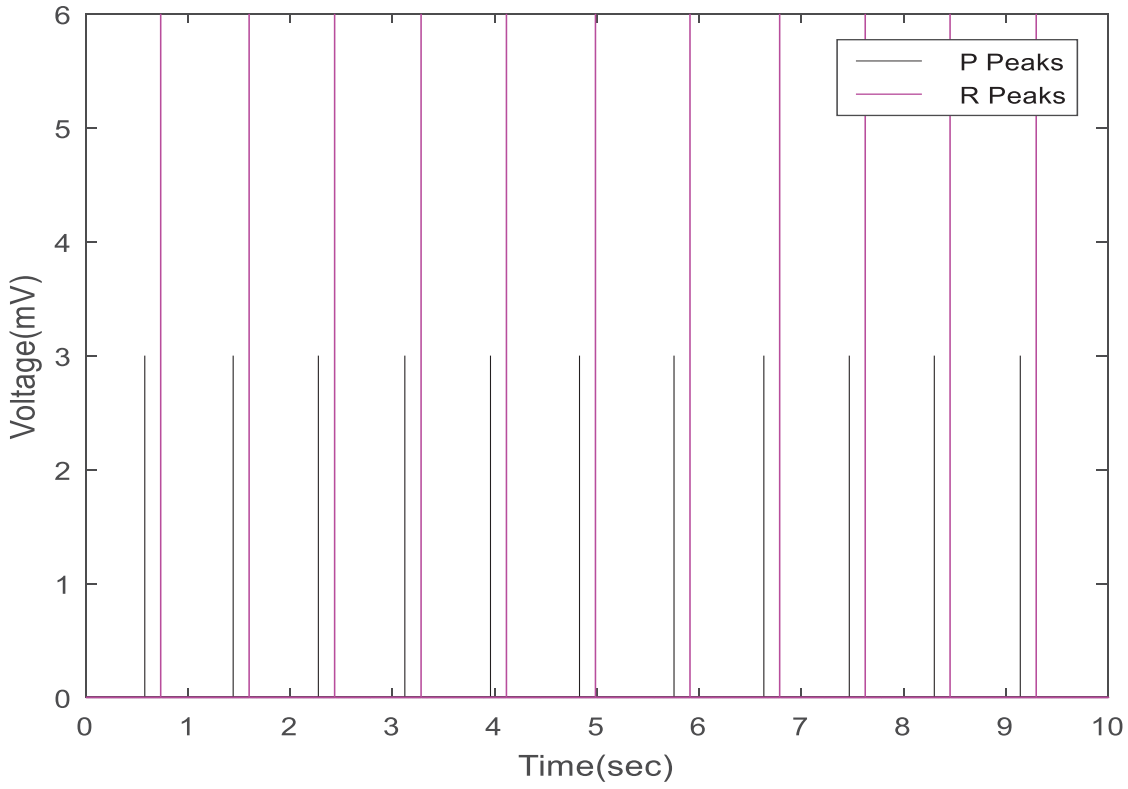

FIGURE 62. Concatenated detected peaks for P-R interval estimation in ECG signal 103.

```
The total R peaks in the signal are 11
R-R Interval is not constant!!!!
The signal is abnormal!!!!
Still check P-P Interval???
The total P peaks in the signal are 11
P-P Interval is not constant!!!!
The signal is abnormal!!!!
Still check P-R Interval???
P-R Interval is not constant!!!!
As all the three intervals vary the signal is abnormal!!!!
Please visit a doctor immediately.
```

FIGURE 63. ECG signal 103 characterization.

Signal 105

Figure 64 displays the original ECG signal 105 consisting of the WB artifact, and Figure 65 demonstrates the absence of the spike at 50 Hz in the ECG signal 105 by inspecting its frequency response in dB and Hz. No significant spike is observed at 50 Hz; therefore, there is no effect of the PI artifact on the ECG signal 105.

Figure 66 indicates the removal of the WB artifact from the ECG signal 105. Figure 67 depict the removal of the WGN from the ECG signal 105 with and without eliminating the WB artifact from it. Therefore, by comparing the graphs in Figure 67, it is observed that the signal in which the WB artifact was removed becomes after removing the WGN from it. Thus, the peaks and valleys of the waves in the ECG signal are clearly distinguished for its detection.

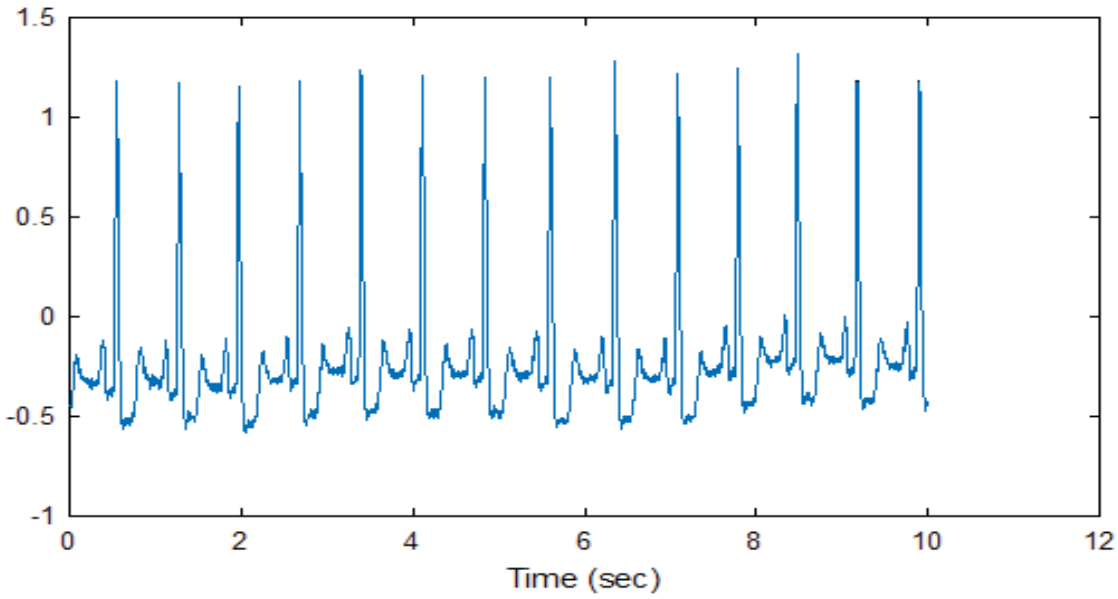

FIGURE 64. ECG signal 105.

Figures 68 and 69, respectively, display the detected peaks of the R-waves and P-waves in the ECG signal 105 by using the hard threshold technique of the wavelets. The algorithm accurately detects the peaks of the R-waves and P-waves. Therefore, the processing of the signal using the wavelets does not change the morphology of the ECG signal. Figure 70 demonstrates

the concatenation of the peaks of the R-waves and P-waves of the ECG signal 105 for calculating the P-R interval. Figure 71 describes that the ECG signal 105 is abnormal as all the three intervals vary along the length of the signal. The algorithm also calculates the total number of the R-waves and P-waves present in the ECG signal 105, which is displayed in Figure 71.

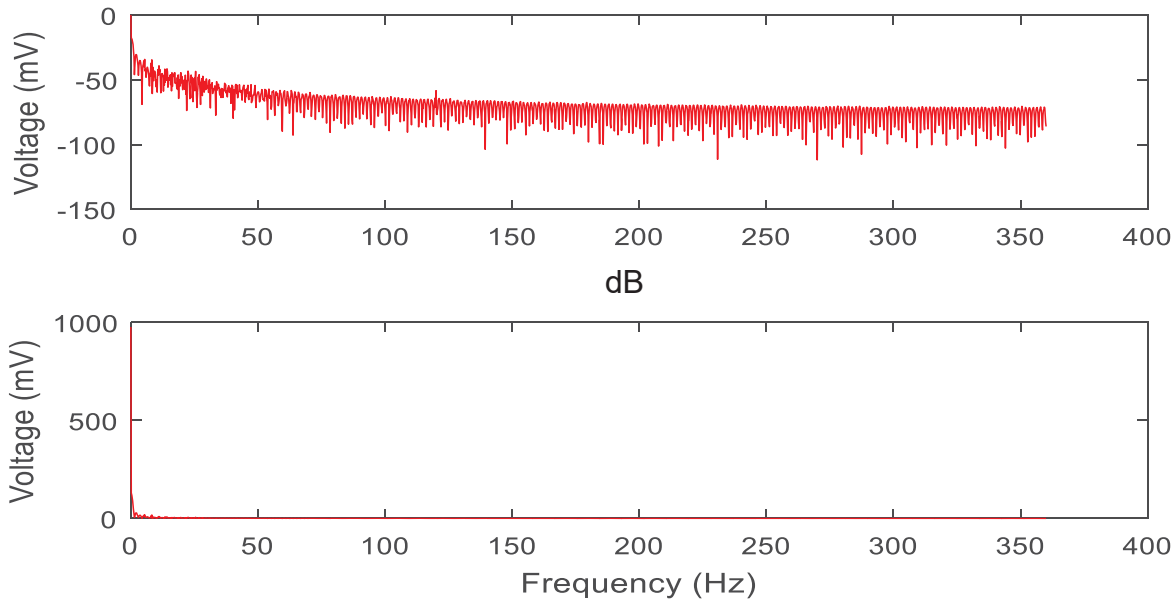

FIGURE 65. Check for spike at 50 Hz in dB and Hz in signal 105.

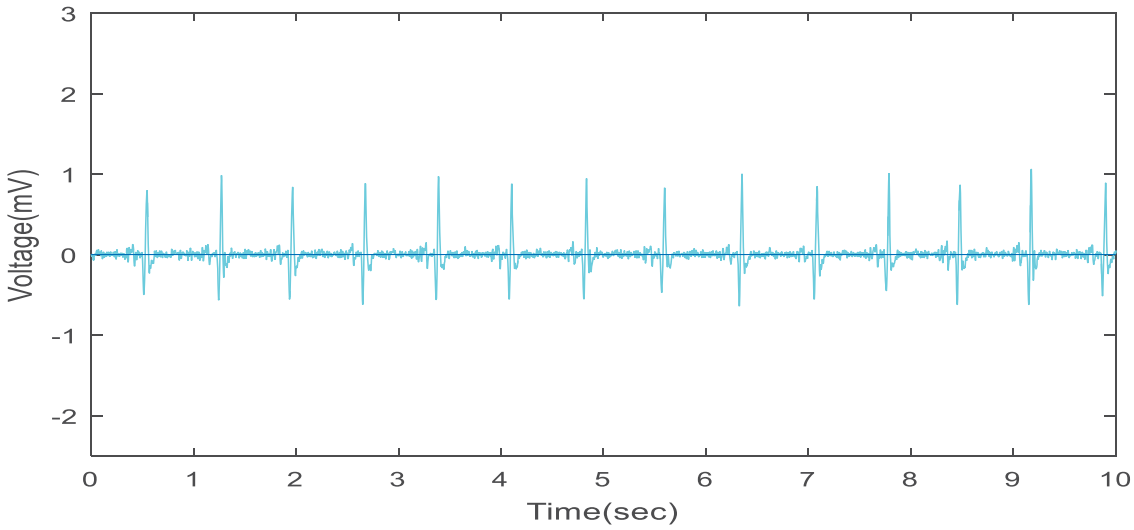

FIGURE 66. WB removed in ECG signal 105.

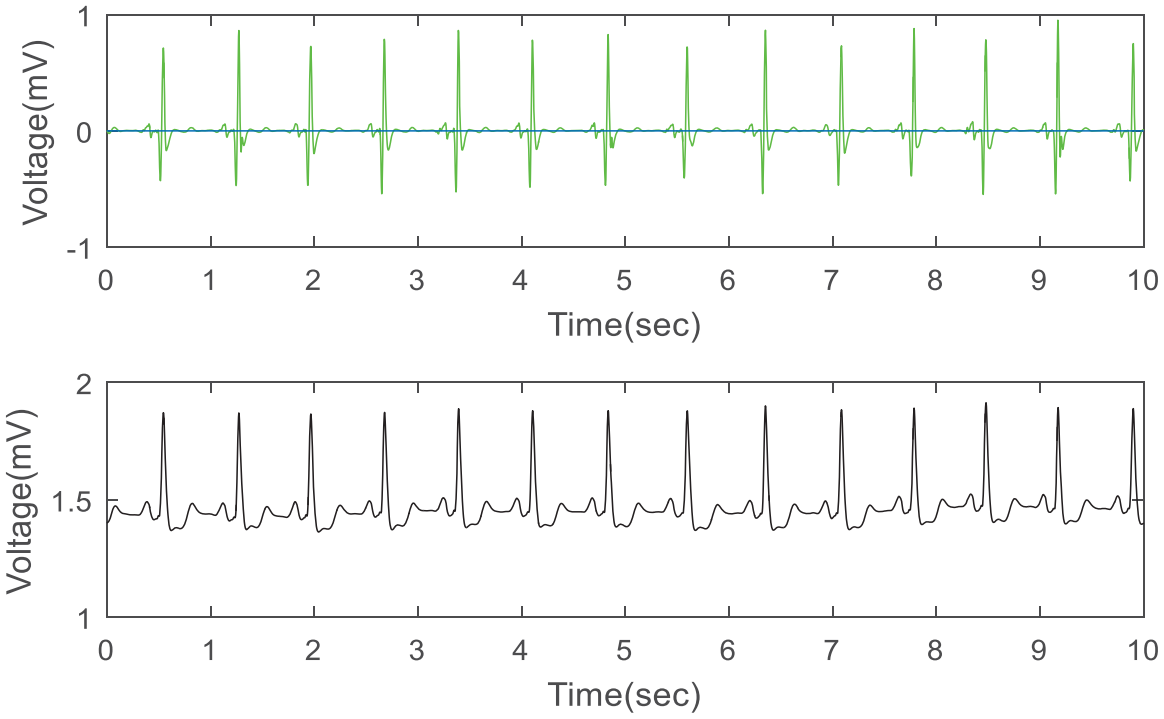

FIGURE 67. WGN removed in ECG signal 105 with and without eliminating the WB artifact.

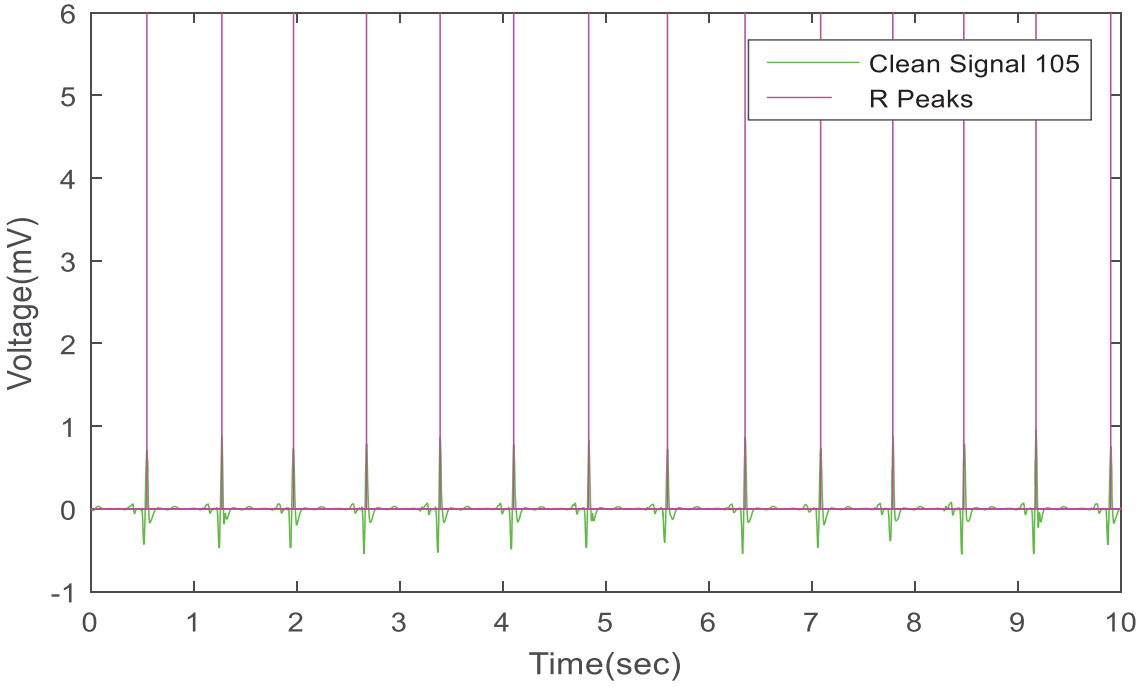

FIGURE 68. Detected peaks of R-waves in ECG signal 105.

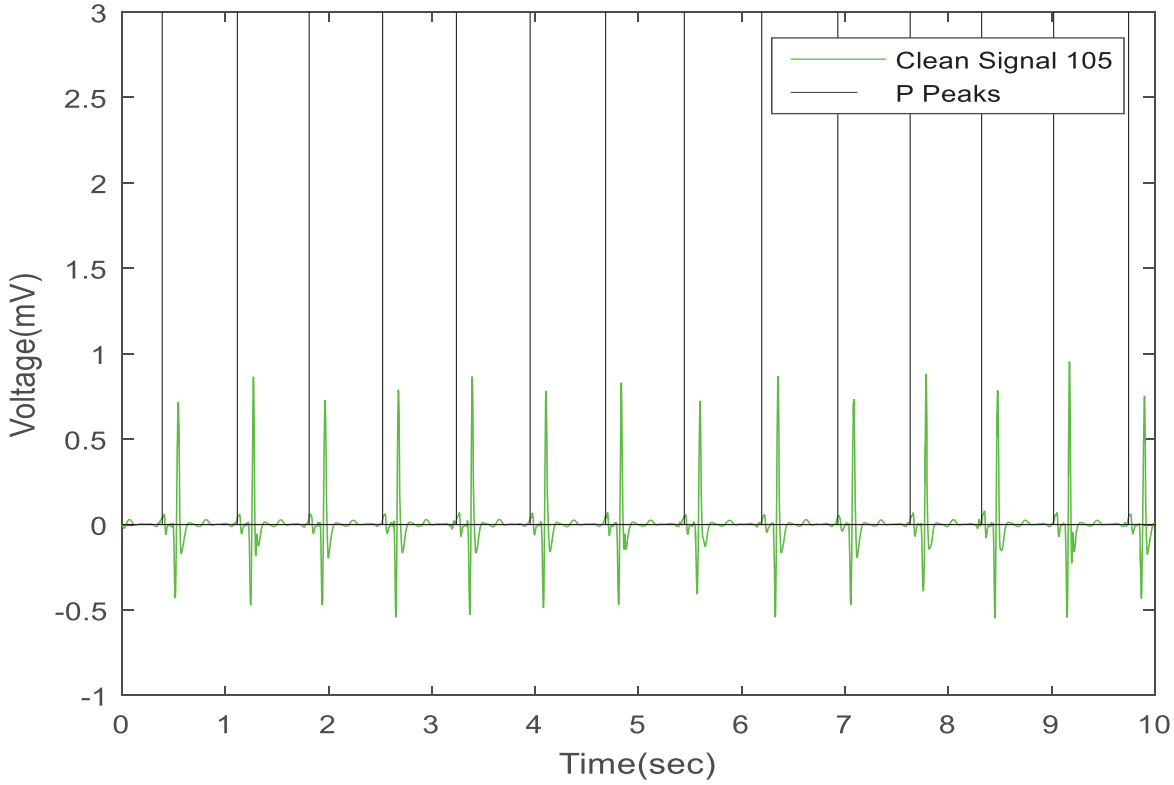

FIGURE 69. Detected peaks of P-waves in ECG signal 105.

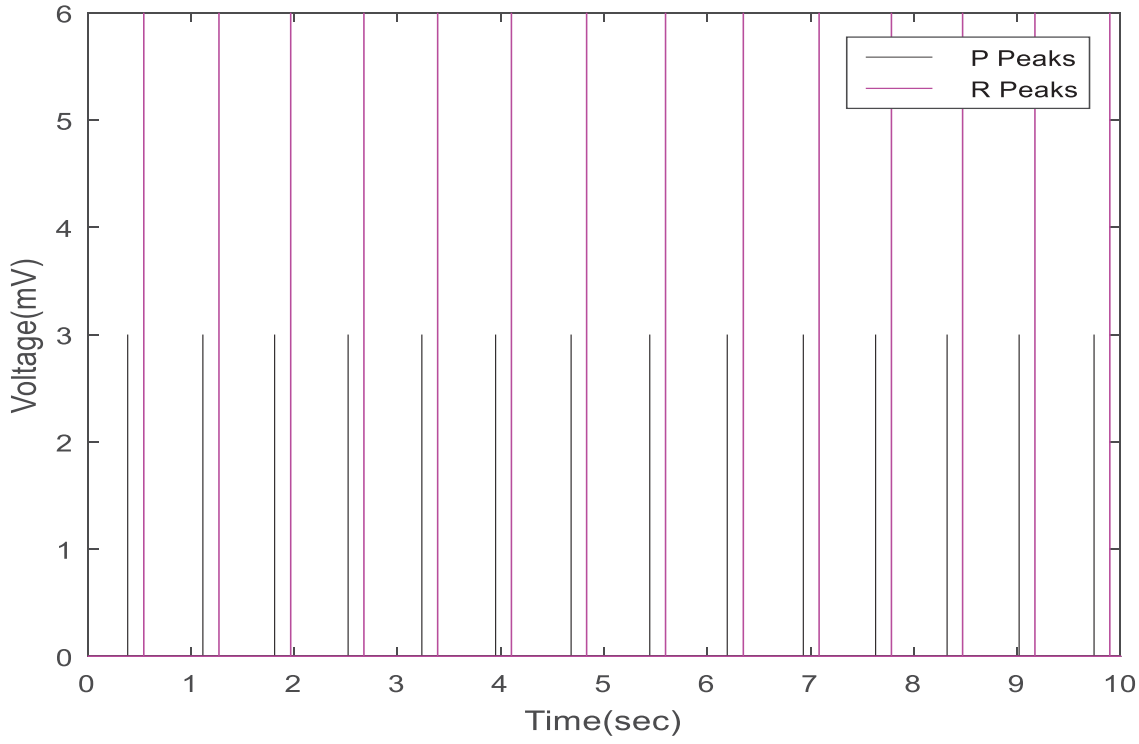

FIGURE 70. Concatenated detected peaks for P-R interval estimation in ECG signal 105.

```
The total R peaks in the signal are 14
R-R Interval is not constant!!!!
The signal is abnormal!!!!
Still check P-P Interval???
The total P peaks in the signal are 14
P-P Interval is not constant!!!!
The signal is abnormal!!!!
Still check P-R Interval???
P-R Interval is not constant!!!!
As all the three intervals are varying, the signal is abnormal!!!!
Please visit a doctor immediately.
```

FIGURE 71. ECG signal 105 characterization.

Signal 119

Figures 72 and 73, respectively, show the original ECG signal 119 consisting of the WB artifact and the check for the interference of the power supply on the ECG signal 119 by converting it to the frequency domain and observing its frequency response in dB and Hz. There is no effect of the PI artifact on the ECG signal 119 as no significant spike is observed at 50 Hz.

Figure 74 depicts the removal of the WB artifact from the ECG signal 119, and Figure 75 removes the WGN from the signal in which the WB artifact with and without eliminating the WB artifact from the signal. Therefore, by comparing both the graphs in Figure 75, it can be realized that the signal becomes clean after removing the WGN and WB artifact. Figure 75 proves that by removing the WGN before the detection stage distinguishes the peaks and valleys of the waves in the ECG signal.

Figures 76, 77, and 78, respectively, display the peaks of the R-waves, P-waves, and its concatenation for calculating the P-R interval. The accurate detection of the peaks of the waves

in the ECG signal does not change the morphology of the ECG signal. Figure 79 describes the ECG signal 119 as abnormal since all the three intervals vary along the length of the signal. It also shows the total number of peaks of the waves in the ECG signal.

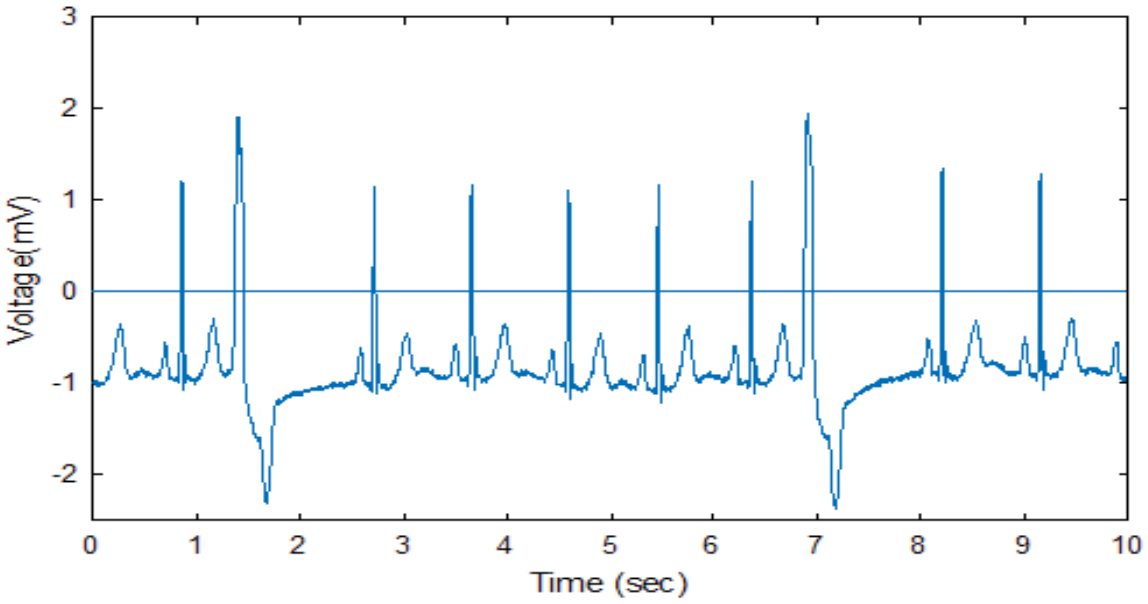

FIGURE 72. ECG signal 119.

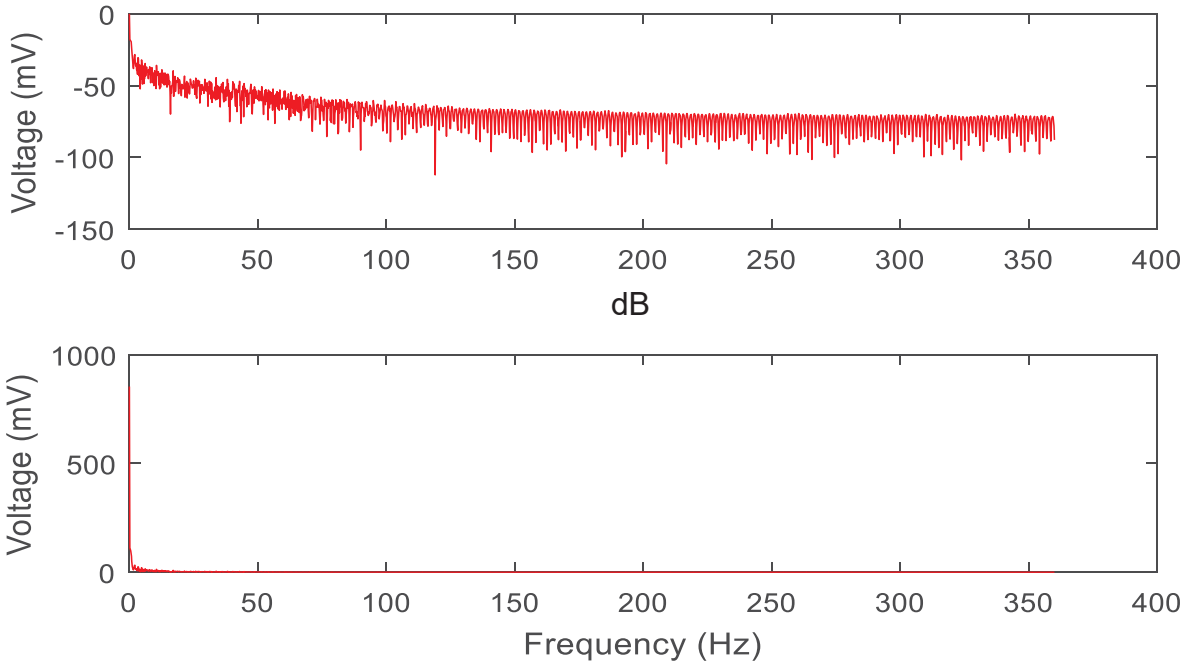

FIGURE 73. Check for spike at 50 Hz in dB and Hz in signal 119.

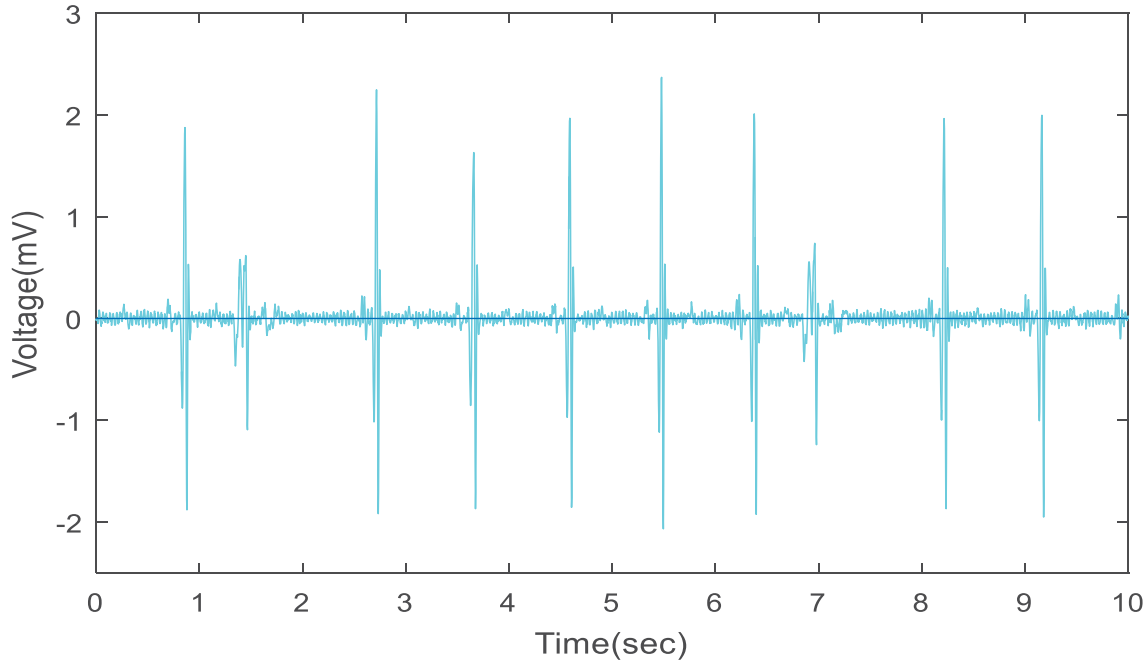

FIGURE 74. WB removed in ECG signal 119.

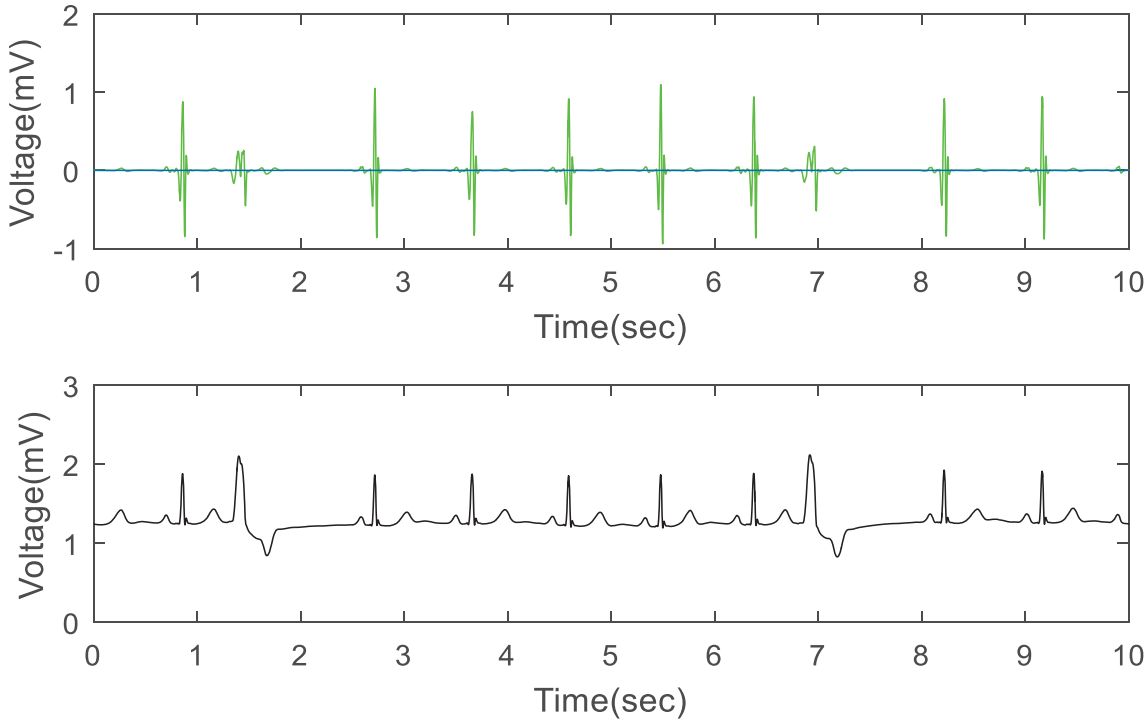

FIGURE 75. WGN removed in ECG signal 119 with and without eliminating the WB artifact.

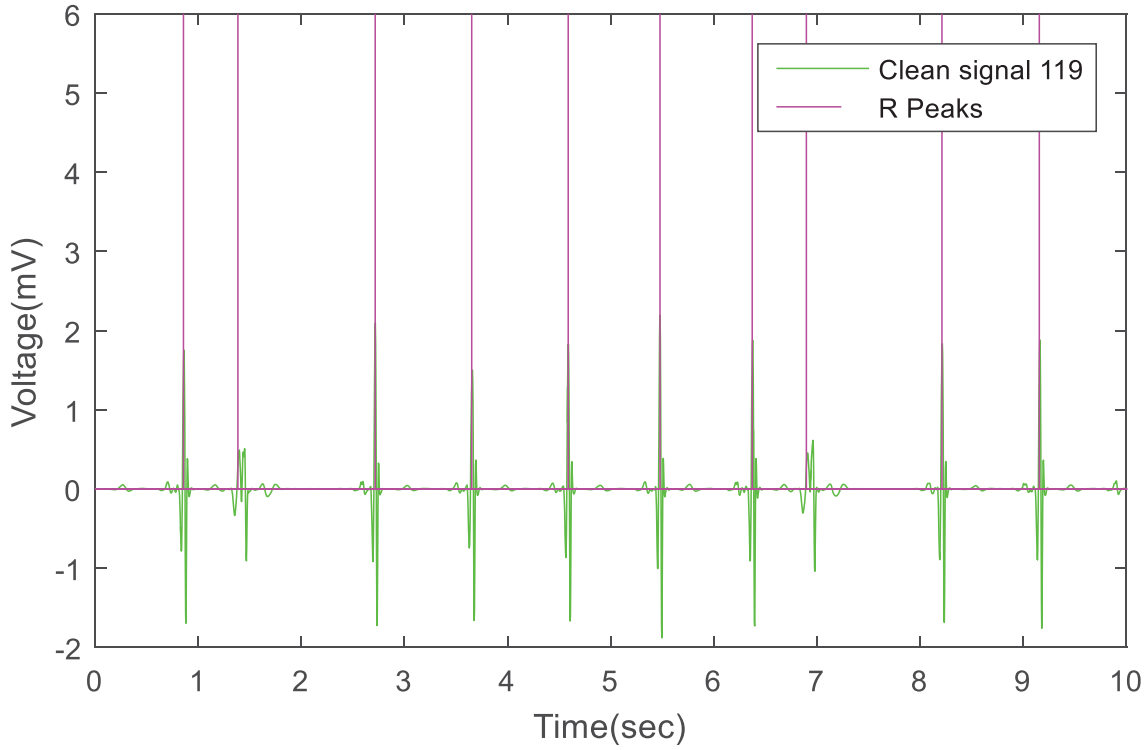

FIGURE 76. Detected peaks of R-waves in ECG signal 119.

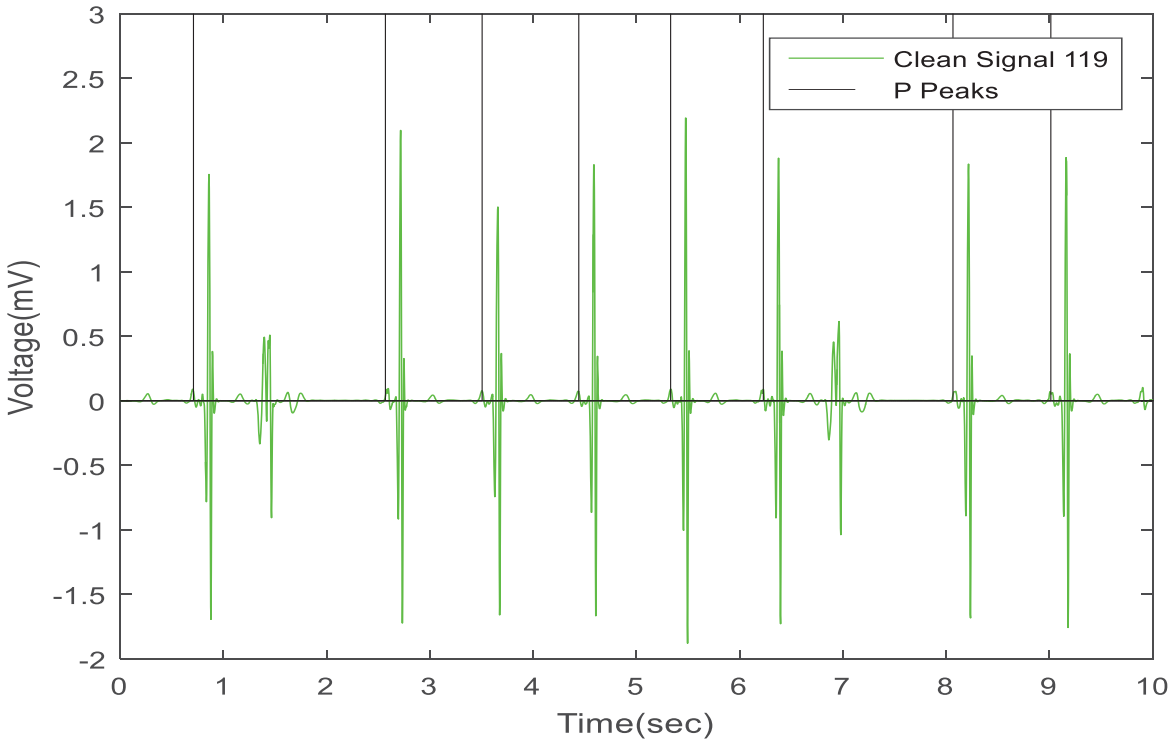

FIGURE 77. Detected peaks of P-waves in ECG signal 119.

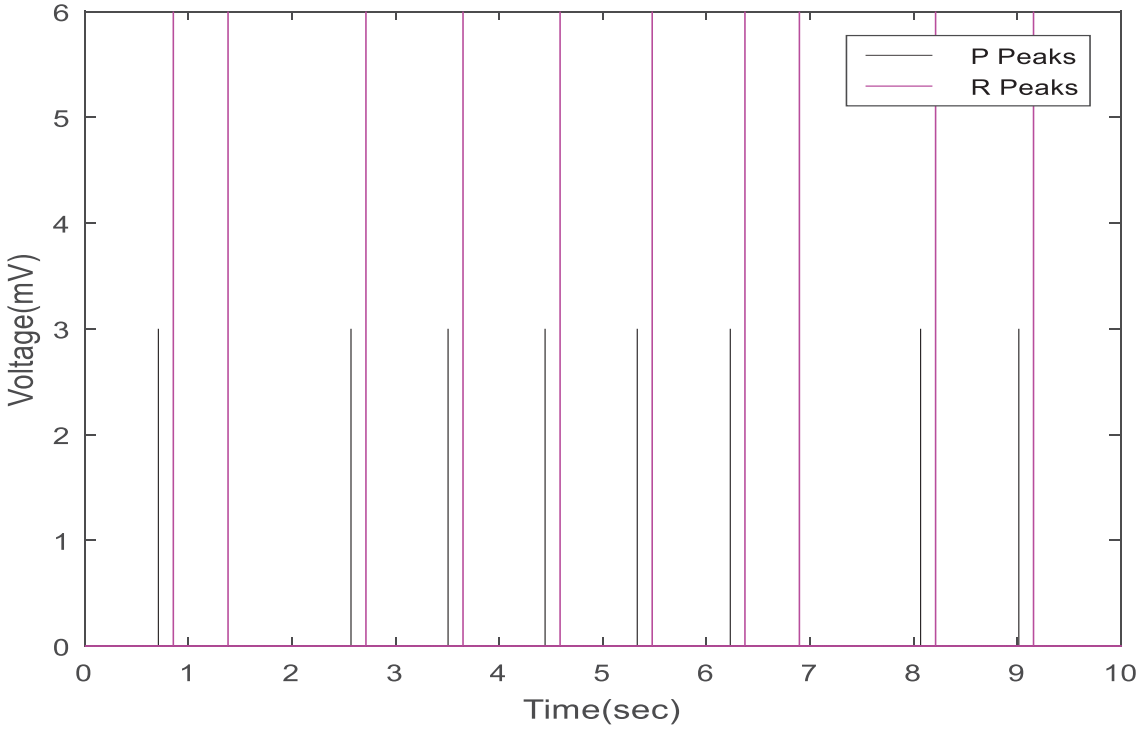

FIGURE 78. Concatenated detected peaks for P-R interval estimation in ECG signal 119.

```
The total R peaks in the signal are 10
R-R Interval is not constant!!!!
The signal is abnormal!!!!
Still check P-P Interval???
The total P peaks in the signal are 8
P-P Interval is not constant!!!!
The signal is abnormal!!!!
Still check P-R Interval???
P-R Interval is not constant!!!!
As all the three intervals are varying, the signal is abnormal!!!!
Please visit a doctor immediately.
```

FIGURE 79. ECG signal 119 characterization.

Signal 16272

Figures 80, 81, and 82, respectively, display the original ECG signal 16272 along with the WB artifact, the signal's frequency response in dB and Hz, and the deduction of the WB artifact from it. Figure 81 clearly signifies the absence of the spike at 50 Hz, and thus the signal is free from the effect of the PI artifact.

Figure 83 confirms the successful removal of the WGN from the ECG signal 16272 in with and without eliminating the WB artifact. Therefore, by comparing both the graphs in Figure 83, it is realized that the signal becomes clean after removing the WGN. Figure 83 proves that by removing the WGN before the detection stage distinguishes the peaks and valleys of the waves in the ECG signal.

Figures 84, 85, and 86, respectively, display the detected peaks of the R-waves, P-waves, and its concatenation to estimate the P-R interval in the ECG signal 16272. Figure 87 describes the ECG signal 16272 as normal due to the three intervals remaining constant along the length of the signal. It also calculates the total number of the R-waves and P-waves present in the ECG signal 16272.

Signal 17052

Figures 88, 89, and 90, respectively, display the original ECG signal 17052 with the presence of the WB artifact, the frequency response of the signal in dB and Hz, and the elimination of the WB artifact from the signal. No significant spike is observed at 50 Hz in Figure 89. Therefore, there is no effect of the PI artifact on the ECG signal 17052.

Figure 91 depicts the removal of the WGN from the ECG signal 17052 with and without removing the WB artifact. The comparison of both the graphs in Figure 91 clearly depicts the clean signal after removing the WGN and the WB artifact.

Figures 92, 93, and 94, respectively, display the detected peaks of the R-waves, P-waves, and its concatenation for estimating the P-R interval in the ECG signal 17052. Figure 95 describes the ECG signal 17052 as normal as all the three intervals remain constant along the length of the signal. The algorithm also calculates the total number of the R-waves and P-waves present in the ECG signal 17052.

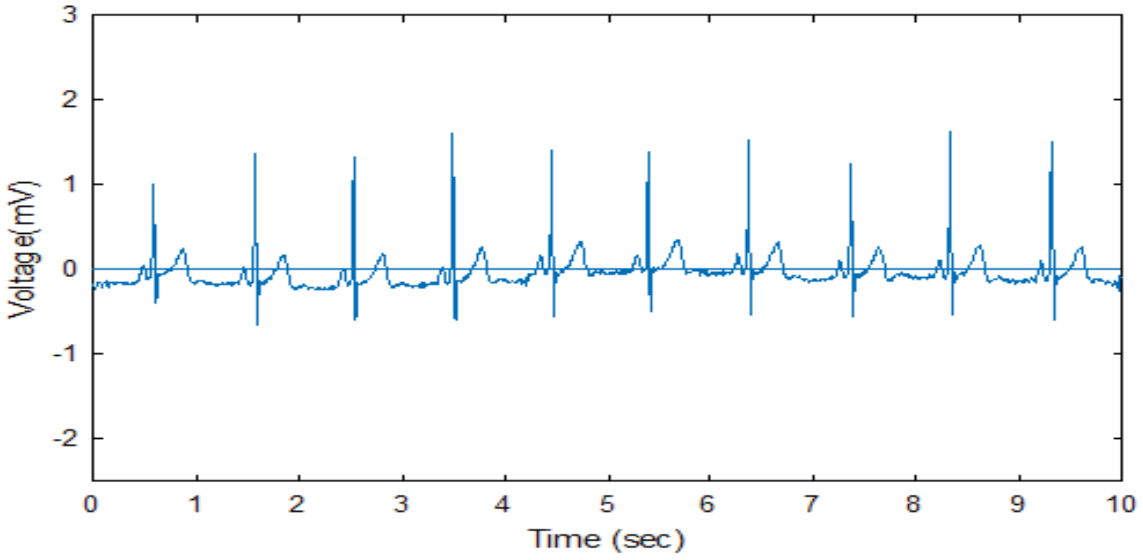

FIGURE 80. ECG signal 16272.

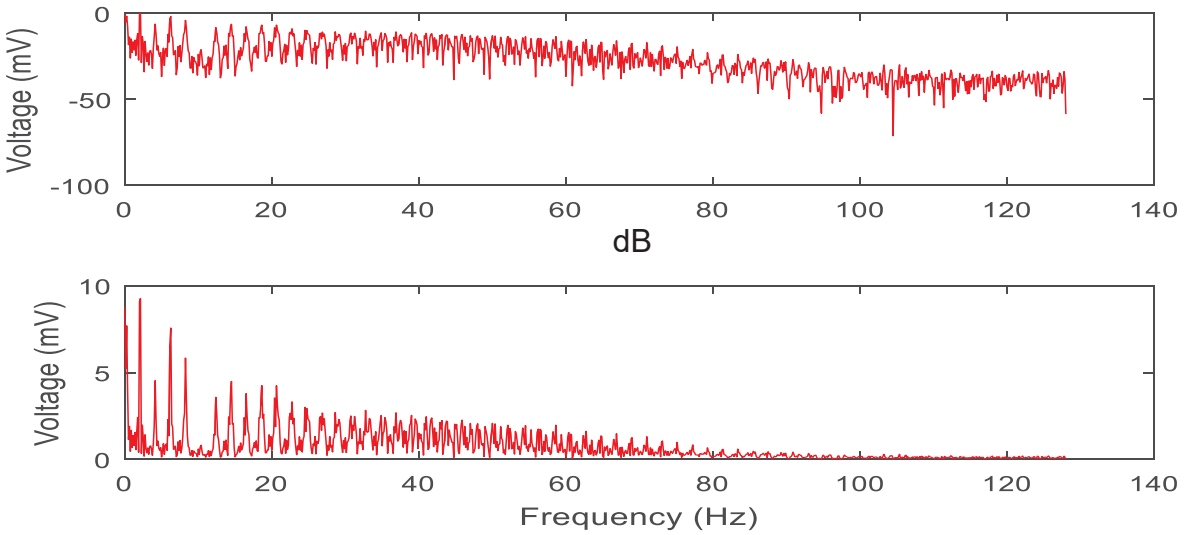

FIGURE 81. Check for spike at 50 Hz in dB and Hz in signal 16272.

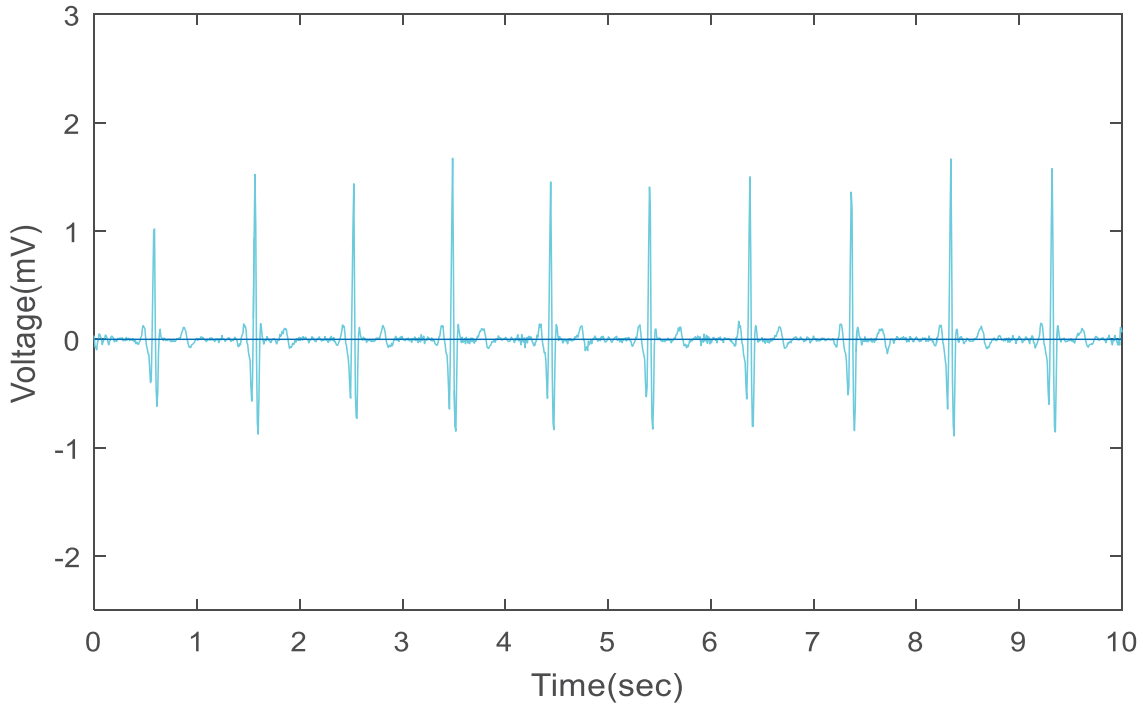

FIGURE 82. WB removed in ECG signal 16272.

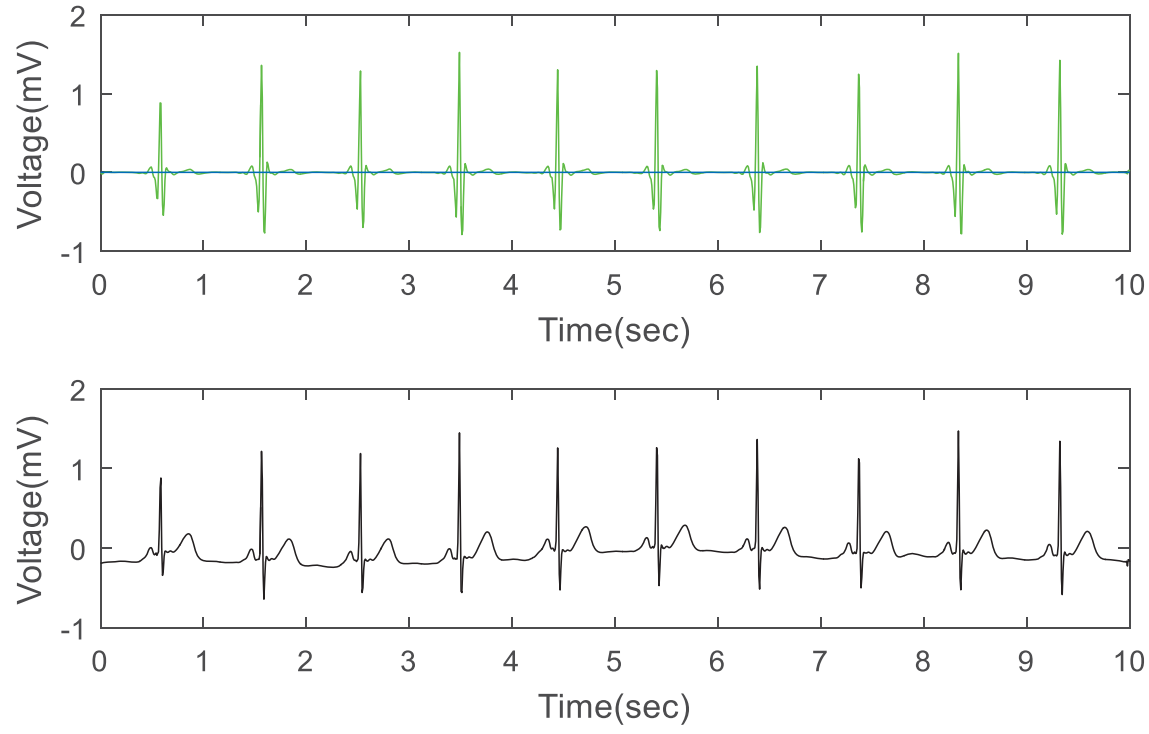

FIGURE 83. WGN removed in ECG signal 16272 with and without eliminating the WB artifact.

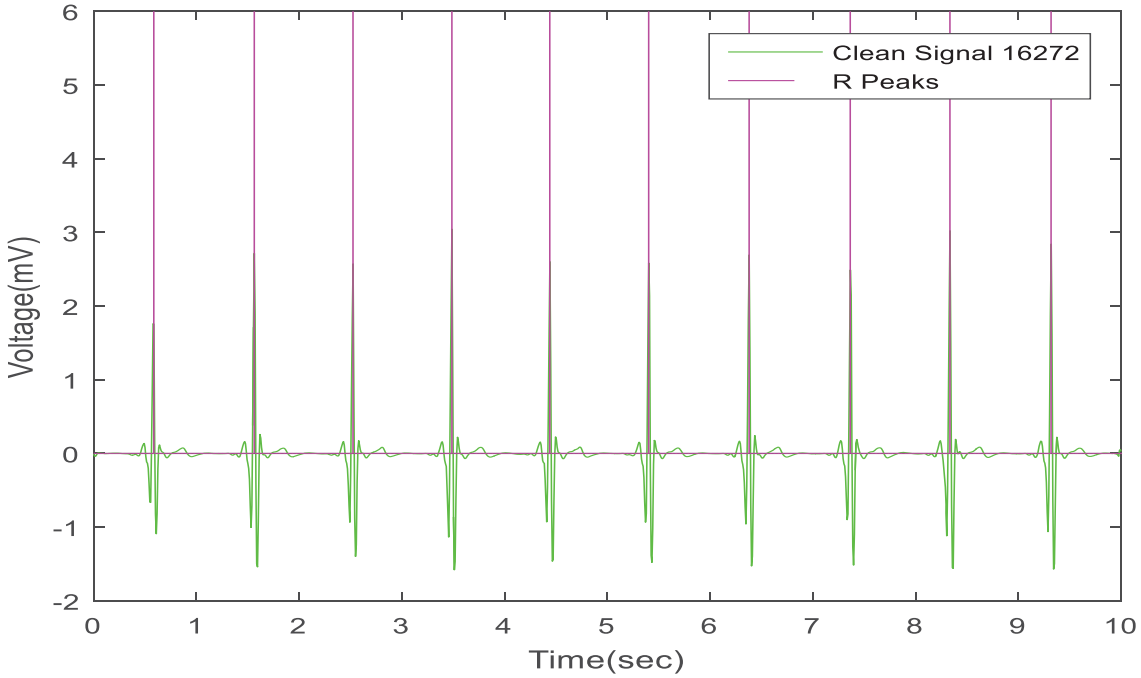

FIGURE 84. Detected peaks of R-waves in ECG signal 16272.

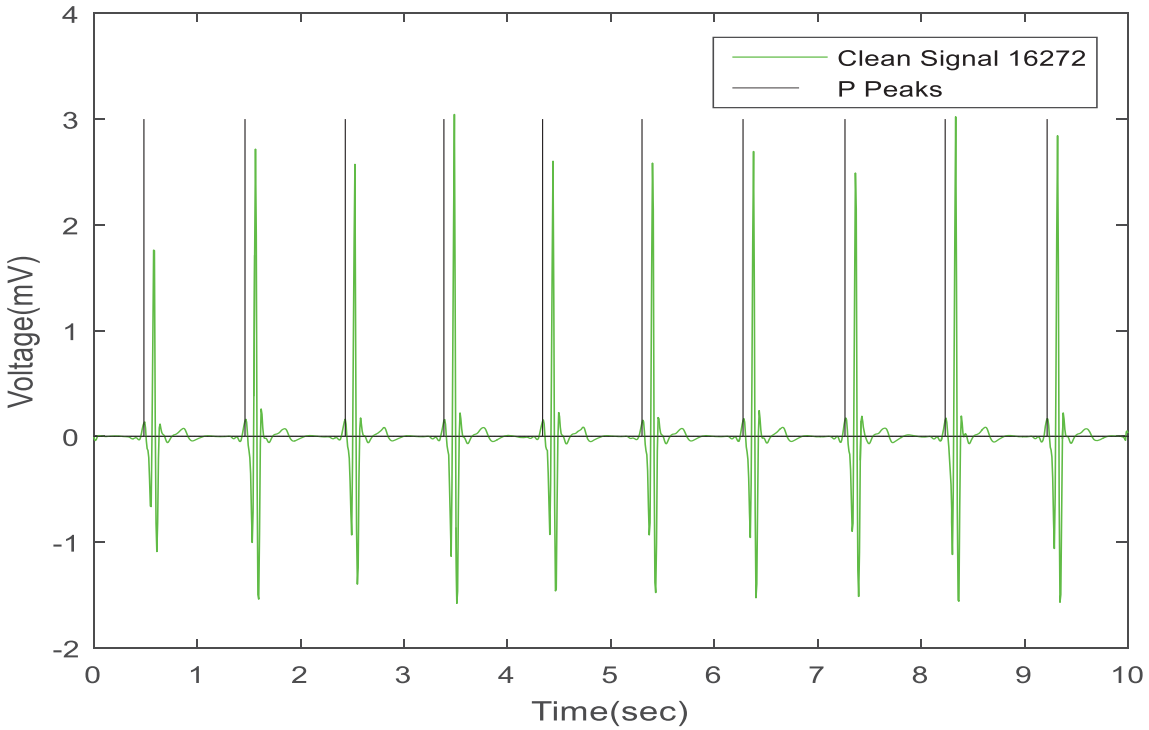

FIGURE 85. Detected peaks of P-waves in ECG signal 16272.

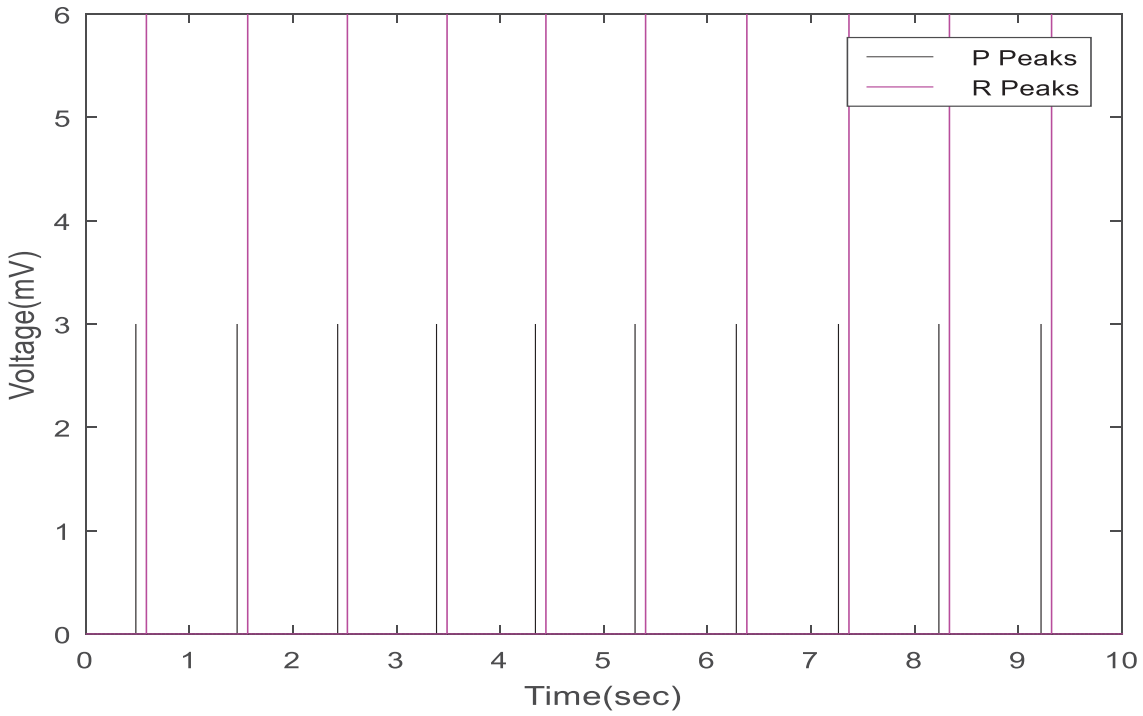

FIGURE 86. Concatenated detected peaks for P-R interval estimation in ECG signal 16272.

```
The total R peaks in the signal are 10
R-R Interval is constant.
Check for P-P Interval.....
The total P peaks in the signal are 10
P-P Interval is constant.
Check for P-R Interval.
P-R Interval is constant.
The signal is normal.
```

FIGURE 87. ECG signal 16272 characterization.

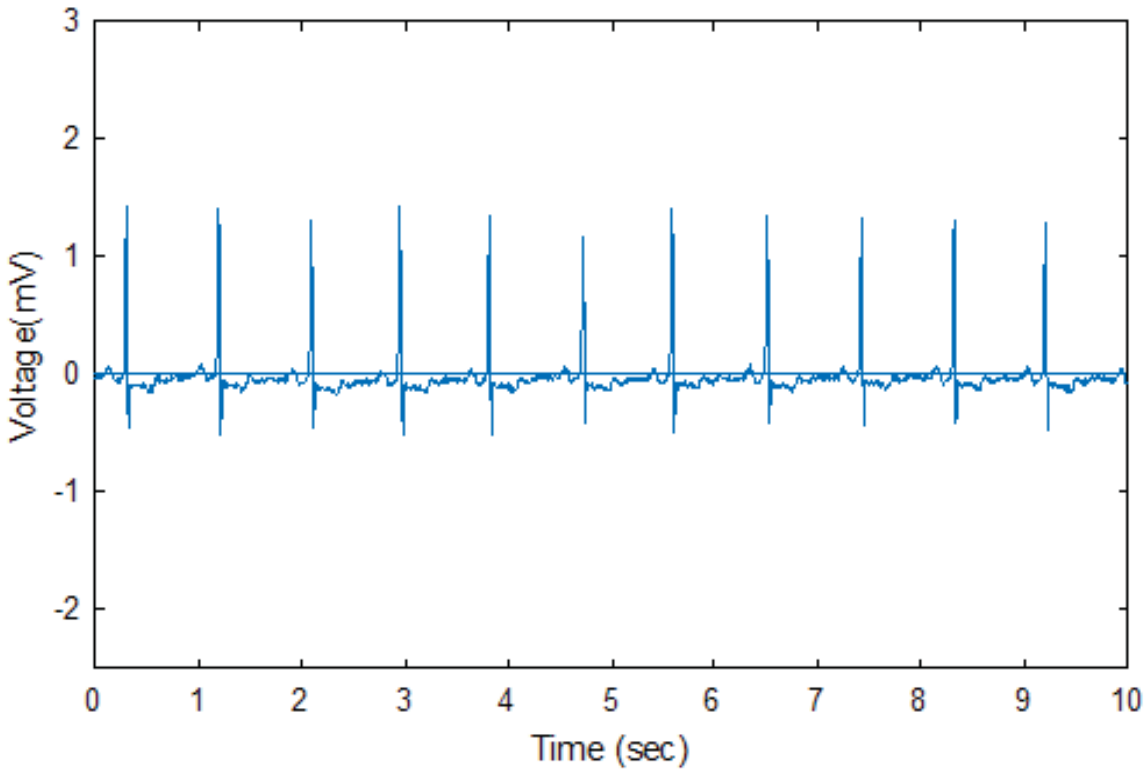

FIGURE 88. ECG signal 17052.

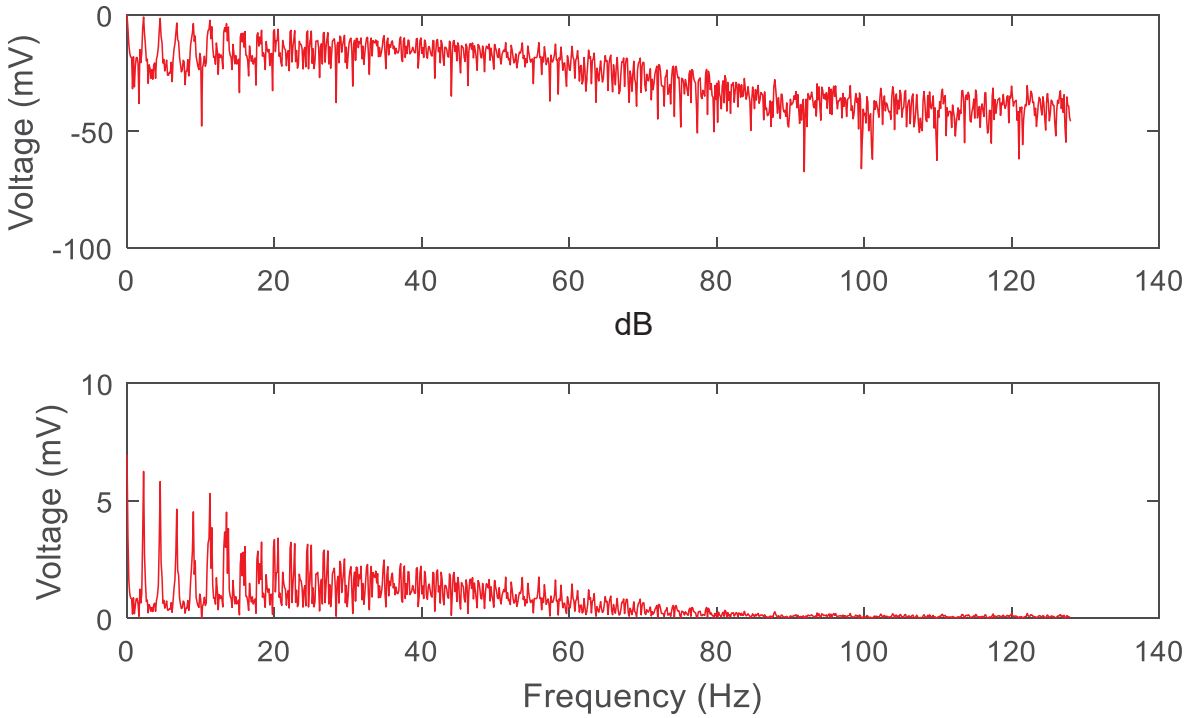

FIGURE 89. Check for spike at 50 Hz in dB and Hz in signal 17052.

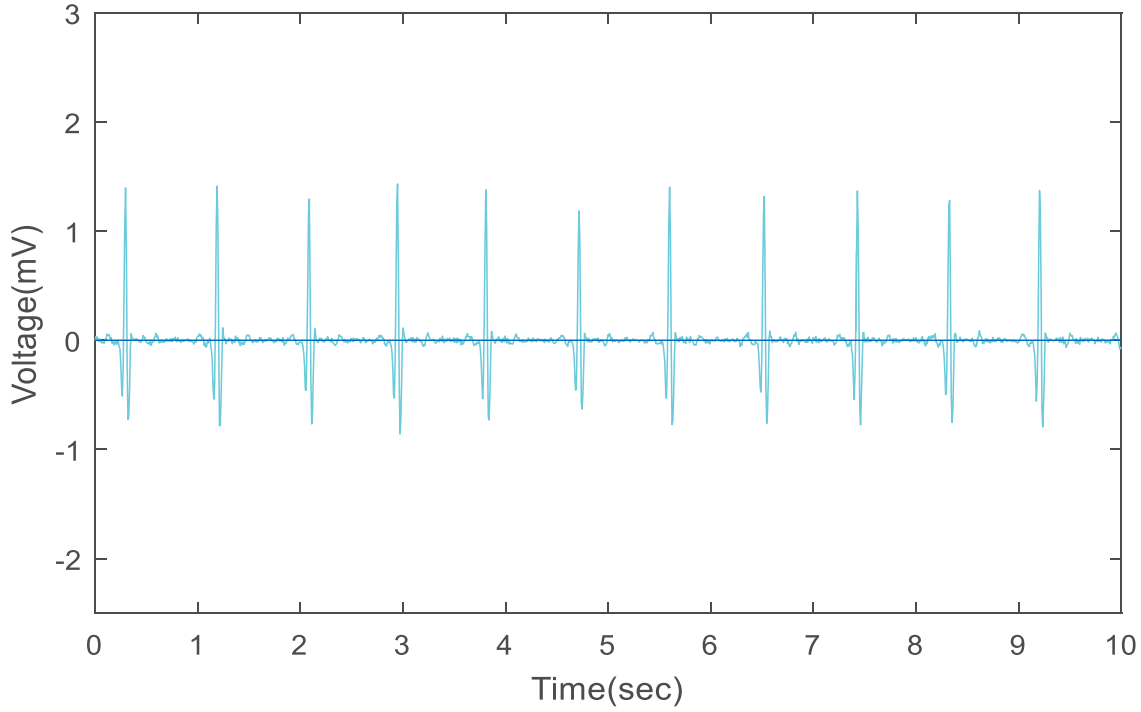

FIGURE 90. WB removed in ECG signal 17052.

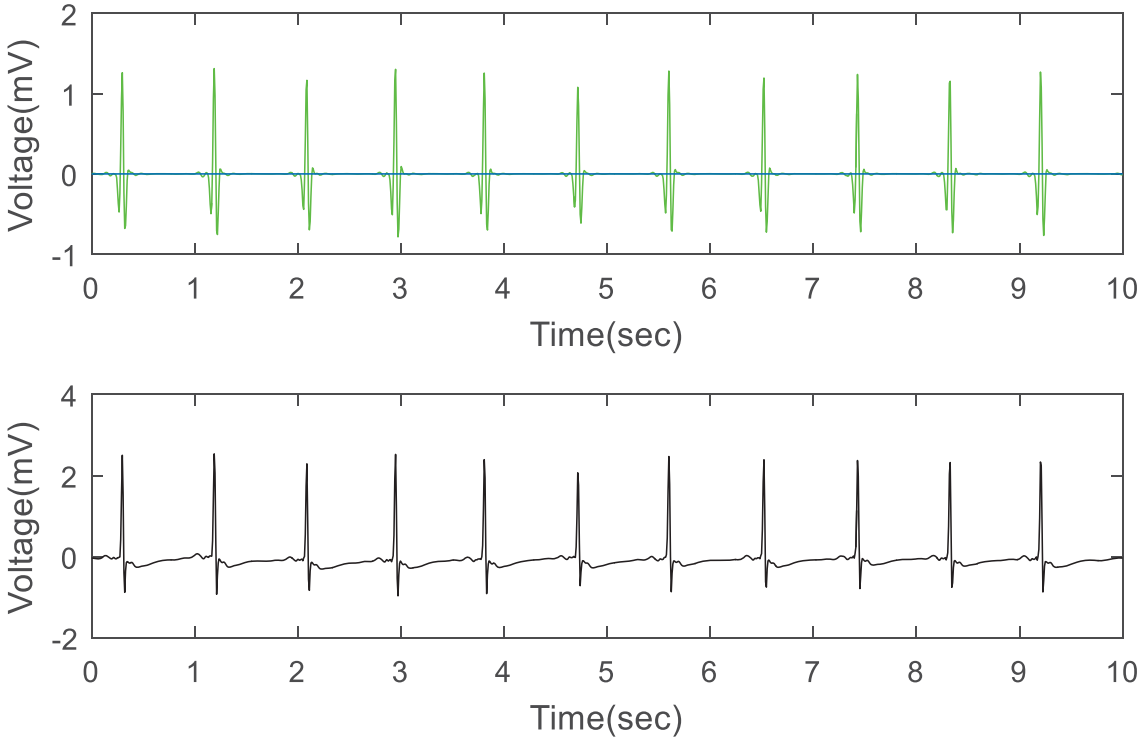

FIGURE 91. WGN removed in ECG signal 17052 with and without removing the WB artifact.

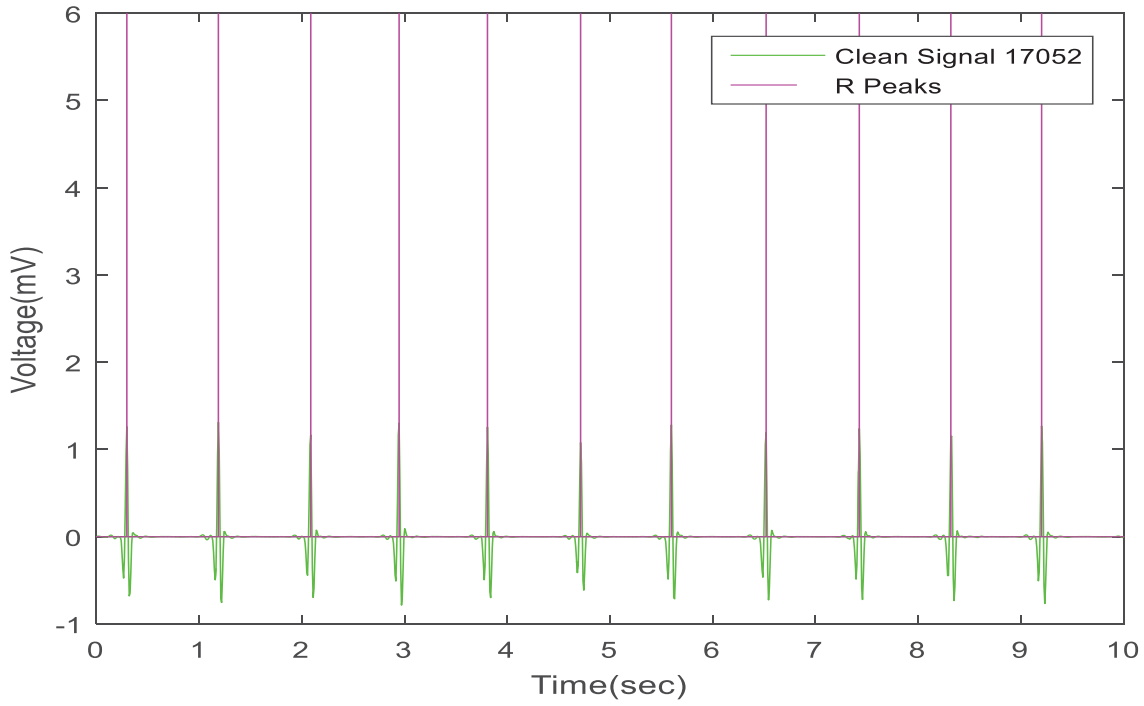

FIGURE 92. Detected peaks of R-waves in ECG signal 17052.

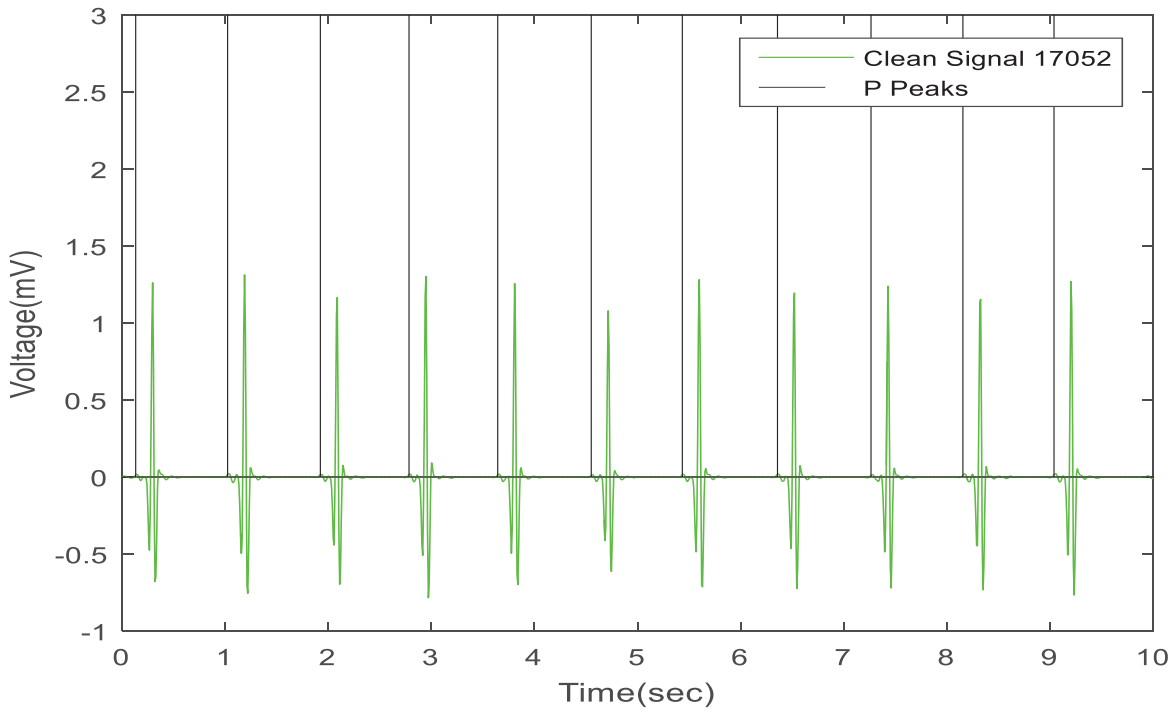

FIGURE 93. Detected peaks of P-waves in ECG signal 17052.

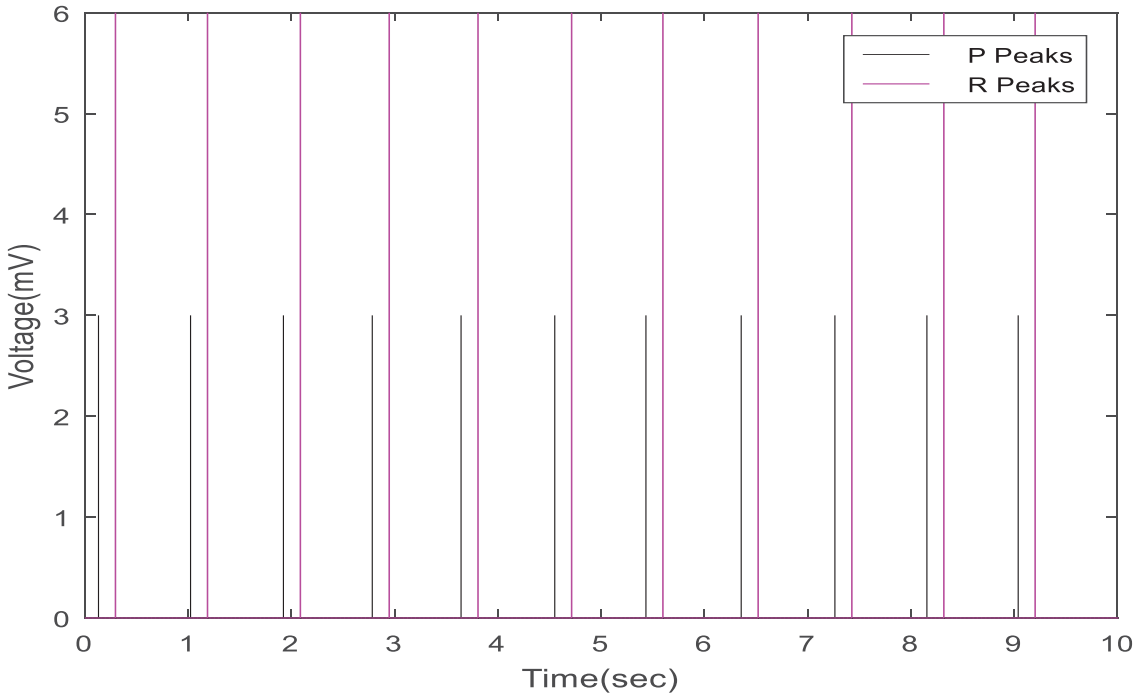

FIGURE 94. Concatenated detected peaks for P-R interval estimation in ECG signal 17052.

```
The total R peaks in the signal are 11
R-R Interval is constant.
Check for P-P Interval....
The total P peaks in the signal are 11
P-P Interval is constant.
Check for P-R Interval....
P-R Interval is constant.
The signal is normal.
```

FIGURE 95. ECG signal 17052 characterization.

Signal 17453

Figure 96 displays the original ECG signal 17453 obtained from the database. This ECG signal consists of the WB artifact. Figure 97 demonstrates whether a spike is present at 50 Hz in the ECG signal 17453 or not by inspecting its frequency response in dB and Hz. Fortunately, no significant spike is observed at 50 Hz. Therefore, there is no effect of the PI artifact on the ECG signal 17453.

Figure 98 indicates the elimination of the WB artifact from the ECG signal 17453. Figure 99 confirms the removal of the WGN from the ECG signal 17453 with and without eliminating the WB artifact. Therefore, by comparing both the graphs in Figure 99, it can be realized how clean the signal becomes after removing the WGN. Figure 99 proves that by removing the WGN before the detection stage distinguishes the peaks and valleys of the waves in the ECG signal.

Figures 100 and 101, respectively, display the detected peaks of the R-waves and P-waves of the ECG signal 17453 by using the hard threshold technique of the wavelets. The accurate peaks of the R-waves and P-waves are detected with the algorithm described in Chapter 4. Therefore, the execution of the signal processing using the wavelets does not change the morphology of the ECG signal. Figure 102 demonstrates the concatenation of the peaks of the R-waves and P-waves of the ECG signal 17453 for estimating the P-R interval.

Figure 103 describes that the ECG signal 17453 is abnormal as the R-R interval is not constant along the length of the signal. The algorithm also calculates the total number of the R-waves and P-waves present in the ECG signal 17453. Figure 103 also displays the total R-waves and P-waves present in the signal.

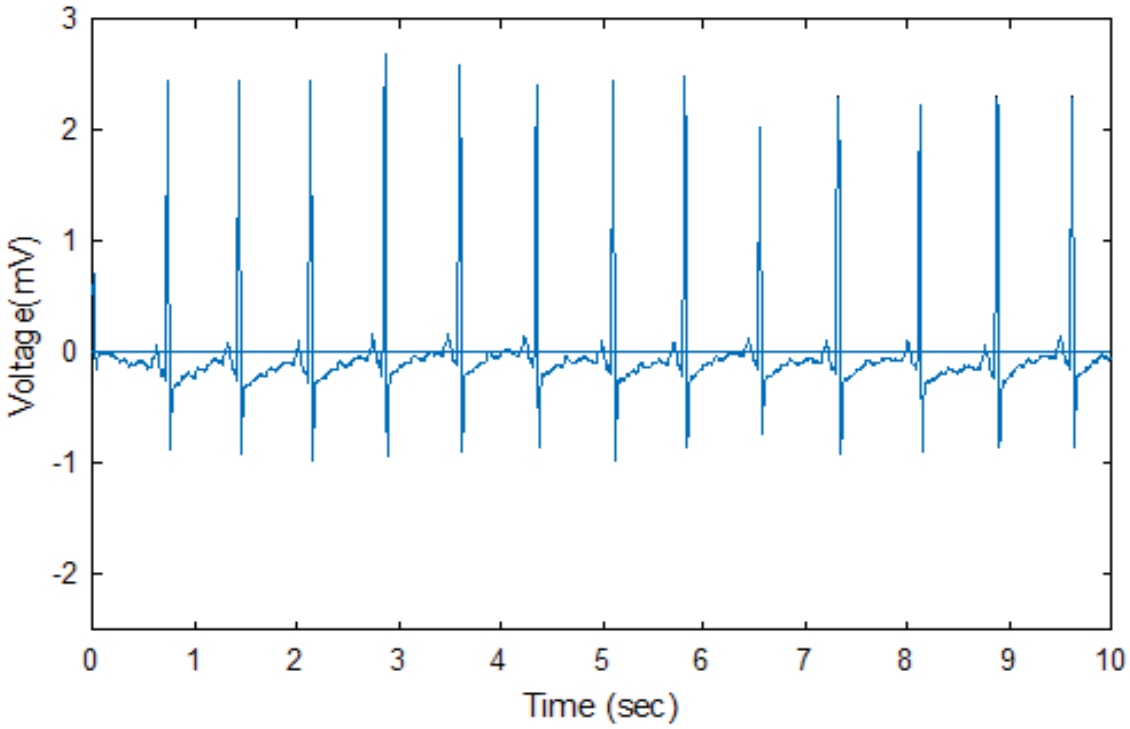

FIGURE 96. ECG signal 17453.

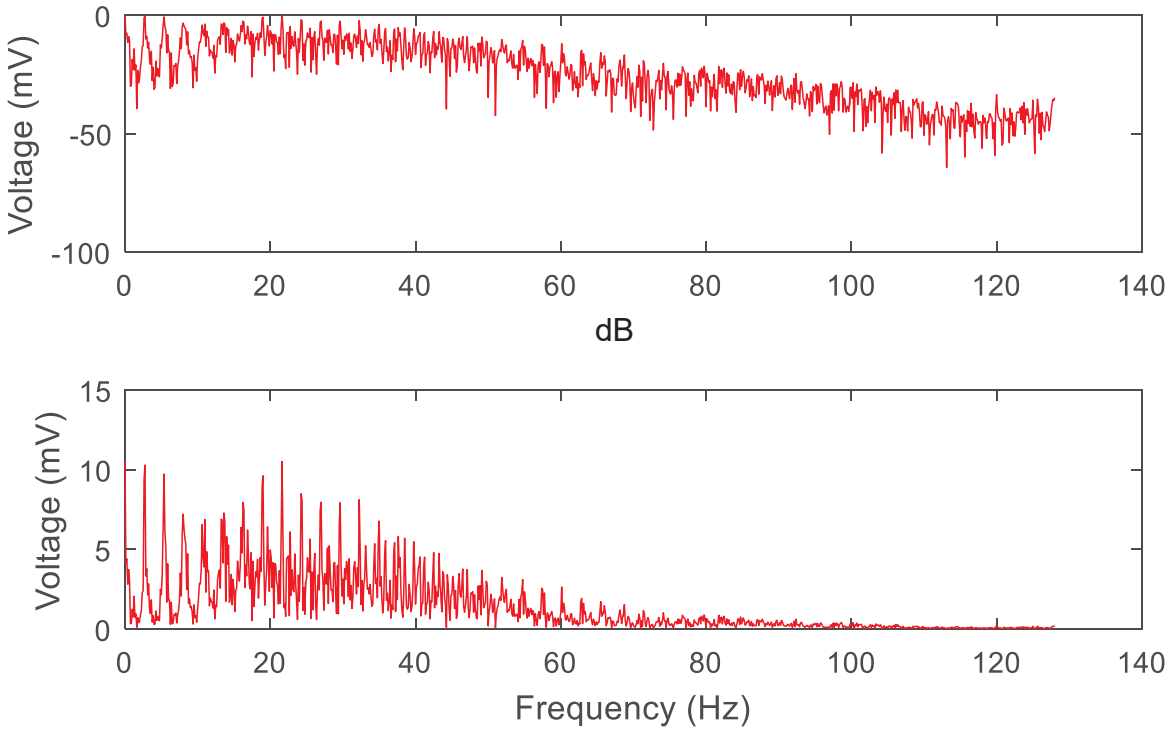

FIGURE 97. Check for spike at 50 Hz in dB and Hz in signal 17453.

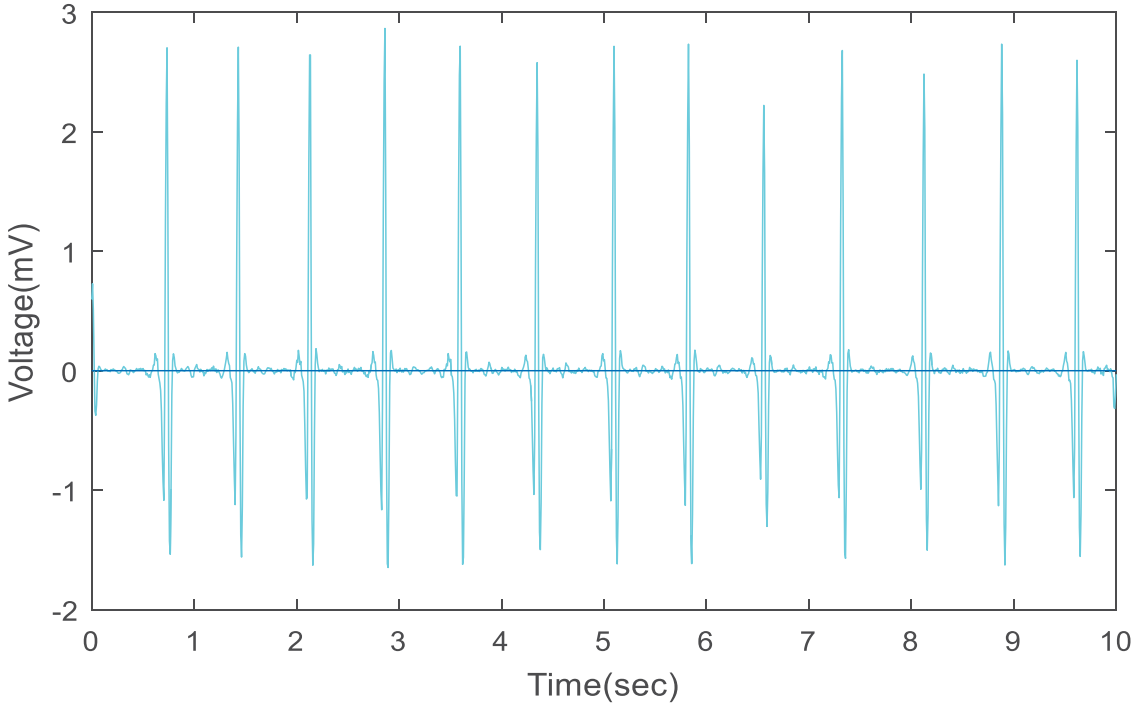

FIGURE 98. WB removed in ECG signal 17453.

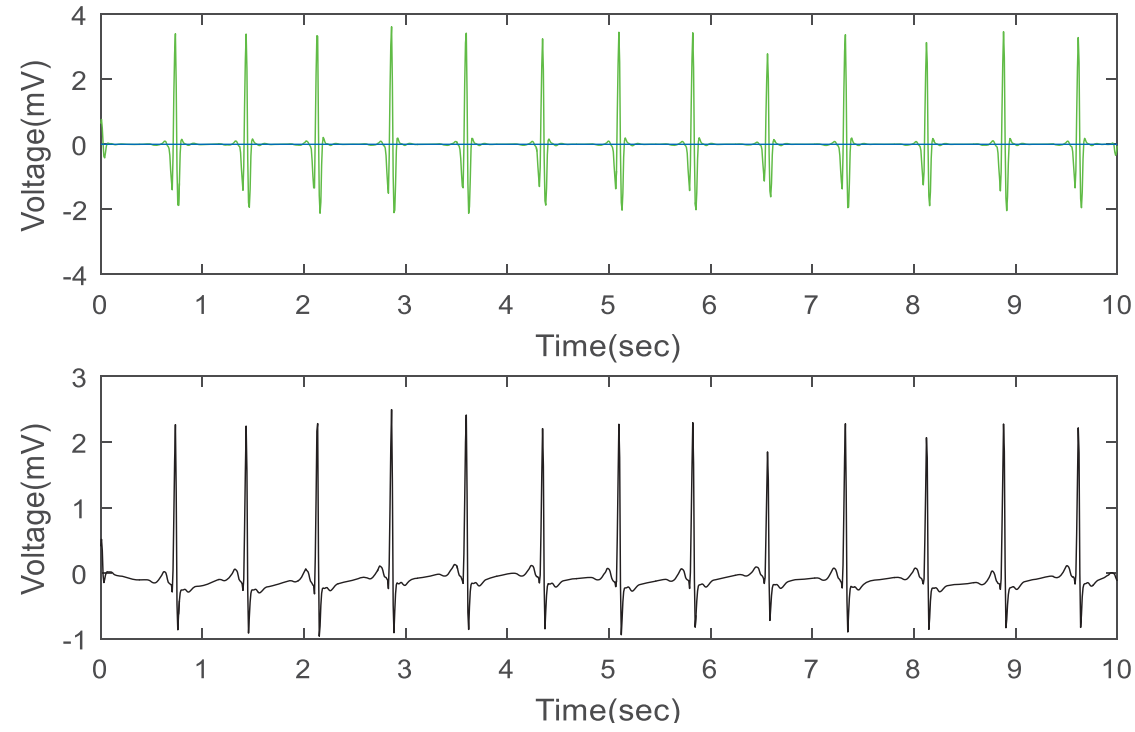

FIGURE 99. WGN removed in ECG signal 17453 with and without eliminating the WB artifact.

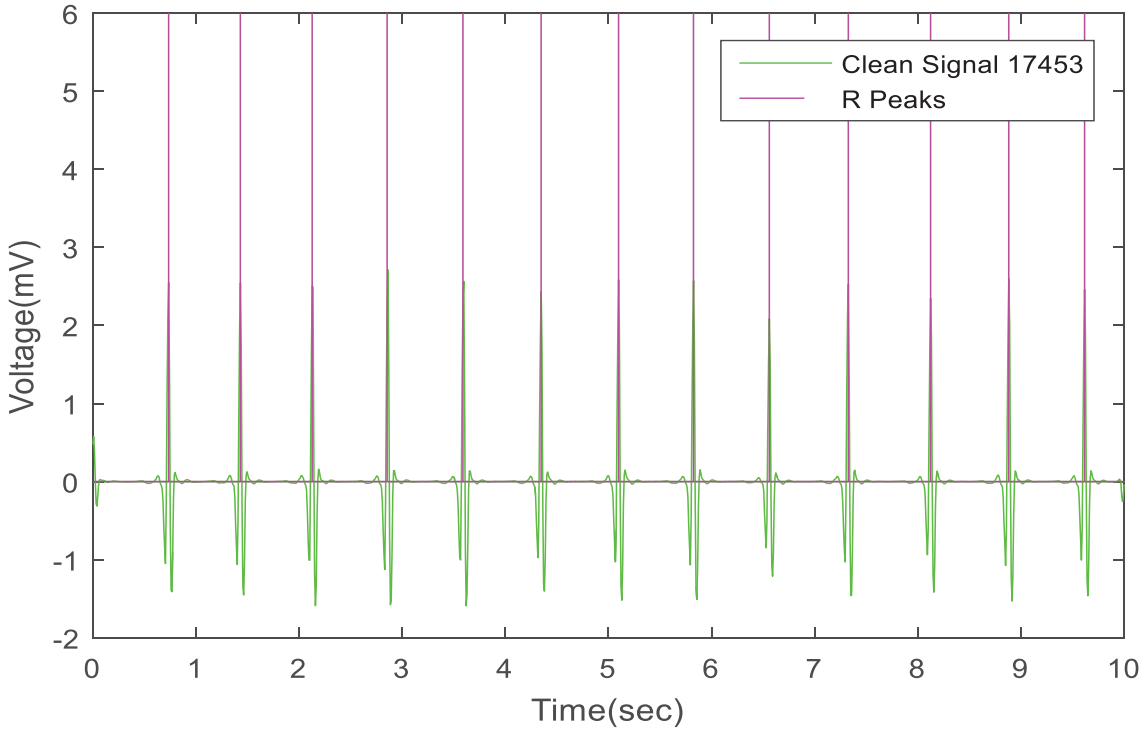

FIGURE 100. Detected peaks of R-waves in ECG signal 17453.

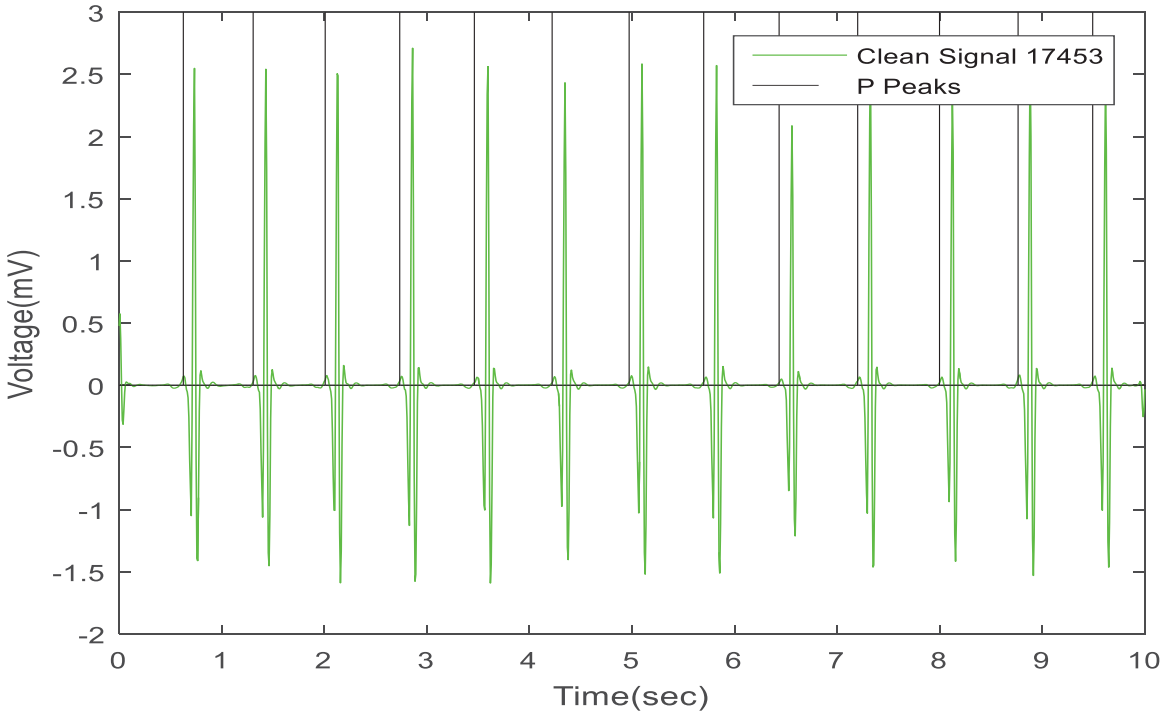

FIGURE 101. Detected peaks of P-waves in ECG signal 17453.

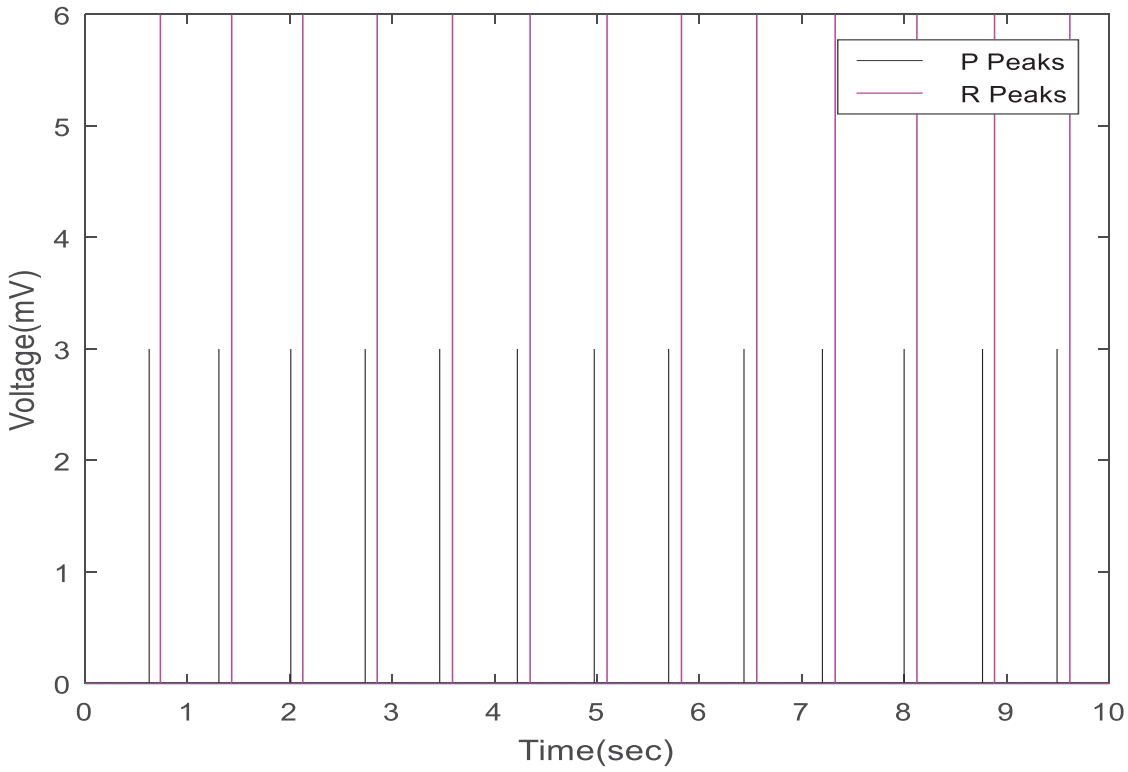

FIGURE 102. Concatenated detected peaks for P-R interval estimation in ECG signal 17453.

```
The total R peaks in the signal are 13
R-R Interval is not constant.
The signal is abnormal..
Check P-P Interval....
The total P peaks in the signal are 13
P-P Interval is constant!!!!
Check P-R Interval....
P-R Interval is constant.
The signal is abnormal as the R-R interval varies.
```

FIGURE 103. ECG signal 17453 characterization.

APPENDIX B

MATLAB CODE

```
clc;
clear all;
close all;
% The code describes the characterization of ECG signal to be a normal
% signal or an abnormal signal in steps as described in the algorithm
thyval=1243; % threshold value
refval = 850; % reference peak value
tolref = 249; % reference tolerance value
const = 55; % constant refrence value
rpeakx=1; % x axis for the detection of R peaks of the ECG signal
rpeakdistance=0; % distance between two R peaks in the ECG signal
rpeaktotal=0; % total peaks
count=1;  % counter in detecting r peaks
count2=1; % Counter 2 in detecting p peaks
ucount1=1; % counter 1 in detecting interval
prdetectionvalue=1; % initialization for detection of PR interval
prdistancecalculation=0; % distance between two PR intervals
totalprpeaks=0; % total peaks in the PR interval
count3=1; % counter in detecting PR interval
% Load Signal from the database
load ('105m.mat'); % load signal
figure(1); % plot number
plotATM('105m'); % Database signal plotting function
hold on;
line([0 10], [0 0]); % horizontal line at 0V for reference
ylabel('Voltage(mV)'); % labelling y axis
axis([0 10 -2.5 3]) % setting axis range
title('Original Signal 105'); % title of the plot
l=linspace(0,10,3600); % Creating samples of the signal
% Checking the interference of power supply on the signal
samplefrequency=360; % sampling frequency
sampletime = 1/samplefrequency;  % sampling time
lengthsignal = 3600;  % total length of the signal
t = (0:lengthsignal-1)*sampletime; % Time vector
pointnfft = 2^nextpow2(lengthsignal); % Generating n point fft
totalsamples=val; % Assigning value to the samples
frequencyresponse = fft(totalsamples,pointnfft)/lengthsignal; % generating frequency response
using fft
r=linspace(0,1,pointnfft/2+1); % samples according to the length of the signal
fadjustfrequencyresponse = samplefrequency*r; % frequency response of the signal
frequencyresponsenpoint=abs(frequencyresponse(1:pointnfft/2+1)); % Taking absolute value of
the frequency response
k=0:pointnfft-1; % npoint Vector
figure(2); % plot number
subplot(2,1,1);
% observing the frequency response in db
```

```
plot(fadjustfrequencyresponse,20*log10(frequencyresponsenpoint/max(frequencyresponsenpoint
)),'red');
ylabel('Voltage (mV)');
xlabel('db');
title ('Poweline Interference Check in db');
subplot(2,1,2);
% figure('DefaultAxesFontSize',20,'DefaultAxesFontName', 'Times New Roman');
% observing the frequency response in Hertz
plot(fadjustfrequencyresponse,frequencyresponsenpoint,'red');
xlabel('Frequency (Hz)');
ylabel('Voltage (mV)');
title ('Poweline Interference Check in Hz');
% Removing the Wandering Baseline from the ECG signal
% generating filter coefficients
[decomposelowpasscoeff,decomposehighpasscoeff,recomposelowpasscoeff,recomposehighpassc
oeff] = wfilters('db4');
% Calculating one level of discrete wavelet transform
[approxcoeff,detailcoeff] = dwt(val,decomposelowpasscoeff,decomposehighpasscoeff);
% reconstructing the signal using inverse discrete wavelet transform
reconstructedsignal =
idwt(approxcoeff,detailcoeff,recomposelowpasscoeff,recomposehighpasscoeff);
wandereliminated=val-reconstructedsignal; % wandering baseline removed
figure(3);
subplot(2,1,1);
plotATM('105m'); % plotting original ECG signal
hold on;
line([0 10], [0 0]); % horizontal line at 0V for reference
ylabel('Voltage(mV)');
axis([0 10 -2.5 3]) % seetting axis range
title('Original Signal 105');
subplot(2,1,2);
plot(l,wandereliminated.*10^10,'cyan'); % plotting wandering baseline removed signal
hold on;
line([0 10],[0 0]); % horizontal line at 0V for reference
xlabel('Time(sec)');
ylabel('Voltage(mV)');
axis([0 10 -2.5 3]) % setting axis range
title('Eliminated Wandering Baseline');
% Eliminating white Gaussian noise from the ECG Signal
% removing white Gaussian noise at level 4 in original signal using universal threshold
% technique
signaldenoise = wden(val,'modwtsqtwolog','s','mln',4,'db4');
figure(4);
% plotting original ECG signal
subplot(3,1,1);
plotATM('105m'); % original signal plot
```

```
hold on;
line([0 10], [0 0]); % horizontal line at 0V for reference
ylabel('Voltage(mV)');
axis([0 10 -2.5 3]) % setting axis range
title('Original Signal 105');
% plotting clean signal
subplot(3,1,2);
plot(l,signaldenoise.*1.5*10^-3,'black'); % plotting denoised signal
hold on;
line([0 10], [1.4 1.4]); % horizontal line at 1.4V for reference
xlabel('Time(sec)');
ylabel('Voltage(mV)');
title('Signal denoised without wandering baseline removal');
% removing white Gaussian noise at level 4 in wandering baseline removed signal using
universal threshold
% technique
signeldenoise = wden(wandereliminated,'modwtsqtwolog','s','mln',4,'db4');
subplot(3,1,3);
plot(l,signeldenoise.*10^10,'green'); % plotting noise free signal
hold on;
line([0 10], [0 0]); % horizontal line at 0V for reference
xlabel('Time(sec)');
ylabel('Voltage(mV)');
title('Signal denoised without wandering baseline removal');
% Logic for finding peaks of R waves in the ECG Signal
cleanlengthsig=length(signaldenoise);
%Logic for determining tentative peak location
for i = 1:cleanlengthsig
   if signaldenoise(1,i) > thyval
         peakvalreferencec(i)=refval;
   else
      peakvalreferencec(i)=0;
   end
end
rpeaks=zeros(1,lengthsignal); % calculating non peak values
%Logic for determining exact peaks
for i=1:cleanlengthsig
   if peakvalreferencec(i) > 0 && peakvalreferencec(i)==peakvalreferencec(i-1)
      rpeaks(i)=0;
   elseif peakvalreferencec(i)>0
      rpeaks(i)=6;
   else
      rpeaks(i)=0;
   end
end
figure(5);
```

```
plot(l,signeldenoise.*10^10,'green'); % noise free signal
hold on;
line([0 10], [0 0]); % horizontal line at 0V for reference
stem (l,rpeaks,'Marker','none','LineWidth',0.5,'Color',[1 0 1]);
xlabel('Time(sec)');
ylabel('Voltage(mV)');
title('R Peaks detected in signal 105');
legend('Clean signal 105','R Peaks');
% Logic for detecting R-R intervals
for count=1:cleanlengthsig
   if rpeaks(count)==0
      rpeakdistance=rpeakdistance+1;
   else
      rpeakx(count)=rpeakdistance;
      rpeakdistance=rpeakdistance+1;
      continue;
   end
end
count=1; % resetting counter

rpeakstotal1=zeros(1,14); % reference for R peaks
for count=1:lengthsignal-37
   if rpeakx(count)~=0
      rpeaktotal=rpeaktotal+1;
      rpeakstotal1(ucount1)=rpeakx(count);
      ucount1=ucount1+1;
   else
      continue;
   end
end
rpeaktotal=rpeaktotal-1; % removing the extra peak detected by the loop
%Print the total peaks in the signal
% fprintf('\nThe total R peaks in the signal are %d\n',rpeaktotal);
%determining the distance between two peaks
for ppeaks=1:rpeaktotal + 1
   if rpeakstotal1(ppeaks)~=1
      ap1(count2)=rpeakstotal1(ppeaks);
      count2=count2+1;
   else
      continue;
   end
end
rintervalestimate=0; % interval value
% tolerance calculation
for count=2:rpeaktotal
   rintervalvalue=abs(ap1(count)-ap1(count-1));
```

```
    if rintervalvalue>tolref
        rintervalestimate=rintervalestimate+1;
    else
        continue;
    end
end
% determining normal or abnormal signal
if rintervalestimate==rpeaktotal - 1
    display('R-R Interval is constant.');
    display('Check P-P Interval...');
else
    display('R-R Interval is not constant!!!!');
    display('The signal is abnormal!!!!');
    display('Still check P-P Interval???');
end
% Logic for determinig Peaks of P waves in the ECG signal
 ppeaksinitialize=zeros(1,lengthsignal);
  % determining tentative peaks of the signal
for i=1:cleanlengthsig-const
    if signaldenoise(1,i)> refval+(2*const)&&signaldenoise(i+const)-signaldenoise(i)>tolref-9
        ppeaksinitialize(i)=1300;
    else
        ppeaksinitialize(i)=0;
    end
end
% determining exact peaks of the signal
countppeaks=zeros(1,lengthsignal);
for i=1:cleanlengthsig
    if ppeaksinitialize(i) > 0 && ppeaksinitialize(i-1)==ppeaksinitialize(i)
        countppeaks(i)=0;
    elseif ppeaksinitialize(i) > 0
        countppeaks(i)=3;
    else
        countppeaks(i)=0;
    end
end
figure(6);
plot(l,signeldenoise.*10^10,'green'); % noise free signal
hold on;
line([0 10],[0 0]); % reference line at 0V
stem (l,countppeaks,'Marker','none','LineWidth',0.2,'Color',[1 1 0]); % plot for detection of peaks
of P waves in the ECG signal
xlabel('Time(sec)');
ylabel('Voltage(mV)');
title('P Peaks detected in clean signal 105');
legend('Clean Signal 105','P Peaks');
```

```
%Logic for determining P-P intervals
for count=1:cleanlengthsig
   if countppeaks(count)==0
      rpeakdistance=rpeakdistance+1;
   else
      rpeakx(count)=rpeakdistance;
      rpeakdistance=rpeakdistance+1;
      continue;
   end
end
count=1;
ucount1=1;
rpeakstotal1=zeros(1,rpeaktotal);
for count=1:lengthsignal-92
   if rpeakx(count)~=0
      rpeaktotal=rpeaktotal+1;
      rpeakstotal1(ucount1)=rpeakx(count);
      ucount1=ucount1+1;
   else
      continue;
   end
end
rpeaktotal=rpeaktotal-1;
%Print the total P peaks in the signal
%fprintf('The total P peaks in the signal are %d\n',rpeaktotal);
count2=1;
for ppeaks=1:15
   if rpeakstotal1(ppeaks)~=1
      ap1(count2)=rpeakstotal1(ppeaks);
      count2=count2+1;
   else
      continue;
   end
end
rintervalestimate=0;
for count=2:14
   rintervalvalue=abs(ap1(count)-ap1(count-1));
   if rintervalvalue>tolref
      rintervalestimate=rintervalestimate+1;
   else
      continue;
   end
end
if rintervalestimate==rpeaktotal-1
   display('P-P Interval is constant.');
   display('Check P-R Interval...');
```

```
else
   display('P-P Interval is not constant!!!!');
   display('The signal is abnormal!!!!');
   display('Still check P-R Interval???');
end
% Detect PR Intervals
prpeaksforinterval = countppeaks + rpeaks;
figure(7);
stem (l,countppeaks,'Marker','none','LineWidth',0.2,'Color',[1 1 0]); % plotting peaks of P waves
of the ECG signal
hold on;
stem (l,rpeaks,'Marker','none','LineWidth',0.5,'Color',[1 0 1]); % plotting peaks of R waves of the
ECG signal
xlabel('Time(sec)');
ylabel('Voltage(mV)');
title('Detected P Peaks and R Peaks with the Denoised Signal 105');
legend('P Peaks','R Peaks');
% Logic for determining PR interval
for count3=1:cleanlengthsig
   if prpeaksforinterval(count3)==0
      prdistancecalculation=prdistancecalculation+1;
   else
      prdetectionvalue(count3)=prdistancecalculation;
      prdistancecalculation=prdistancecalculation+1;
      continue;
   end
end
count3=1;
uintervalpr1=1;
totalprpeaksdeterminep=zeros(1,28);
for count3=1:lengthsignal-37
   if prdetectionvalue(count3)~=0
      totalprpeaks=totalprpeaks+1;
      totalprpeaksdeterminep(uintervalpr1)=prdetectionvalue(count3); % ap stores the value of pr
      uintervalpr1=uintervalpr1+1;
   else
      continue;
   end
end
totalprpeaks=totalprpeaks-1;
peakprc1=1;
for counter1=1:29
   if totalprpeaksdeterminep(counter1)~=1
      a1p1(peakprc1)=totalprpeaksdeterminep(counter1);
      peakprc1=peakprc1+1;
   else
```

```
        continue;
    end
end
printervalestimate=0;
printervaltolerance=0;
for count3=2:2:28
    x1t=abs(a1p1(count3)-a1p1(count3-1));
    if x1t>59
        printervalestimate=printervalestimate+1;
    else
        printervaltolerance=printervaltolerance+1;
        continue;
    end
end
if printervalestimate==rpeaktotal-2
    display('P-R Interval is constant.');
    display('The signal is normal.');
else
    display('P-R Interval is not constant!!!!');
    display('As all the three intervals are varying, the signal is abnormal!!!!');
    display('Please visit a doctor immediately.');
end
```

REFERENCES

REFERENCES

[1] D. C. Schechter, "*Diagnostic Electrocardiography by Michael C. Ritota, MD, D. Sc., JB Lippincott Co., Philadelphia, 1969, 174 pp. $15.00*," *CHEST Journal,* vol. 57, pp. 596-596, 1970.

[2] B. J. Aehlert, *ECGs Made Easy.* St. Louis: Elsevier Health Sciences, 2015.

[3] M. B. Conover, *Understanding Electrocardiography: Physiological and Interpretive Concepts.* St. Louis: Mosby, 1980.

[4] M. AlGhatrif and J. Lindsay, "A brief review: History to understand fundamentals of electrocardiography," *Journal of Community Hospital Internal Medicine Perspectives,* vol. 2, 2012.

[5] J. Kubicek, M. Penhaker and, R. Kahankova, "Design of a synthetic ECG signal based on the Fourier series," *Proc. Intl. Conf. Advances in Computing, Communications and Informatics (ICACCI, 2014),* 2014, pp. 1881-1885.

[6] J. W. Hurst and R. J. Myerburg, *Introduction to Electrocardiography.* New York City: McGraw-Hill Companies, 1973.

[7] M. E. Silverman, R. J. Myerburg, and J. W. Hurst, *Electrocardiography, Basic Concepts and Clinical Application.* New York City: McGraw-Hill Companies, 1983.

[8] A. Graps, "An introduction to wavelets," *IEEE Computational Science and Engineering,* vol. 2, pp. 50-61, 1995.

[9] I. Daubechies, *Ten Lectures on Wavelets.* Philadelphia: SIAM, vol. 61, 1992.

[10] C. Torrence and G. P. Compo, "A practical guide to wavelet analysis," *Bull. Am. Meteorol. Soc.,* vol. 79, pp. 61-78, 1998.

[11] P. E. McSharry, G. D. Clifford, L. Tarassenko, and L. A. Smith, "A dynamical model for generating synthetic electrocardiogram signals," *IEEE Transactions on Biomedical Engineering,* vol. 50, pp. 289-294, 2003.

[12] G. D. Clifford and P. E. McSharry, "A realistic coupled nonlinear artificial ECG, BP and respiratory signal generator for assessing noise performance of biomedical signal processing algorithms," in *Proc. of SPIE,* 2004, pp. 291.

[13] J. Ackora-Prah, A. Y. Aidoo and, K. B. Gyamfi, "An artificial signal generating function in MATLAB™," *Applied Mathematical Sciences*, vol. 7, pp. 2675-2686, 2013.

[14] G. A. Kumar and S. Vegi, "Analyzing of an ECG signal mathematically by generating synthetic-ECG, " *International Journal of Engineering And Science*, vol. 4, pp. 39-44, 2015.

[15] P. M. Agante and J. P. Marques de Sa, "ECG noise filtering using wavelets with soft-thresholding methods," in *Computers in Cardiology,* vol. 26, pp. 535-538, 1999.

[16] M. Z. U. Rahman, R. A. Shaik, and D. R. K. Reddy, "Noise cancellation in ECG signals using computationally simplified adaptive filtering techniques: Application to biotelemetry," *Signal Processing: An International Journal (SPIJ),* vol. 3, pp. 1-12, 2009.

[17] Y. Sharma and A. Shrivastava, "Periodic noise suppression from ECG signals using novel adaptive filtering techniques," *International Journal of Electronics, Computer Science, and Engineering,* vol. 1, pp. 681-685, 1956.

[18] Z. H. Slimane and A. Naït-Ali, "QRS complex detection using Empirical Mode Decomposition," *Digital Signal Processing,* vol. 20, pp. 1221-1228, 2010.

[19] M. Kaur and B. Singh, "Comparison of different approaches for removal of baseline wander from ECG signal," in *Proceedings of the International Conference & Workshop on Emerging Trends in Technology,* 2011, pp. 1290-1294.

[20] M. Ayat, M. B. Shamsollahi, B. Mozaffari, and S. Kharabian, "ECG denoising using modulus maxima of wavelet transform," in Proc. *2009 Annual International Conference of the IEEE Engineering in Medicine and Biology Society,* 2009, pp. 416-419.

[21] R. Kumar and P. Patel, "Signal denoising with interval dependent thresholding using DWT and SWT," *International Journal of Innovative Technology and Exploring Engineering (IJITEE)* vol.1, pp. 2278-3075, 2012.

[22] M. Alfaouri and K. Daqrouq, "ECG signal denoising by wavelet transform thresholding," *American Journal of Applied Sciences,* vol. 5, pp. 276-281, 2008.

[23] S. Chen, H. Chen, and H. Chan, "A real-time QRS detection method based on moving-averaging incorporating with wavelet denoising," *Comput. Methods Programs Biomed.,* vol. 82, pp. 187-195, 2006.

[24] K. Tan, K. Chan, and K. Choi, "Detection of the QRS complex, P-wave and T wave in electrocardiogram," in *Proc. 2000 1st Intl. Conf. Advances in Medical Signal and Information Processing* (IEE Conf. Publ. no. 476), 2000, pp. 41-47.

[25] D. Nithya and S. Ravindrakumar, "Detection of cardiovascular abnormalities using peak detection and adaptive thresholding: A synthetic and real time approach," in *2012*

International Conference on Computing, Communication and Applications, 2012, pp. 1-5.

[26] S. Mahmoodabadi, A. Ahmadian, and M. Abolhasani, "ECG feature extraction using daubechies wavelets," in *Proceedings of the 5th IASTED International Conference on Visualization, Imaging and Image Processing,* 2005, pp. 343-348.

[27] Y. Zhong, L. Xu, L. Yan, Y. Shen, and S. Wang, "Adaptive R-wave detection method in dynamic ECG with heavy EMG artifact," in *Proc. 2012 Intl. Conf. Information and Automation (ICIA),* 2012, pp. 83-87.

[28] M. Bahoura, M. Hassani, and M. Hubin, "DSP implementation of wavelet transform for real time ECG wave forms detection and heart rate analysis," *Comput. Methods Programs Biomed.,* vol. 52, pp. 35-44, 1997.

[29] Cuiwei Li, Chongxun Zheng, and Changfeng Tai, "Detection of ECG characteristic points using wavelet transforms," *IEEE Transactions on Biomedical Engineering,* vol. 42, pp. 21-28, 1995.

[30] I. Nouira, A. B. Abdallah, M. H. Bedoui, and M. Dogui, "A robust R peak detection algorithm using wavelet transform for heart rate variability studies," *International Journal on Electrical Engineering and Informatics,* vol. 5, pp. 270-283, 2013.

[31] M. Akay, *Time Frequency and Wavelets in Biomedical Signal Processing.* (IEEE Press series in biomedical Engineering). Piscataway, New Jersey: IEEE Press, 1998.

[32] U. Zaka, B. A. Baloch, M. Alam, and I. Touqir, "Detection of peaks of ECG signal using wavelet transform," in *Proc. 2014 Natl. Software Engineering Conf. (NSEC),* 2014, pp. 43-47.

[33] I. Daubechies, "Where do wavelets come from? A personal point of view," *Proceedings of the IEEE,* vol. 84, pp. 510-513, 1996.

[34] A. Boggess and F. J. Narcowich, *A First Course in Wavelets with Fourier Analysis.* New Jersey: John Wiley & Sons, 2015.

[35] D. F. Walnut, *An Introduction to Wavelet Analysis.* Boston: Springer Science & Business Media, 2013.

[36] F. Nazan Ucar, M. Korurek, and E. Yazgan, "A noise reduction algorithm in ECG signals using wavelet transform," in *Proc. 1998 2nd Intl. Conf. Biomedical Engineering Days,* 1998, pp. 36-38.

[37] Mahipal Singh Chaudhary, Rajiv Kumar Kapoor, and Akshay Kumar Sharma, "Comparison between different wavelet transforms and thresholding techniques for ECG

denoising," in *Proc. 2014 Intl. Conf. Advances in Engineering and Technology Research (ICAETR),* 2014, pp. 1-6.

[38] M. Vetterli and C. Herley, "Wavelets and filter banks: Theory and design," *IEEE Transactions on Signal Processing,* vol. 40, pp. 2207-2232, 1992.

[39] A. L. Goldberger, L. Amaral, L. Glass, J. M. Hausdorff, P. Ivanov, R.G. Mark, J.E. Mietus, G. B. Moody, C. K. Peng, and H. E. Stanley. PhysioBank, PhysioToolkit, and PhysioNet: Components of a New Research Resource for Complex Physiologic Signals. *Circulation* 101(23):e215-e220; 2000 (June 13). PMID: 10851218; doi: 10.1161/01.CIR.101.23.e215

[40] O. Shultseva and J. Hauer, "Implementation of adaptive filters for ECG data processing," in *Proc. 2008 IEEE Region 8th Intl. Conf. Computational Technologies in Electrical and Electronics Engineering, (SIBIRCON 2008),* 2008, pp. 206-209.

[41] S. Sharma and R. P. Narwaria, "Noise reduction from ECG signal using adaptive filter algorithm," in *International Journal of Engineering Research and Technology,* 2014, vol. 3, pp. 437-440.

[42] A. Sharma, S. Toshniwal, and R. Sharma, "Noise reduction technique for ECG signals using adaptive filters," in *International Journal of Recent Research and Review*, vol. 7, pp. 82-86, 2014.

[43] D. Cyrill, J. McNames, and M. Aboy, "Adaptive comb filters for quasiperiodic physiologic signals," in *Proc. 2003 25th Intl. Conf. Engineering in Medicine and Biology Society (IEEE),* 2003, vol. 3, pp. 2439-2442.

[44] P. R. Bokde and N. K. Choudhari, "Implementation of Adaptive filtering algorithms for removal of Noise from ECG signal," *International Journal of Circuit Theory and Applications*, vol.6(I), pp. 51-56, 2015.

[45] R. S. Kumari, S. Bharathi, and V. Sadasivam, "Design of optimal discrete wavelet for ECG signal using orthogonal filter bank," in *Proc. 2007 Intl. Conf. Conference on Computational Intelligence and Multimedia Applications,* 2007, pp. 525-529.

[46] N. M. Arzeno, Z. Deng, and C. Poon, "Analysis of first-derivative based QRS detection algorithms," *IEEE Transactions on Biomedical Engineering,* vol. 55, pp. 478-484, 2008.

[47] S. Chouakri, F. Bereksi-Reguig, and A. Taleb-Ahmed, "QRS complex detection based on multi wavelet packet decomposition," *Applied Mathematics and Computation,* vol. 217, pp. 9508-9525, 2011.

[48] J. Kubicek, M. Penhaker, and R. Kahankova, "Design of a synthetic ECG signal based on the Fourier series," in *Proc. 2014 Intl. Conf. Advances in Computing, Communications and Informatics (ICACCI, 2014),* 2014, pp. 1881-1885.

[49] C. Chandrakar and M. Kowar, "Denoising ECG signals using adaptive filter algorithm," *International Journal of Soft Computing and Engineering (IJSCE),* vol. 2, pp. 120-123, 2012.

[50] J. Lee and G. Lee, "Design of an adaptive filter with a dynamic structure for ECG signal processing," *International Journal of Control, Automation, and Systems,* vol. 3, pp. 137-142, 2005.

[51] S. A. Rehman and R. R. Kumar, "Performance comparison of adaptive filter algorithms for ECG signal enhancement," *International Journal of Advanced Research in Computer and Communication Engineering,* vol. 1, pp. 2278-1021, 2012.

[52] J. Baraniak, J. Hauer, N. Schuhmann, and G. Leugering, "Implementation of adaptive filters for biomedical applications," in *Russian-Bavarian Conference on Bio-Medical Engineering,* 2007, pp. 169.

[53] A. Deo, M. Bandil, D. Singh, and A. Wadhwani, "Denoising ECG signals with adaptive filtering algorithm & patch based method," *International Journal of Computer Networks and Wireless Communications (IJCNWC),* vol. 3501, 2013.

[54] W. Zgallai, "The application of adaptive LMF quadratic and cubic Volterra filters to ECG signals," *International Journal of Computer Theory and Engineering,* vol. 7, pp. 337, 2015.

[55] A. Gyaourova, C. Kamath, and I. K. Fodor, "Undecimated wavelet transforms for image de-noising," *Report, Lawrence Livermore National Lab., CA,* vol. 18, 2002.

[56] J. Pan and W. J. Tompkins, "A Real-Time QRS Detection Algorithm," *IEEE Transactions on Biomedical Engineering,* vol. BME-32, pp. 230-236, 1985.

[57] B. Kohler, C. Hennig, and R. Orglmeister, "The principles of software QRS detection," *IEEE Engineering in Medicine and Biology Magazine,* vol. 21, pp. 42-57, 2002.

[58] S. K. Sahoo, A. K. Subudhi, B. Kanungo, and S. K. Sabut, "Feature extraction of ECG signal based on wavelet transform for arrhythmia detection," in *Proc. 2015 Intl. Conf. Electrical, Electronics, Signals, Communication and Optimization (EESCO),* 2015, pp. 1-5.

[59] P. S. Hamilton and W. J. Tompkins, "Quantitative investigation of QRS detection rules using the MIT/BIH arrhythmia database," *IEEE Transactions on Biomedical Engineering,* vol. BME-33, pp. 1157-1165, 1986.

[60] Y. D. Kumar and A. Prasad, "ECG abnormalities detection using doppler shift method," in *Proc. 2014 4th Intl. Conf. Advanced Computing & Communication Technologies,* 2014, pp. 493-497.

[61] B. B. Hubbard, "The world according the wavelets: The story of a mathematical technique in the making," Massachusetts: *Ak Peters,* pp. 227-229, 1996.

[62] M. W. Frazier, *An introduction to wavelets through linear algebra.* Berlin: Springer Science & Business Media, 2006.

[63] A. Jensen and A. la Cour-Harbo, *Ripples in mathematics: The discrete wavelet transform.* Berlin: Springer Science & Business Media, 2001.

[64] J. S. Walker, *A primer on wavelets and their scientific applications.* Boca Raton, Florida: CRC press, 2008.

[65] M. V. Wickerhauser, "Adapted wavelet analysis from theory to software," Massachusetts: *AK Peters*, 1994.

[66] S. G. Mallat, "A theory for multiresolution signal decomposition: The wavelet representation," *IEEE Transactions on Pattern Analysis and Machine Intelligence,* vol. 11, pp. 674-693, 1989.

[67] T. Domider, E. Tkacz, P. Kostka, and A. Wrzesniowski, "A new approach to the p-wave detection and classification based upon application of wavelet neural network," in *Proc. 2001 23rd Intl. Conf. Engineering in Medicine and Biology Society (IEEE),* 2001, pp. 1758-1760.

[68] J. P. Madeiro, P. C. Cortez, J. A. Marques, C. R. Seisdedos, and C. R. Sobrinho, "An innovative approach of QRS segmentation based on first-derivative, Hilbert and wavelet transforms," *Med. Eng. Phys.,* vol. 34, pp. 1236-1246, 2012.

[69] A. Ghaffari, H. Golbayani, and M. Ghasemi, "A new mathematical based QRS detector using continuous wavelet transform," *Comput. Electr. Eng.,* vol. 34, pp. 81-91, 2008.

[70] S. W. Lee and B. H. Nam, "Peak detection of ECG signal using wavelet transform and radial basis functions," in *Proc. 1999 38th Intl. Conf. SICE Annual,* 1999, pp. 1067-1070.

[71] C. Ye, M. T. Coimbra, and B. V. K. Vijaya Kumar, "Arrhythmia detection and classification using morphological and dynamic features of ECG signals," in *Proc. 2010 Intl. Conf. IEEE Engineering in Medicine and Biology,* 2010, pp. 1918-1921.

[72] C. Saritha, V. Sukanya, and Y. N. Murthy, "ECG signal analysis using wavelet transforms," *Bulg. J. Phys.,* vol. 35, pp. 68-77, 2008.

[73] J. Sahambi, S. Tandon, and R. Bhatt, "Using wavelet transforms for ECG characterization. An on-line digital signal processing system," *IEEE Engineering in Medicine and Biology Magazine,* vol. 16, pp. 77-83, 1997.

[74] A. Mukherjee and K. K. Ghosh, "An efficient wavelet analysis for ECG signal processing," in *Proc. 2012 Intl. Conf. Informatics, Electronics & Vision (ICIEV),* 2012, pp. 411-415.

[75] H. Sato, "A consideration on scaling functions of wavelets," in *Proc. 2008 Intl. Symposium on Information Theory and its Applications (ISITA 2008),* 2008, pp. 1-6.

[76] E. Goldberger, *How to Interpret Electrocardiograms in Terms of Vectors: A Practical Manual.* Thomas, 1968.